Doctoral Dissertation

Optimization of skylight design for enhanced daylight performance in museum interiors using genetic algorithms and multi-objective optimization

September

2024

Kai Li

Fukuda Laboratory
Architecture Course
Graduate School of Environmental Engineering
The University of Kitakyushu
Japan

PREFACE

In a world grappling with deteriorating natural environments and acute energy shortages, the substantial energy consumption attributed to buildings presents a formidable challenge. Thus, setting goals to reduce building energy usage and mitigate environmental impacts is crucial. However, achieving these objectives must not compromise the comfort of building occupants. Efficiently harnessing natural light not only reduces energy dependency but also enhances the quality of building usage. Building performance simulation and advanced computational methods in the early design stages empower us to set precise performance objectives and explore viable strategies to minimize environmental degradation. Despite the complexity of real-world scenarios and the potential differences between simulated and observed results, these simulations are instrumental in understanding the interplay between design parameters and building performance. Focusing on indoor natural lighting environments and specific building types, this thesis uncovers opportunities for performance optimization and efficiency improvements in the early design phases, considering environmental and structural aspects. This research, augmenting contemporary studies on similar themes, identifies significant areas requiring further exploration and is poised to enrich the design field and aid stakeholders in making informed architectural decisions.

DEDICATION

I dedicate a tiny contribution of this thesis to the field of knowledge, to teachers, my parents, my family, my friends, my alma mater, and my institutions.

ACKNOWLEDGEMENT

First and foremost, I extend my deepest gratitude to my advisor, Professor Hiroatsu Fukuda, for his invaluable guidance and support throughout my doctoral studies. His insights into research methodologies and academic practices have been crucial to my development. His mentorship in my research field and detailed feedback on my dissertation writing have not only taught me the intricacies of my study area but also how to excel as a scholar.

I would also like to express my appreciation to my thesis committee members, Professor Bart Dewancker, Professor Koji Takasu and Professor Imai, whose insightful comments and suggestions have greatly assisted me in refining my dissertation. I am thankful for the academic staff at The University of Kitakyushu.

Special thanks go to the members of the Fukuda Laboratory: Xiao Yuling, Yao Wenying, Xu Shipeng, Jiayi Shi, and my seniors Rendy Perdana Khidmat, Zhang Tao, Zhang Li, and Zhou Rui. Your support, encouragement, and advice have been invaluable throughout my time as a student.

Most importantly, I wish to express my profound gratitude to my parents. My mother, who guided and supported me during the most confusing times of my life, helping me find my direction again. My father, whose life philosophies and teachings continue to inspire and guide me daily through memories. Although he could not witness this achievement, his influence is woven through every part of my journey. I am deeply thankful for the role they have played in shaping who I am today.

ABSTRACT

In a world grappling with deteriorating natural environments and acute energy shortages, the substantial energy consumption attributed to buildings presents a formidable challenge. Thus, setting goals to reduce building energy usage and mitigate environmental impacts is crucial. However, achieving these objectives must not compromise the comfort of building occupants. Efficiently harnessing natural light not only reduces energy dependency but also enhances the quality of building usage. Building performance simulation and advanced computational methods in the early design stages empower us to set precise performance objectives and explore viable strategies to minimize environmental degradation. Despite the complexity of real-world scenarios and the potential differences between simulated and observed results, these simulations are instrumental in understanding the interplay between design parameters and building performance. Focusing on indoor natural lighting environments and specific building types, this thesis uncovers opportunities for performance optimization and efficiency improvements in the early design phases, considering environmental and structural aspects. This research, augmenting contemporary studies on similar themes, identifies significant areas requiring further exploration and is poised to enrich the design field and aid stakeholders in making informed architectural decisions.

Keywords: Daylight performance, Multi-objective optimization (MOO), Gallery skylight, Parametric simulation, Visual comfort

Table of Contents

List of Figures

List of Tables

Nomenclature

ACI	:	Annual cumulative illuminance
ASE	:	Annual Sunlight Exposure
ASEi	:	Each value in optimal ASE outcome
ASE_{max}	:	Minimum value of ASE optimization set
ASE_{min}	:	Maximum value of ASE optimization set
ATL	:	Atlanta
Cfa	:	Koppen climate classification for humid subtropical climates
CIE	:	Commission Internationale de l'Éclairage
CORE	:	The processor's core
CPU	:	Central Processing Unit
DA	:	Daylight Autonomy
DAYSIM	:	Daylighting analysis software
DF	:	Daylight Factor
DGP	:	Daylight Glare Probability
EPW	:	*EnergyPlus* weather data
EQ	:	Indoor Environmental Quality credit in LEED
FF	:	Fitness Function
FF_i	:	Fitness function equation
GA	:	Generative Algorithm / Genetic Algorithm
GB	:	Giga byte
GH	:	Grasshopper
GPU	:	Graphic Processing Unit
HypE	:	An algorithm for fast Hypervolume-Based Many-Objective Optimization
IESNA	:	Illuminating Engineering Society of North America
LEED	:	Leadership in Energy and Environmental Design
LEED v4.1	:	Standard for green building design, construction, operations, and performance
LM	:	Lighting Measurement
MOO	:	Multi-Objective Optimization
NSGA	:	Optimization techniques

PC	:	Personal Computer
RAD	:	RADIANCE software engine
RGB	:	Red, Green, Blue
RTX	:	Ray Tracing Texel eXtreme
SDA	:	Spatial Daylight Autonomy
sDA	:	Each value in optimal sDA outcome
SFR	:	Skylight to Floor Ratio
SPEA	:	Strength Pareto Evolutionary Algorithm
SST	:	Sawtooth-Shaped Toplight
sUDI	:	Each value in optimal sUDI outcome
TMY	:	Typical meteorological year
UDI	:	Useful Daylight Illuminance
UDI_i	:	Each value in optimal UDI outcome
UDI_{max}	:	Minimum value of UDI optimization set
UDI_{min}	:	Maximum value of UDI optimization set
US	:	The United States
UV	:	Ultraviolet
VDT	:	Video Display Terminals
ρ	:	Surface reflectance
ρB	:	Surface reflectance Blue
ρG	:	Surface reflectance Green
ρR	:	Surface reflectance Red

Chapter 1. Introduction

1.1. General background

Integrating natural light as part of a comprehensive and controlled lighting strategy is essential for sustainable and eco-friendly architectural design. Skylight can be a significant source of daylight for deep-plan buildings and provide additional environmental advantages such as solar gain, reduced energy loss, and natural ventilation [1]. Furthermore, one of the most cost-effective strategies to lower energy consumption in non-residential buildings is to substitute electric lighting, which accounts for about a third of commercial building energy use, with natural daylight [2].

Therefore, incorporating natural light into museum buildings is a critical feature of sustainable architecture, with most environmental building certifications awarding credits for adequate daylighting levels. However, designing skylight to achieve optimal natural light distribution within a building can be complex due to the various parameters affecting light distribution. White Arkitekter recognizes this challenge as an opportunity to expand their knowledge base and has proposed the study associated with this thesis.

By offering architects guiding principles for museum daylight design from the outset of a project, substantial time and money can be saved, significantly enhancing the potential for an optimized solution. This allows for greater focus on detailed aspects, leading to higher quality results. Although many daylight simulation programs are available to designers, they can be cumbersome and difficult to use in the early design stages. However, parametric design has made this optimization process more accessible to experienced designers.

The objective of this thesis is to delve into the relationship between daylight and museum design and to develop guidelines that will be readily accessible to architects and engineers. These guidelines will assist in designing effective atria from the beginning of a project, thereby improving the quality of architectural design practices concerning daylight access. Critical questions about museum design will be addressed through parametric studies of 3D models using Grasshopper for Rhinoceros and both static and dynamic daylight simulations with Honeybee for Grasshopper.

1.2. Daylight and electric light

The use of natural light in architecture has gained significant attention in the context of global energy conservation efforts. Harnessing daylight not only aligns with sustainable building practices but also offers extensive benefits to human well-being and building performance. This section explores the importance of incorporating natural light in building designs, emphasizing the dual benefits it brings to both occupants and structures.

Daylighting in architecture is increasingly advocated not only for its aesthetic and perceptual qualities but also for its pivotal role in reducing reliance on artificial lighting, which is a major consumer of electrical energy. Buildings designed to maximize natural light use less energy for lighting during daylight hours, which can significantly reduce overall energy consumption. Additionally, daylight is dynamic in intensity and quality throughout the day and year, which can enhance the visual comfort of indoor environments and contribute to the thermal comfort during various seasons.

Daylight is both carbon-free and cost-effective, playing a significant role in energy conservation when properly utilized. In museums, the strategic use of daylight can significantly reduce the need for electric lighting, which can comprise up to 20% of a museum's total energy consumption. However, uncontrolled daylight can pose challenges, such as overheating spaces or over-illuminating artworks. Therefore, museum projects must develop and implement both active and passive lighting solutions to manage light, heat, and UV radiation effectively. Table 1.2.1 illustrates the advantages and disadvantages of daylight and electric light.

Table 1.2.1 Comparison of daylight and electric light

Daylight	Electric Light
Benefits	**Benefits**
• Improved visitor experience • Carbon-free and cost-free	• Enhanced flexibility in lighting scenarios • Ability to tune lighting according to visitor and curator preference

• Link to the outside world and sky conditions	• Tailored lighting specific to application
• Improved staff well-being	• Tunable color temperature and illuminance level
• Variation in lighting condition and ambiance of galleries	• Presence-based control systems reduce illumination exposure to artwork
• Changing color temperature during the course of the day	• Lighting only during operating hours
• Correct light color and color rendering	• Retrievable pre-programmed lighting scenes
Drawbacks	**Drawbacks**
• Potential to overheat the gallery space	• Potentially high maintenance/life cycle costs
• Potential to over-light gallery	• Potentially high energy costs if not using high-efficiency luminaire systems
• Dynamic lighting scenario does not fit exhibit	• Potentially monotone and tiring lighting scenarios

1.3. Advantages of daylight

The primary objective of daylighting is clearly outlined in the daylighting chapter of the LEED certification. It specifies that "the intent of the daylighting chapter is to connect building occupants with the outdoors, reinforce circadian rhythms, and reduce the use of electrical lighting by introducing daylight into the space" [3,4]. To fully grasp the significance of effective daylighting within a building, it is essential to consider its relationship to sustainability. The benefits of incorporating daylight into buildings can be explained through three interconnected aspects of sustainability: environmental, social, and economic. These aspects are discussed in the following sections to elucidate the advantages of daylighting.

1.3.1. Social benifits

Natural light provides a spectrum that closely resembles daylight, which is optimal for human vision. It reduces the risk of eye strain and headaches associated with poor artificial lighting. The dynamic quality of natural light, with changes in intensity and angle throughout the day, helps maintain the human circadian rhythm, promoting better sleep patterns and overall health. Natural light enhances the colors and textures of materials used in interiors, making spaces appear larger and more welco ming. It can transform the ambiance of a room, influencing the aesthetics and the perceived value of the space.

Incorporating daylight into deep-plan buildings helps occupants gain a sense of orientation, time, weather, and the outside world [5]. Natural light is known to positively influence human health, productivity, and our biological clock. This internal clock, which manages our sleep-wake cycles (or circadian rhythms), is regulated by the brain's production of melatonin, which is synthesized in the dark. Studies reveal that exposure to bright light (> 1500 lux) through the eyes inhibits melatonin production by the pineal gland in the brain. Elevated melatonin levels induce drowsiness, while lower levels promote alertness, thus playing a crucial role in maintaining our circadian rhythms. Dr. Alfred J. Lewy's research indicated that light therapy could benefit patients experiencing winter depression by affecting their melatonin levels.

Access to natural light has been linked to higher productivity in workplace studies. Employees in environments with ample daylight report higher levels of energy and less fatigue. In educational settings, natural light correlates with improved student performance and concentration, likely due to better mood and alertness facilitated by exposure to daylight. In a literature review by Edwards and Torcellini (2002), several studies were presented showing that office workers in spaces with natural light or window views had increased productivity. Their review also noted that natural light enhances attention and alertness during the post-lunch dip and can boost alertness for monotonous tasks. They also mentioned quicker recovery times for hospital patients and reduced stress levels for doctors and nurses. Additionally, Edwards and Torcellini highlighted numerous studies on the academic benefits of daylighting, such as improved test scores, accelerated learning rates by 20–26%, better attendance by 1.6–1.9%, and improved behavior A literature review of the effects of natural light on building occupants [6–8].

1.3.2. Environmental benifits

Buildings utilizing natural light reduce their reliance on artificial lighting, which can significantly decrease energy costs. Properly designed windows and skylights can illuminate spaces more efficiently than artificial lights, particularly during peak daylight hours, leading to lower electricity consumption and enhanced environmental sustainability. Integrating natural light effectively reduces a building's carbon footprint by decreasing energy consumption.

An essential element of environmentally conscious design is the reduction of artificial lighting by incorporating daylight into buildings. To understand the scale of artificial lighting usage today, one can examine its electricity consumption. According to the International Energy Agency, artificial lighting accounts for nearly 20% of global electricity use, comparable to the annual electricity production of nuclear power worldwide [9]. Beyond the significant energy consumption, artificial lighting systems generate substantial waste. In an article discussing the environmental impact of artificial lighting, Páramo (2008) identifies three types of waste: material waste (bulbs and lighting systems), energy consumption (heat, UV, and electromagnetic radiation), and light pollution [10]. The heat generated by artificial lighting increases the cooling load on a building's mechanical cooling system. Reducing the use of artificial lighting can decrease building cooling loads by 10-20% [11]. Implementing daylighting strategies not only reduces a building's energy consumption but also lowers carbon dioxide emissions, thereby mitigating the greenhouse effect.

Sustainable design practices that incorporate optimal use of daylight not only save energy but also reduce harmful environmental impacts. This approach aligns with global sustainability goals, promoting healthier and more eco-friendly living environments.

1.3.3. Economic benifits

Integrating natural daylight into a building significantly reduces the need for electrical lighting, thereby lowering energy consumption. With fewer artificial lights generating less heat, the cooling load on the mechanical system decreases, leading to overall lower energy expenses. According to the US National Institute of Building Sciences, optimal daylighting strategies can cut a building's total energy costs by up to one third [11]. In addition to lower energy bills, smaller artificial lighting systems mean reduced material usage and lower maintenance costs.

A study by the British Council for Offices (BCO) on how office design impacts building performance revealed that employee salaries constitute about 85% of an office building's operational costs over a 25-year period. Compared to this, other costs are negligible. Therefore, enhancing office worker productivity has a much more significant financial impact than any savings on other factors. The study also highlights that well-designed lighting and properly daylit environments can boost office worker productivity by 3–20%, underscoring the financial benefits of good daylighting [12].

1.4. Advantages of computer simulation and MOO

The integration of computational tools in architectural design has revolutionized the way architects approach daylight analysis and optimization.

1.4.1. Early Stage Simulation

Computational simulations enable architects to visualize and analyze the impact of natural light early in the design process. By simulating various lighting scenarios, architects can adjust the design to achieve optimal daylight penetration and distribution before the construction phase begins. This proactive approach helps in identifying potential issues such as glare, excessive heat gain, or inadequate lighting, which can be costly to rectify after the building is constructed. The ability to iterate designs rapidly in response to simulated outcomes ensures that the final architectural plan is both aesthetically pleasing and functionally superior, minimizing the need for expensive post-construction modifications.

1.4.2. Cost and Time Efficiency

The use of computational models dramatically reduces the time and expense associated with physical model construction. Traditional methods require physical materials, space for model setup, and considerable labor for building and modifying the physical models. Computational modeling, on the other hand, allows for quick adjustments to the design with just a few clicks, significantly cutting down the iteration time. This not only speeds up the design process but also reduces the resources spent on materials and manpower. Moreover, the ability to explore more design alternatives in a shorter time frame enhances the designer's creativity and ability to respond to client feedback or changing requirements effectively.

1.4.3. Accuracy and Comprehensive Analysis

Computational tools provide precise and detailed analyses of how natural light interacts with a building throughout the day and across different seasons. These tools use sophisticated algorithms to model light behavior accurately, including reflections, refractions, and shadows cast by various architectural elements. This level of detail allows designers to understand not only how light enters and moves through a space but also its thermal effects and energy implications. Such comprehensive analysis is essential for creating energy-efficient buildings that adhere to sustainability standards and provide comfortable living or working environments. Furthermore, these simulations can predict the lighting conditions in every corner of a building, ensuring that all spaces are adequately lit and energy-efficient.

Multi-objective optimization (MOO) in architectural design allows for the simultaneous consideration of various factors such as light quality, energy efficiency, and aesthetic values.

Multi-objective optimization allows architects to simultaneously consider multiple design objectives, such as aesthetic appeal, structural integrity, energy efficiency, and cost-effectiveness. By integrating various goals into the design process, MOO helps ensure that no single aspect dominates at the expense of others, leading to a more balanced and holistic architectural solution. For example, in a building project, MOO can help balance the trade-offs between maximizing natural light, minimizing heat gain, and maintaining visual comfort for occupants. This is particularly beneficial in complex projects where differing objectives might otherwise lead to conflicting design decisions.

MOO is crucial for designing buildings that are not only functional and beautiful but also environmentally sustainable. By optimizing for factors such as solar gain, thermal insulation, and daylight use, MOO contributes to reducing a building's carbon footprint and operational costs. For instance, optimizing the placement and sizing of windows using MOO can maximize natural lighting and enhance thermal comfort while minimizing energy use for heating and cooling. This approach aligns with global standards for sustainable design, such as LEED or BREEAM, and helps architects achieve high performance in both environmental and energy metrics.

MOO provides architects with the tools to assess multiple design scenarios under various constraints and priorities. This capability is invaluable for adapting designs to specific client needs or site conditions. For example, an architect can use MOO to evaluate different facade designs based on their performance in different climates or urban settings. Scenario testing with MOO enables designers to anticipate potential challenges and evaluate the impact of different design decisions, such as choosing materials or configurations that optimize energy use while also considering factors like local climate conditions and building orientation. The use of MOO fosters innovation in architectural design by encouraging exploration of non-traditional solutions that meet complex requirements. It pushes designers to think outside the conventional frameworks and explore new combinations of materials, technologies, and form factors that might not be considered using a single-objective optimization approach.

1.5. Problem statement and research question

Despite advances in computational simulation for architectural design, there are notable gaps in research. Specifically, while the current models and tools have improved, they still struggle with real-time dynamic assessments and comprehensive integration into traditional design processes. These simulations are becoming more critical as daylighting and energy conservation become key components of sustainable design projects.

However, the development of methods that seamlessly incorporate these simulations into standard architectural practices remains a challenge.

Natural light displays highly dynamic characteristics that vary with the time of day, season, and geographic location, introducing significant challenges in its simulation and application in architecture. The ability to accurately forecast natural light behavior is critical because it influences a wide range of design decisions, from window placement and orientation to the choice of materials and the design of the building's facade. Architects need to predict how different light levels and qualities will impact the space throughout the day and year to optimize both the energy efficiency and occupant comfort. This requires sophisticated simulation tools that can model the intricate interactions of light with the built environment, accounting for factors such as reflection, absorption, and scattering.

Integrating advanced computational simulations effectively into the traditional architectural design process poses several challenges. Many existing practices rely on more intuitive and less quantitative methods of design, making the shift to data-driven, simulation-based approaches difficult. Given the aforementioned challenges and research gaps, this research seeks to answer the following question:

-How can architectural design processes be adapted to better accommodate the dynamic and complex behaviors of natural light, ensuring effective integration of computational simulation tools into traditional design workflows?

This question aims to explore methodologies that could bridge the gap between traditional architectural practices and modern computational techniques, enhancing both the practicality and accuracy of natural light simulations in architectural design.

Addressing the complexities of natural light behavior and its integration into architectural practices is crucial for advancing the field of architectural design. By focusing on these challenges, this research intends to provide actionable insights that can help streamline the integration process, promote sustainable design, and ultimately lead to environments that are both aesthetically pleasing and functionally superior.

1.6. Aims and objectives

Building upon the challenges identified in the use of natural light simulation and its integration into architectural design, this research aims to advance the use of computational tools in architecture. It seeks to develop models and strategies that enhance the accuracy and application of these tools in daily architectural practice.

1.6.1. Optimize Design Accuracy

The goal here is to enhance the precision of computational tools used in simulating natural light, ensuring that the data these tools generate is reliable and detailed. This accuracy is vital for architects when making design decisions that affect both the aesthetics and functionality of a building. Improved simulation tools can predict how light interacts with different materials and architectural features, impacting everything from energy consumption due to heating and lighting needs to how users perceive and interact with the space. By accurately modeling different lighting scenarios throughout the day and year, these tools help in creating spaces that are not only energy-efficient but also comfortable and visually appealing to the occupants.

1.6.2. Promote Sustainable Design Practices

This objective focuses on leveraging enhanced simulation tools to design buildings that make optimal use of natural light, thereby reducing the need for artificial lighting and decreasing overall energy consumption. By doing so, buildings become more sustainable and environmentally friendly. Effective use of simulations can guide the placement of windows, skylights, and other architectural elements to maximize daylight while minimizing heat loss and gain, aligning with sustainable building standards. Encouraging the adoption of these practices promotes not only environmental responsibility but also long-term economic benefits for building owners and occupants through reduced energy costs.

By achieving these objectives, the project aims to provide architects with advanced tools that enable the creation of buildings that are better adapted to their natural environments, enhancing both sustainability and occupant well-being.

1.7. Novelty and contributions

In this field of study, despite the substantial efforts by researchers and practitioners on integrating parametric and multi-objective optimization approaches to address environmental aspects in design [13–16], the exploration extends beyond merely finding optimal solutions. This method encompasses a layered investigation that combines pinpointing trends, roles of design parameters, and the impact of critical parameters on design objectives. However, reports on an all-encompassing optimization approach from inception to ranking design solutions remain relatively scarce. This thesis leverages the generative and parametric methodologies to examine the relationships between design parameters and objectives, aiming to elucidate environmental and structural phenomena, and to identify superior design solutions through a form-finding process that includes assessing trends and roles of parameters. Furthermore, this dissertation introduces a unique design optimization goal applicable across various scales of design. Beyond the primary innovation and contributions of providing a detailed optimization method, which introduces a novel way to execute form-finding, each case study delineates its particular importance. Specifically, every principal experiment introduces fresh insights to the study areas as outlined in Table 1.7.1.

Table 1.7.1. Research novelty and contribution.

Scope and section	Novelty	Contribution
Main	The bigger idea of combining a parametric and MOO using specific regional context and material used.	We propose several platforms to investigate the relationship between design parameters and design objectives, while simultaneously optimizing the design objective (target building performance). This contrasts with the traditional design process,

		which is relatively ineffective at identifying problem-specific information.
Chapter 5	This study introduces a novel approach to optimizing natural light distribution in museum spaces using genetic algorithms. The primary innovation lies in the application of genetic algorithms to the geometric configuration of sawtooth skylights, which has not been extensively explored in previous research. The integration of advanced computational tools such as Octopus and Ladybug for year-round sunlight simulations further adds to the originality, as these tools are leveraged to precisely define shading system parameters and settings, ensuring a high level of accuracy and effectiveness in the optimization process.	Enhanced Daylight Management: The study provides a robust method for optimizing skylight configurations to achieve better natural light distribution while minimizing glare and protecting exhibits, which is crucial for museum environments. Innovative Methodology: By utilizing genetic algorithms combined with iterative simulations, the research offers a forward-thinking approach that can be applied to other architectural design challenges involving complex lighting scenarios. Practical Applications: The findings are directly applicable to real-world scenarios, particularly for buildings oriented at non-polar directions. The optimized skylight configurations presented in this study can be implemented to improve energy efficiency and visual comfort in museum spaces. Tool Integration: The research showcases the effective use of Octopus and Ladybug tools in the optimization process,

		demonstrating their potential in architectural design and performance simulation.
Chapter 6	This study introduces a novel approach to optimizing natural light distribution in museum interiors through the use of point skylight systems. The primary innovation lies in the application of the Octopus genetic algorithm plugin and Ladybug tool for daylight simulations, which has not been extensively explored in previous research. The study focuses on optimizing the skylight system's design parameters, including skylight height and shading panel angles, to achieve optimal daylight performance while meeting medium sensitivity exhibit standards from IESNA.	Enhanced Daylight Management: The study demonstrates how optimized point skylight systems can effectively block direct sunlight and reduce indoor glare, while maintaining the annual cumulative illuminance (ACI) below 480,000 lux and increasing the annual effective Useful Daylight Illuminance (UDI) to 75%. Innovative Methodology: By utilizing advanced computational tools and genetic algorithms, the research offers a forward-thinking approach to evaluating and optimizing daylight performance in museum interiors. Practical Applications: The findings provide practical design guidelines, showing that specific skylight dimensions and shading panel angles can significantly enhance indoor lighting conditions. These guidelines can be directly applied to museum design projects to improve energy efficiency and exhibit preservation. Case Study Validation: Using Renzo Piano's High Museum Expansion as a case study, the research validates

		its methods and findings, providing a real-world application and demonstrating the feasibility of the proposed optimization approach.

1.8. Thesis structure

The thesis divided into three main parts. First is the introduction consisting of Chapters 1 and 2, methodology in Chapter 3, and body of the thesis that consists of Chapters 4, 5, and 6, and lastly the discussion and conclusion that is in Chapter 7 and 8. More specifically, this thesis consists of 8 chapters presented in Table 1.8.1.

Table 1.8.1. Thesis structure

Chapter 1. Introduction	This chapter discusses the research background, offering a broader perspective. Additionally, it outlines the problem statement, scope, and objectives of the research, as well as the originality and contributions of this study.
Chapter 2. Literature review	This chapter lists and explains the literature that forms the conceptual foundation of this study. It presents the most recent and relevant research on parametric multi-objective optimization and building performance simulation. Additionally, the chapter includes a summary of the methodologies employed in this thesis. It covers the overall workflow, parametric platform, environmental simulation, and optimization methods. Each subsection introduces its topic and concludes with a comprehensive and contextually relevant explanation of the methods used.
Chapter 3. Methodology	This chapter provides an overview of the methodologies used in this dissertation. It discusses the overall workflow, parametric platform, environmental simulation, and optimization processes. Each section introduces its topic and concludes with a detailed and

	contextually relevant explanation of the methods employed.
Chapter 4. Preliminary study	This chapter outlines the prerequisite knowledge necessary before formally commencing the research, which includes an understanding of the variability and types of natural sky light, as well as detailed requirements of natural lighting for various architectural types. This foundational knowledge is critical for framing the research questions and methodology in the study of natural light optimization in buildings.
Chapter 5. Optimizing Natural Lighting Effects in Non-Polar Oriented Museums: A Genetic Algorithm Approach for Sawtooth Skylight Design	This study explores the use of genetic algorithms to optimize sawtooth skylights in museums, enhancing natural light distribution while minimizing glare and meeting exhibit protection standards. Using tools like Octopus and Ladybug, the research conducts year-round simulations and iterative assessments to find the best skylight configurations, particularly for buildings oriented at 45 degrees northeast.
Chapter 6. Parametric Design and Multi-Objective Optimization of Daylight Performance in Gallery Skylight Systems: A Case Study on the High Museum Expansion	This study uses Renzo Piano's High Museum Expansion to explore the optimization of point skylight systems for natural lighting in museums. Utilizing computer modeling, Ladybug for simulations, and the Octopus genetic algorithm, it improves visual comfort and protects exhibits. Findings show that skylights with specific dimensions and angles enhance lighting conditions, maintaining annual cumulative illuminance below 480,000 lux and increasing useful daylight illuminance to 75%.
Chapter 7. Discussion	This chapter provides a synopsis of the scenarios discussed in the previous chapter. It will outline the contributions and standings of each case study within their respective research domains. Additionally, the

	limitations of this research and recommendations for future studies will also be discussed.
Chapter 8. Conclusion	This chapter summarizes the scenarios discussed in the preceding chapter. It describes the contributions and status of each case study within their respective fields of research. Furthermore, the limitations of this study and subsequent recommendations are addressed. Additionally, this chapter encapsulates the comprehensive parametric and multi-objective optimization platform applied to a specific case, along with each conclusion and analysis.

Figure 1.1 explains the logic of this thesis. The main idea is to implement computational methods at the early stages of architectural design to assess whether this approach can lead to potential optimization and efficiency. The study will explore computational methods in two different cases, targeting visual comfort and light intensity. The conclusions of the chapters will answer the questions and reveal deeper investigations such as trends between parameters and objectives, and the most influential parameters driving design objectives in each case. The final conclusion will determine if the proposed methods can achieve optimization and identify trends and roles of dynamic variables or design parameters across all experiments. Additionally, the reliability of the proposed method will be explored, and the final conclusions will be compared with the research questions and hypotheses discussed in Chapter 1.

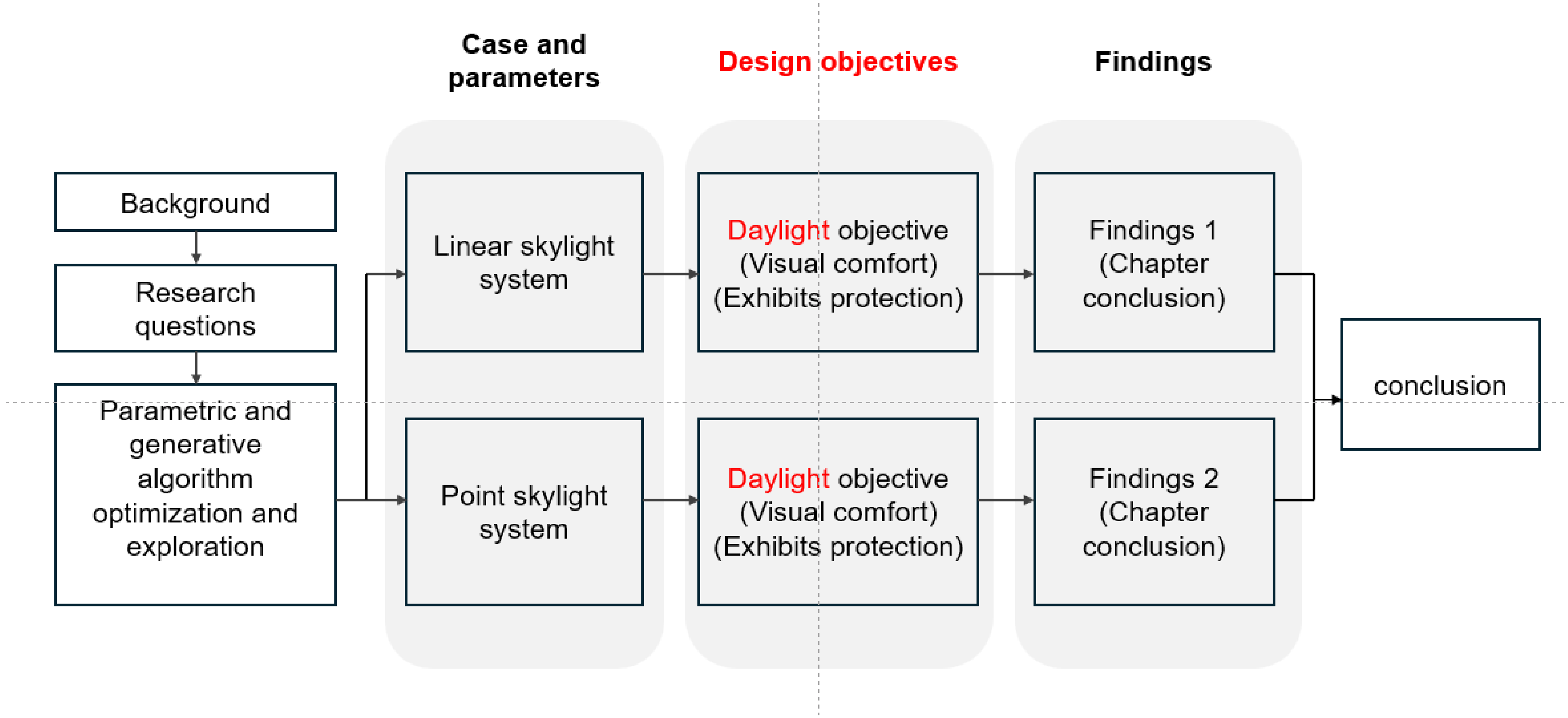

Figure 1.1 The scheme and the logic behind the thesis

Chapter 2. Literature review

2.1. Daylight in standards and certifications

The American LEED [4] rating system and the British BREEAM [17] rating system are distinct environmental certification frameworks that offer diverse criteria for creating environmentally responsible buildings. One of these criteria ensures that the daylighting requirements are fulfilled within the occupied areas of a building. Furthermore, there are numerous standards available to assist designers in incorporating daylight into their designs.

2.1.1. LEED v4

The latest version of LEED sets criteria for assessing the quantity and quality of daylight using computer simulations. Good daylighting criteria can be met through one of three options outlined in the certification. The first option involves conducting annual computer simulations to demonstrate that certain levels of spatial daylight autonomy (sDA) and annual sunlight exposure (ASE) are achieved in specific areas. The second option requires designers to use computer models to show that illuminance levels range from 300 to 3000 lux at 9 a.m. and 3 p.m. on a clear-sky equinox day in designated areas. The third option specifies that illuminance levels must be between 300 and 3000 lux during any hour from 9 a.m. to 3 p.m. at the appropriate work plane height in specified areas. For this option, two measurements are required as detailed in the certification [4].

2.1.2. BREEAM

In BREEAM, meeting just one criterion is insufficient; instead, a combination of two criteria must be met. The certification outlines methods for measuring the daylight factor, average daylight illuminance, uniformity, sky view from desk height, and room depth criterion. For instance, a zone is considered adequately daylit if 80% of the floor area receives an average daylight illuminance of 200 lux for 2650 hours annually or meets an average daylight factor according to specific values based on different latitudes. In addition to one of these criteria, a specific uniformity ratio must be achieved, or a specific point daylight factor must be met based on different latitudes. Alternatively, daylighting points can also be achieved by ensuring a view of the sky from desk height and meeting the room depth criterion, which is defined as

where

- d = room depth,
- w = room width,
- HW = window head height from floor level,
- RB = average reflectance of surfaces in the rear half of the room.

Finally, the standard mandates that designers evaluate the necessity of glare control using shading systems. It also provides a framework for achieving exemplary level criteria to earn innovation credits, along with a timeline detailing the evidence required to demonstrate compliance with these criteria [17].

LEED and BREEAM both employ more complex methods through dynamic daylight evaluation. In the literature reviewed, the most common daylight metric is the daylight factor, likely due to its simple calculation method and the fact that everyday computers have only recently become powerful enough to handle the intensive calculations required for dynamic daylight simulations.

2.2. Research on Indoor Daylighting and Skylight Systems

In recent years, the application of natural daylight in architectural design, particularly in museums and libraries, has gained significant attention due to its numerous benefits. The primary aim of utilizing natural light in these buildings is to enhance energy efficiency, improve the visual comfort of occupants, and ensure the preservation of artifacts. As global concerns about sustainability and energy consumption continue to rise, integrating natural daylight into building design has become an essential strategy for reducing reliance on artificial lighting and minimizing environmental impact.

Museums and libraries, as institutions that serve both educational and cultural purposes, face unique challenges in balancing adequate lighting for display and preservation needs. Museums require careful management of light to protect sensitive artifacts from photodegradation, while libraries must provide sufficient illumination for reading and research activities. Furthermore, both types of buildings benefit from the psychological and physiological advantages that natural light offers to visitors and staff, such as increased well-being, productivity, and satisfaction.

This literature review aims to explore the latest research and developments in the field of indoor natural daylighting and skylight systems in museums and libraries. By examining a comprehensive range of studies, this review seeks to identify effective strategies for optimizing natural light usage, evaluate the impacts on energy efficiency and occupant comfort, and highlight the technological advancements in daylighting systems. The motivation for conducting this literature review is to provide a solid foundation for future research and practical applications in architectural design. By understanding the benefits and challenges associated with natural daylight in museums and libraries, architects, engineers, and facility managers can make informed decisions that enhance the sustainability and functionality of these important cultural and educational spaces.

2.2.1. Indoor Lighting in Museums

Varandani et al. [18]conducted a study to explore the use of skylights and other passive design strategies to optimize daylighting in museums and art galleries. They utilized parametric simulation techniques to analyze the impact of various design strategies on daylight performance. Their findings indicated that optimized skylight designs could significantly improve energy efficiency while minimizing potential damage to artifacts. This study highlighted the importance of adjusting skylight position, size, and shading devices to ensure adequate and evenly distributed daylight. The significance of their work lies in providing sustainable lighting solutions that protect exhibits while enhancing energy efficiency.

Ignacio Acosta et al. [19] utilized Lightscape 3.2 software to simulate various rooms with three different skylight shapes. After conducting trials, the researchers concluded that, for this type of skylight with a height/width ratio of 4/3, the curved shape resulted in an approximately 3.5% increase in average daylight factors compared to the rectangular shape. Conversely, the sawtooth shape led to a decrease of approximately 3.5% in average daylight factors under overcast sky conditions in a room.

Behar et al. [20] focused on restoring natural light in art museums. They investigated how modern technologies and design methods, such as laser-cut panels, could be used to restore and optimize the performance of natural light while adhering to current preservation standards. Their study found that it is possible to maintain the artistic and functional quality of the original design while meeting contemporary conservation requirements. The significance of this research lies in its dual focus on maintaining historical integrity and improving current museum lighting conditions.

EmmanuelOyebade's [21] research at the Nigerian National War Museum examined sustainable daylighting techniques to enhance internal visibility. The study assessed existing daylighting technologies' shortcomings and proposed the use of automated louvered skylights. The results showed that these systems could sustainably improve internal visibility by adjusting according to external lighting conditions. This research is significant for its practical application in enhancing museum lighting quality and energy efficiency.

Sharif-Askari and Abu-Hijleh [22] conducted a comprehensive review of environmental conditions in museums. Their research focused on evaluating the indoor environmental parameters such as temperature, relative humidity, lighting, and air quality, and their impact on artifact preservation and energy consumption. The study reviewed existing literature and case studies to identify the best practices and technologies for maintaining optimal conditions in museums. They found that integrating advanced environmental control systems and energy-efficient lighting can significantly enhance the preservation of artifacts while reducing energy usage. The significance of their work lies in providing a holistic approach to museum environmental management, emphasizing the balance between artifact protection and sustainability.

Kesner's analysis of museum lighting environments identified significant issues in managing daylight to protect artifacts while meeting visitor expectations. The study found that existing lighting conditions often fail to meet the needs of both decision-makers and visitors, particularly in daylit galleries. Kesner highlighted the necessity of informed decision-making based on documented evidence to improve museum lighting design [23].

2.2.2. Toplighting systems by different researchers globally

Windows are openings in a building envelope that permit light and air to enter indoor spaces. These spaces can be categorized into two primary types: openings in the sidewalls of a building and apertures in the roof, commonly referred to as rooflights. The terms used by building professionals for these classifications are side-lighting and toplighting, respectively.

This study emphasizes the importance of toplighting systems, highlighting their potential benefits. Toplighting allows designers greater flexibility in source placement, facilitating more uniform sky illumination and enhancing privacy and security [24]. However, these systems face limitations, including structural design challenges, electrical and mechanical system integration, fire safety considerations, and their application in tall buildings due to their capacity to illuminate only the upper floors [24].

The Lighting Guide LG10 publication (1999) [25,26], titled 'Daylighting and Window Design,' identifies several categories of rooflights. It highlights shed roof, monitor, and sawtooth as the most common toplighting systems as shown in Figure 2.1.

Toplighting systems can feature horizontal, vertical, tilted, or domed glazing, according to Phillips[5], Kroelinger[24], and Ruck and Aschehoug [27].

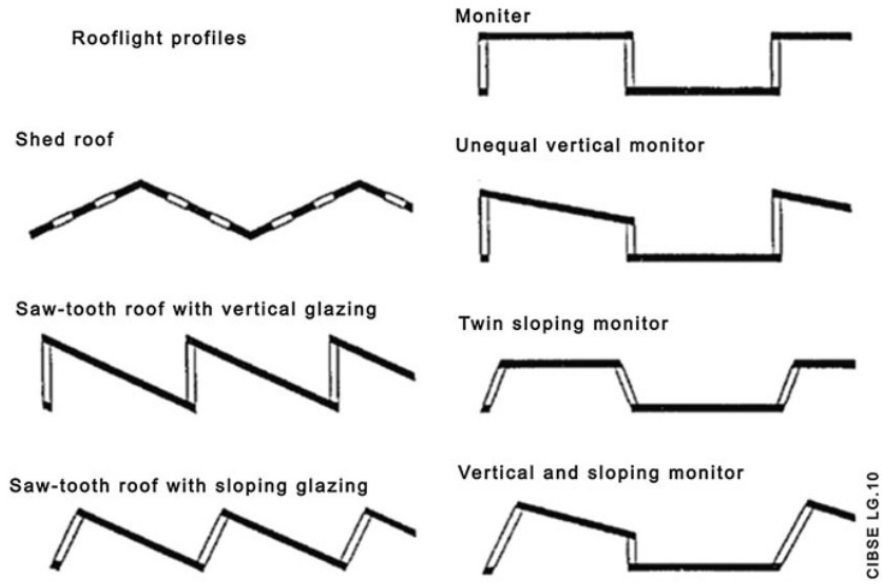

Figure 2.1 Most common types of toplighting systems published by lighting guide LG10.

Figure 2.2 and Figure 2.3 summarizes multiple studies on different aspects and types from various locations worldwide, particularly in areas with high levels of solar radiation. The surveys aim to highlight critical design concepts specific to different regions and indicate the characteristics of these global system designs. A toplight system can be uniformly spread over a wide area and is highly effective in sustainable design. Table 2.2.1 outlines the specific tasks and localized conclusions for each system.

Overall, the aforementioned studies suggest that toplight systems are practical and can complement electric lighting across various climatic conditions. These systems bring the dynamic quality of the outdoor environment indoors. The interplay between sunlight and cloud movements creates a more stimulating atmosphere than constant indoor lighting. The dramatic, ever-changing light levels produced by these systems evoke a positive response from people and enhance the perception of color, texture, and shape. Despite these advantages, daylighting designers must consider several critical factors when designing toplighting systems. These factors include visual and thermal comfort, heat loss and gain, seasonal and daily variations in daylight availability, and integration with electric lighting systems, roofing structures, and HVAC design [28].

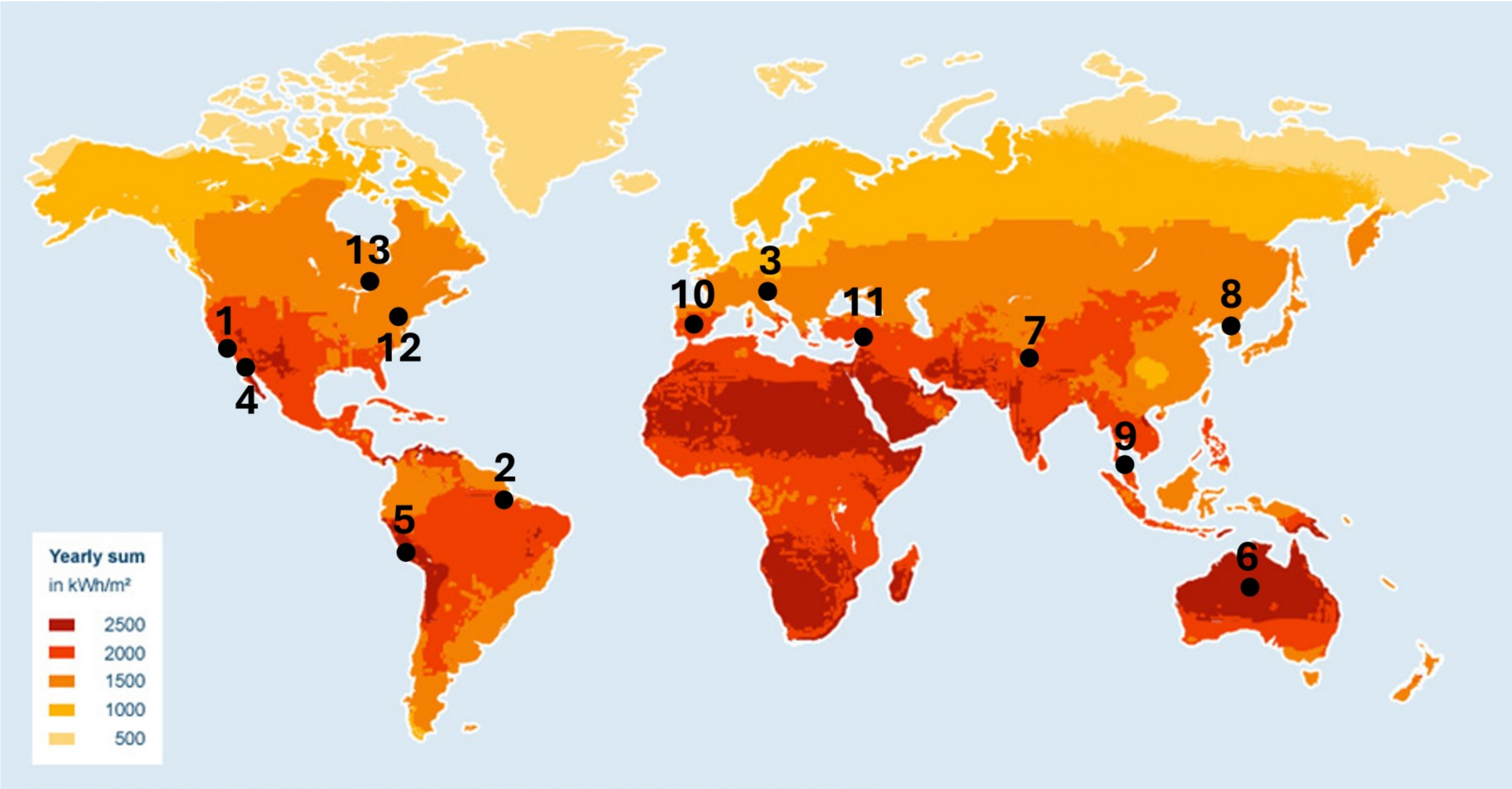

Figure 2.2 Location of surveys implemented according to the Global irradiance [29]: (1) Lee et al. [30]; (2) Cabús and Pereira [31]; (3) Kristl and Krainer [32]; (4) McHugh et al. [33]; (5) Beltran [34]; (6) Darula et al. [35]; (7) Chel et al. [36]; (8) Kim and Chung [37]; (9) Yunus et al. [38]; (10) Acosta et al. [39]; (11) Yildirim et al. [40]; (12) Ghobad et al. [41]; (13) Laouadi et al. [42].

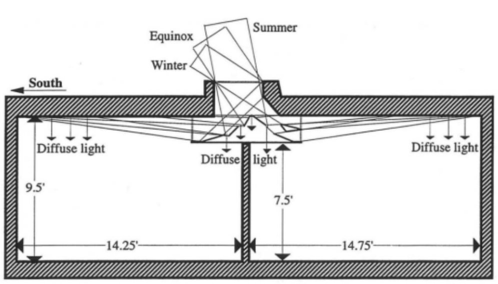

(1) Lee et al. [30]

California, USA/North America—Hot and usually dry climate

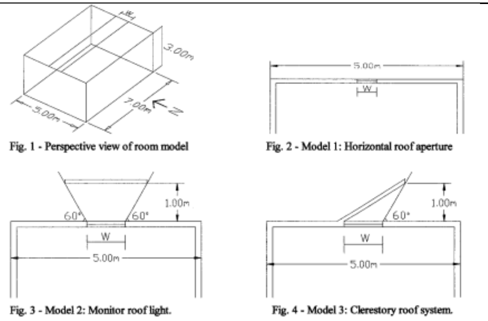

(2) Cabús and Pereira [31]

Brazil/South America —Tropical hot and humid climate

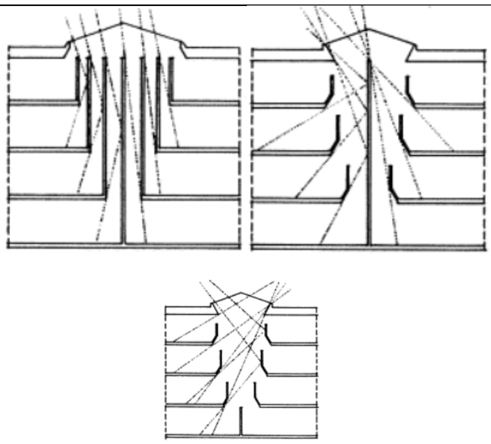

(3) Kristl and Krainer [32]

Slovenia/EuropeHumid subtropical with continental climate

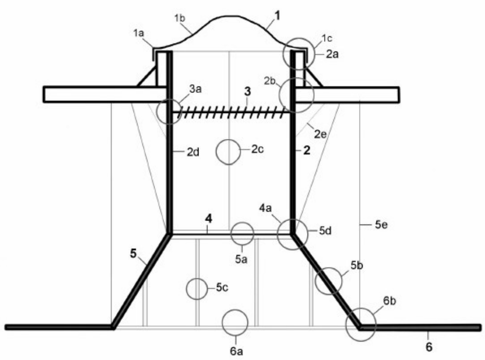

(4) McHugh et al. [33]

California USA/North America—Hot and dry climate

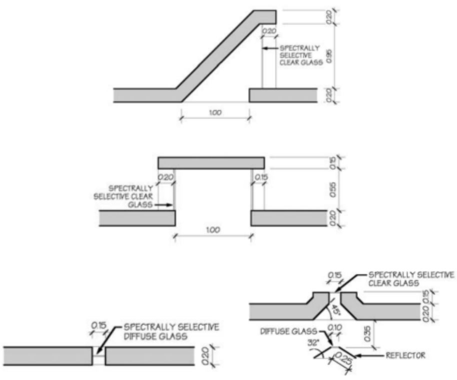

(5) Beltran [34]

Lima, Peru—Tropical climate

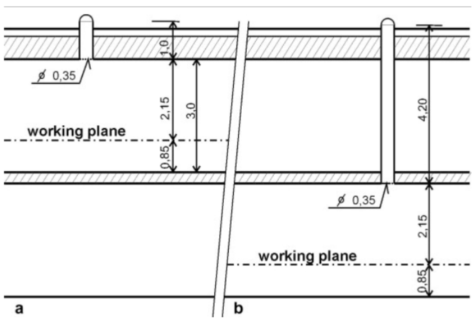

(6) Darula et al. [35]

Australia/Australia—Desert climate

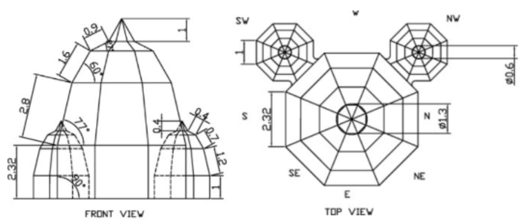

(7) Chel et al. [36]

Delhi, India/AsiaHumid —subtropical climate

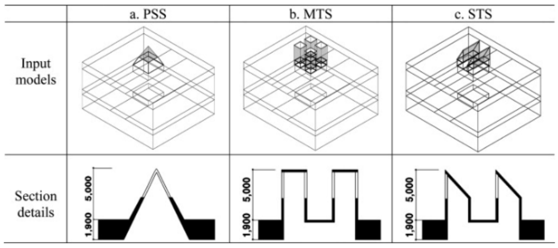

(8) Kim and Chung [37]

Seoul, South Korea/Asia—Humid subtropical and humid continental climate

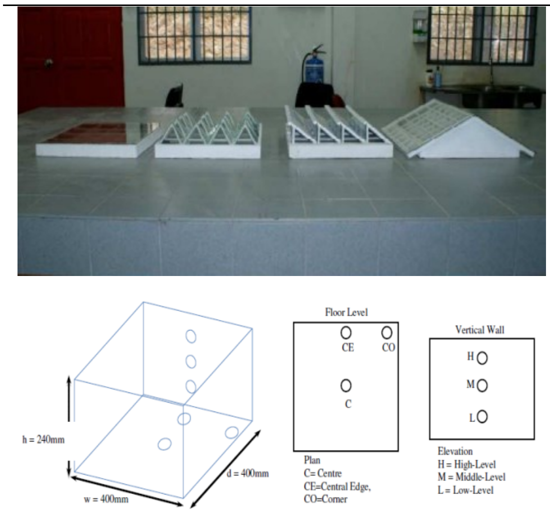

(9) Yunus et al. [38]

Malaysia—Tropical hot and humid climate

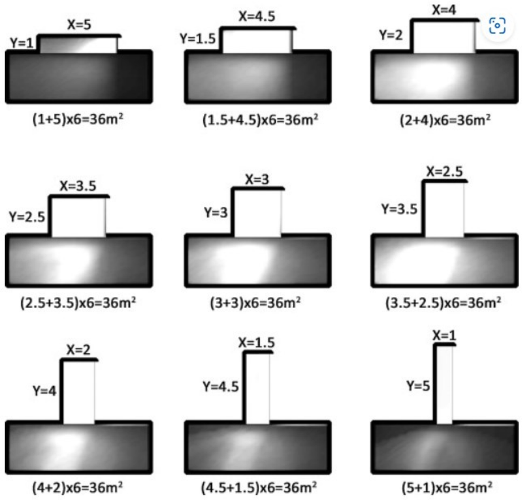

(10) Acosta et al. [39]

Madrid, Spain/Europe —Mediterranean climate

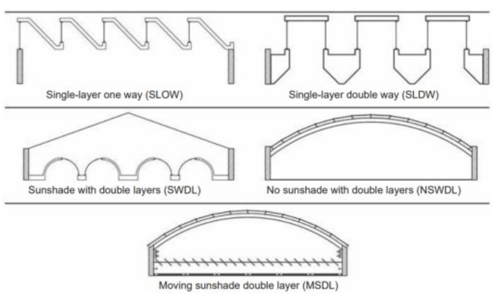

(11) Yildirim et al. [40]

Ankara, Turkey/Asia — Continental climate

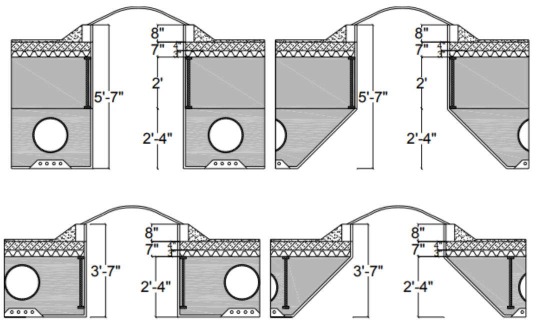

(12) Ghobad et al. [41]

Boston, MA/North America — Continental climate

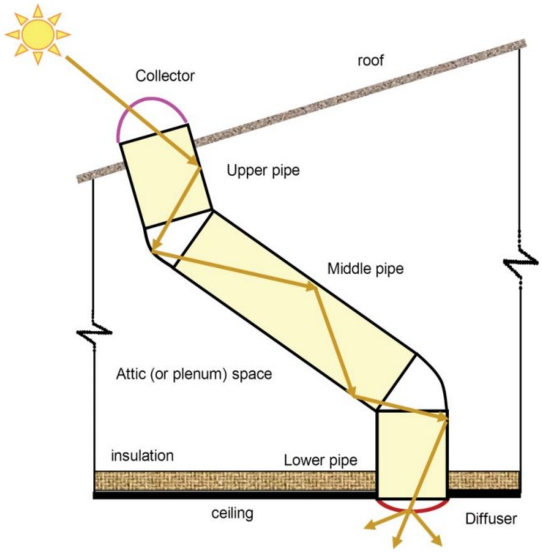

(13) Laouadi et al. [42]

Ontario, Canada — Humid continental

Figure 2.3 Toplighting systems by different researchers globally [26]

Table 2.2.1 Summary of Figure 2.3 [26]

Authors	Types	Designs	Conclusions
Lee et al. [30]	Skylight	The skylight design comprises three systems: skylight opening and light well, a reflector array, and a lower diffusing panel *Location: California, USA/North America—Hot and usually dry climate*	The design improves light redirection and achieves balance throughout a deep perimeter space by employing geometry and a special prismatic film to reflect direct sunlight throughout the year
Cabús and Pereira [31]	Skylight, monitor, and sawtooth roof	The study compared three toplighting methods. Sunlight and skylight, along with shading devices, were employed to create various models.	The study concluded that opening systems are able to capture and redistribute some direct sunlight and can produce well-lit spaces with minimum heat gain. Internal surface reflectance was found

		Location: Brazil/South America —Tropical hot and humid climate	to be important for work-plane illuminance
Kristl and Krainer [32]	Light wells	Three simple light wells (8 m height) were designed according to three types: individual, semi-individual (where the light well is divided into two individual light wells by a vertical reflecting wall), and combined (where all the apartments are illuminated by a common light well). *Location: Slovenia/EuropeHumid subtropical with continental climate*	The findings revealed that the optimum use of natural daylight is achieved by using semi-individual light wells with wide upper and narrow lower parts, into which the reflecting wall is placed. In this method, the topmost floors are lit mostly by direct light, whereas the ground and first floors are illuminated by both direct and reflected light from the inclined mirrored wall
McHugh et al. [33]	Splayed skylight wells	This study considered two parts of light wells: splay and throat. *Location: California USA/North America—Hot and dry climate*	The design allows daylight to spread as broadly as possible whilst reducing glare from overly bright surfaces
Beltran [34]	Skylights	This study examined the daylight performance of traditional and innovative toplighting systems: skylights with diffusing glazing, sawtooths, clerestories, roof monitors, skylights with splayed wells, and reflectors and	The findings indicated that skylights with reflectors provide the best overall daylight and thermal performance among all the systems. Skylights with reflectors provide uniform light all throughout the space (500 lux). Roof monitors

		diffusers beneath the aperture. All these designs involve high-performance glazing. *Location: Lima, Peru—Tropical climate*	introduce the most uniform and highest illuminance levels. Toplighting systems with sufficient solar control and proper use of reflective surfaces can deliver good daylight illumination and conserve energy.
Darula et al. [35]	Tubular light	Original tubular light guides with a transparent hemispherical cupola positioned on a roof gather all sunlight and skylight obtainable at ground level throughout a year. *Location: Australia/Australia—Desert climate*	The study found that the luminous effectiveness of tubular light guides in tropical regions is high because of long sunshine durations and dominant high solar altitudes. However, in areas with a temperate climate, these two features are poor, particularly during cold seasons.
Chel et al. [36]	Skylight	This study examined a mathematical system for an existing skylight combined with a dome-shaped indoor mud house to evaluate the daylight factor grounded on the alterations in the prototype presented by CIBSE. *Location: Delhi, India/AsiaHumid — subtropical climate*	The proposed prototype defines the daylight factor and indoor illuminance of a building with a skylight, which almost meet those in the investigational findings at various vertical levels of the work plane.
Kim and Chung [37]	Skylight: pyramid, monitor	Twenty scaled prototypes were constructed in this research to estimate the	Monitor toplight models were confirmed to be highly effective in cutting off direct

	and sawtooth	daylighting performance. A reflectance value of 70 % was applied for the light well and ceiling, 50 % for the walls, and 30 % for the floors. *Location: Seoul, South Korea/Asia—Humid subtropical and humid continental climate.*	sunlight. Sawtooth guarantees stable daylighting performance. These models were designated as attractive replacements for the current skylight system.
Yunus et al. [38]	Skylights	This study examined the effects of roof forms and internal structural obstructions on daylight levels in atria. Four types were tested in the analysis: structured flat roof, structured pyramidal gridded roof, structured north- and south-facing sawtooth roof, and structured north-east-sloping glazed pitched roof. *Location: Malaysia—Tropical hot and humid climate*	The inclined roof exhibits various patterns of daylight reduction levels. For high angles, complicated roof profiles, and east- and west-facing surfaces, the daylight level decreases to more than half of that in an unobstructed atrium. A west-facing atrium receives more light at all floor levels. During the brightest time of the day, daylight reduction by the structured sawtooth roof is lower than that by the others.
Acosta et al. [39]	Light-scoop skylights	Different types of light-scoop skylights were tested in different room sizes. A light-scoop skylight that is 6 m long and with variable heights of 3, 4.5, and 6 m	The study found that for this type of skylight, a height/width ratio of approximately 4:3 is the best model to ensure maximum daylight levels in a space under overcast sky conditions.

		was placed in the center of the roof. *Location: Madrid, Spain/Europe — Mediterranean climate*	
Yildirim et al. [40]	Roof skylight systems	Five roof skylight systems were considered. These five are single-layer one-way roof skylight system, single-layer double-way roof skylight system, sunshade with double layers, no sunshade with double layers, and moving-sunshade double-layered roof system. *Location: Ankara, Turkey/Asia — Continental climate*	The results revealed that light should be restricted to avoid glare. When sunlight is limited, light should be admitted at a higher rate. The double-layered roof system, which delivers uniform and sustainable lighting in all conditions, demonstrates the best performance compared with the other four roof skylight systems.
Ghobad et al. [41]	Light well	This paper focused on four light wells and ceiling geometries. The glazing area, expressed as the skylight to floor area ratio (SFR), was 5, 6, 7, and 8 %. The transmissivity of the glazing was 40 and 54 %. *Location: Boston, MA/North America—Continental climate*	The study showed that a splayed ceiling integrated with a duct in the structural volume reduces building costs, allows the roof to be lowered, and decreases unwanted thermal gains. The quantity of useful illuminance on the task surface is improved, the variations in illuminance on the task surface are reduced, and the potential light is boosted.

Laouadi et al. [42]	Tubular daylighting devices	The study assumed that tubular daylighting devices transmit sunbeam light, skylight, and surrounding reflected diffuse light. The transmitted and absorbed luminous fluxes rely on device geometry structure and diffuse light intensities. *Location: Ontario, Canada — Humid continental*	The study concluded that the devices include three various units (upper, middle, lower), with elbows joining them at the roof and ceiling levels. The device collectors may take a conical or hemispheric shape or a combination of both. Collector glazing may comprise diffusing elements, reflectors, prisms, or multi-panes distributed along the glazing surface. The ceiling diffusers may be hemispheric or planar and could have multiple prismatic or diffusing.

2.3. Computational approach in design

2.3.1. Generative and Parametric Architecture

Parametric design has revolutionized architectural practice, allowing architects to explore a wide range of design possibilities through computational methods. Parametric design is a process based on algorithmic thinking that enables the expression of design intent through the relationships between elements. By defining these relationships, parameters can be manipulated to alter the outcome, enabling a dynamic and flexible approach to design. This method leverages software to handle complex computations and generate numerous design iterations quickly, facilitating optimization and innovation.

The roots of parametric design can be traced back to the early 20th century with the advent of digital computing and computer-aided design (CAD). Computer-Aided Design (CAD) made its debut in the architectural field in the early 1970s. The phrases "From Simple to Complex" and "From Form to Code" aptly describe the evolution of modern architecture. The advent of computers has ushered in a paradigm shift from traditional to parametric design. This advancement has revolutionized the workflow for static graphic primitives into a highly controlled process. In the digital era, it is essential to apply a standard approach to design. To achieve the high standards expected in design and to address performance and efficiency concerns, harnessing the immense potential of digital systems is essential.

However, it wasn't until the 1980s and 1990s that parametric design began to gain traction, largely due to advancements in software capabilities and the increasing power of personal computers.

Key milestones in the development of parametric design include early digital design explorations in the 1960s and 1970s using mainframe computers and early CAD systems. The 1980s and 1990s saw the advancement of software, with the development of sophisticated tools like AutoCAD and later Rhino, enabling more complex and precise modeling. From the 2000s to the present, the introduction of scripting and visual programming languages, such as Grasshopper for Rhino, has made parametric design more accessible and powerful.

Coined as "parametricism" by Patrik Schumacher, a partner at Zaha Hadid, this architectural style rebels against traditional design processes, focusing on free-form architectural concepts. According to Schumacher, "Parametric problems can only be resolved with advanced parametric technology"[43]. The parametric method [44–47] offers a multitude of design alternatives that are unattainable with traditional methods. Beyond creating alternative designs based on specific rules, parametric design can also solve complex design challenges that would be too time-consuming for an architect to handle alone. This style is characterized by irregular shapes, curves, lines, and geometry. It is defined by four main characteristics: combining complexity and variety, rejecting the uniformity of utilitarianism, prioritizing shared aspects of urbanism, interior design, architectural marvels, and even fashion, and emphasizing the interdependence and flexibility of all design elements. Additionally, there is a preference for algorithmic, computer-aided design [48].

Parametric design involves creating building parts and technical components based on computational methods, unlike conventional design processes that shape these elements physically. In this approach, the relationship between design intent and design response is governed by criteria and regulations. The term "parametric" refers to the input variables or parameters fed into the algorithms. In Woodbury's 2006 article "Parametric Modelling as a Design Representation in Architecture: A Process Account," a propagation-based system is described. Here, algorithms produce unknown final shapes based on previous parametric inputs through a dataflow model and constraint scheme, where final constraints are determined and algorithms define the foundations (structures, material use, etc.) to meet these constraints. This process is referred to as "form-finding," where the design object is "found" within a propagation-based system [49]. Most parametric designs are displayed in 3D interactive views, with graph nodes representing instances of the nodes associated with the current configuration of the graph's independent variables. The display algorithm depends on the node type: point nodes are displayed as points, line nodes as lines, etc. [50].

Computer-Aided Manufacturing (CAM) has also emerged alongside the advancements in computerization. This marks a significant improvement in production techniques, focusing on bridging the gap in architectural details. CAM facilitates the control and modification of interactions between the virtual design process and actual manufacturing. Data generated during the virtual design phase can be used as primary input for the manufacturing process. In other words, the management of globally integrated processes in architecture has become more precise and detailed. Parametric tools allow for the creation of complex forms and structures that would be challenging or impossible with traditional methods. These include organic shapes, intricate facades, and innovative structural systems. By manipulating parameters, architects can optimize designs for various performance criteria, such as energy efficiency, structural integrity, and material usage. Parametric design allows for easy customization of building components to fit specific site conditions, client requirements, and aesthetic preferences. Using parametric models enhances communication and collaboration among different disciplines involved in the design and construction process, such as engineers, fabricators, and contractors.

Complex computations can be managed with a high degree of flexibility thanks to the control provided by parameters, potentially leading to unexpected or unpredictable outcomes. Additionally, this flexibility opens up possibilities for generating a vast number of design variations, enhancing the freedom in shape creation [51]. The main difference between classical design and generative algorithm design lies in the initial phase of the design process. Figure 2.4 [52] illustrates the comparison between the classical design process and parametric or generative algorithm design processes. Classical design typically has fixed design variables that can be manually explored within the designer's visual imagination. The process starts with a concept and is iteratively examined to improve efficiency. If the initial review results do not meet the desired design goals, further evaluations are conducted. If the second design iteration also fails to meet the criteria, the process is repeated. This cycle continues until the objectives are achieved and the desired performance is obtained.

In contrast, generative algorithm procedures use a top-down approach. Unlike traditional design, which places the goals at the end of the process, generative algorithms set the goals at the beginning. Once the objectives are defined, the next step is to establish dynamic design variables as parameters. The entire system functions like a series of calculators with various functions or source code. This source code is used to determine the design variables that lead to the optimal design solution.

Parametric design represents a significant shift in architectural practice, offering unprecedented control and creativity. Its ability to handle complex geometries and optimize various aspects of building performance makes it an indispensable tool in modern architecture. As computational tools continue to evolve, the potential applications and benefits of parametric design are likely to expand, further transforming the landscape of architectural design.

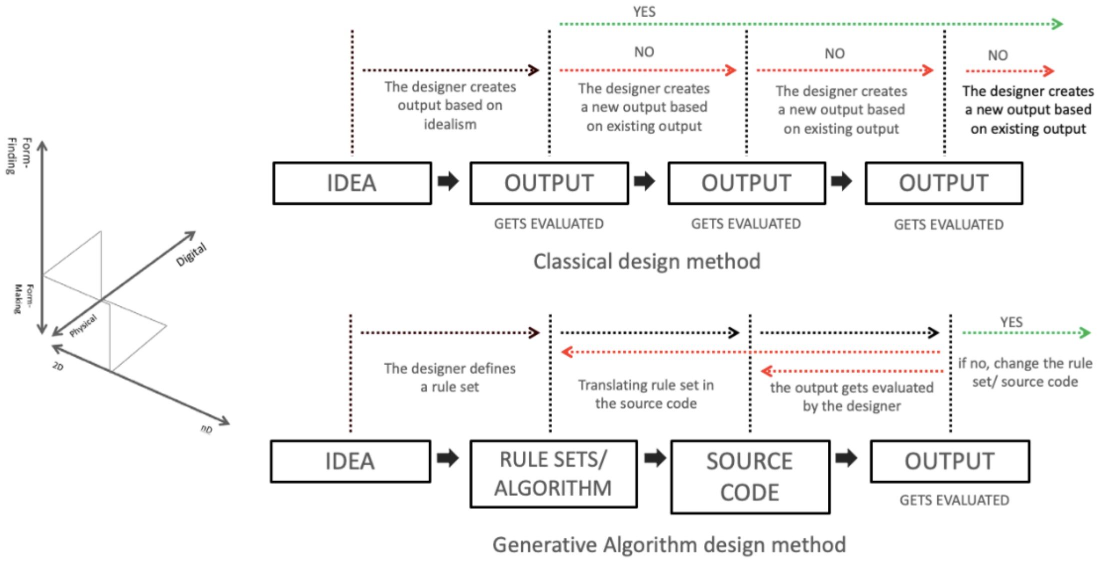

Figure 2.4 Classical design and Genetic Algorithm design processes [52]

2.3.2. Evolutionary computation and MOO

The evolutionary design method and evolutionary optimization draw inspiration from nature, natural processes, and the creativity observed in biological artifacts, all resulting from the highly creative process known as evolution. In computational terms, these processes emulate evolution to integrate creative processes into design thinking and computation, fostering innovative new design methods. Evolutionary computation combines principles from evolutionary biology and computer science [53]. In this genetic system, the concept of "survival of the fittest" enables the reproduction and growth of successive generations, thereby preserving genetic information. For example, in our bodies, gene chromosomes that survived and evolved over long periods encode basic life information, which is replicated in algorithms. This type of search process requires defining intentions or objectives, with the algorithm assisting in finding the optimal design.

On the other hand, multi-objective optimization involves using multiple phenotypes or parameters and multiple genomes or objectives in the search process. This framework comprises parametric model-based form generation, numerical assessment, simulation-based performance evaluation, and multi-objective optimization (MOO). These three elements iterate to generate and evaluate numerous design options. Several designers and researchers use similar methods to support integrated design [54]. In this process, parametric modeling facilitates the association of building elements and the generation of multiple design options while maintaining predefined geometric relationships. Simulations evaluate various facets of these design alternatives. Among the design options included in the optimization process, those with superior performance are identified based on specific evaluation criteria related to the design specifications [55].

The optimization processes and systems used in this research apply the Pareto front principle. The Pareto front, widely accepted and also known as the Pareto frontier or Pareto set, comprises all efficient options generated from multi-objective optimization. This enables observers to focus on efficient options and make trade-offs within this set, rather than examining the entire range of every parameter [56].

2.4. Research on parametric and MOO shading, geometry

Many researchers have been integrating shading and glazing strategies, utilizing parametric computational approaches, and employing Genetic Algorithm (GA) optimization to enhance efficiency and optimization for daylight and visual comfort. Some of these studies have also addressed energy consumption efficiency.

Khidmat et al. [57] employed a parametric and multi-objective optimization approach to investigate the daylight performance of expanded-metal shading in Kitakyushu, Japan. Through computational simulations and optimization analysis, they concluded that the proposed framework successfully met the daylight requirements of LEED v4.1. The framework achieved a 100% reduction in Annual Sunlight Exposure (ASE) and approximately a 50% improvement in Useful Daylight Illuminance (UDI) compared to the baseline model.

Zahra Shirzadnia et al. [58] successfully improved the daylight performance of an old boiler building in a historical factory in Mazandaran, Iran, by employing parametric modeling and optimization algorithms. They achieved a significant reduction of 63.43% in the DA (Daylight Autonomy) metric. Their research provides comprehensive design guidelines for the adaptive reuse of heritage buildings in a humid subtropical climate.

Yi et al. [59] proposed a method that integrates multiple performance criteria into Multi-Objective Optimization (MOO). The aim was to maximize daylighting, maximize structural strength, minimize system weight, and reduce overall material cost. This approach allows for optimized solutions that satisfy requirements across multiple building performance areas, rather than being limited to a specific domain.

Eltaweel et al. [15,60,61] explored advanced louver slats and Venetian blinds to predict natural daylight intensity distribution in a simulated office room in Cairo and New Cairo, Egypt, aiming for a steady daylight illuminance range of 300 lux to 500 lux at 90%. The research found that the proposed parametric control system for the slats and blinds could optimize daylight performance effectively. Fang et al. [62] assessed the daylight and energy performance of a simulated office space in Miami, Atlanta, and Chicago using a parametric framework. By iterating building depth, roof ridge position, skylight dimensions, window dimensions, and louver lengths, the study optimized for UDI and EUI, demonstrating that skylight dimensions were particularly significant.

Gerber et al. [63] introduced a multi-agent system (MAS) in architectural design to help designers explore a wide range of informed solutions by combining generative algorithms and user light preferences. This research concluded that MAS could produce unique design configurations that perform better environmentally than standard façade shading. Grobman et al. [64] compared static and kinetic shading strategies for daylight performance in a Mediterranean climate, showing that dynamic strategies improved the Adjusted Useful Daylight Illuminance (AUDI) by 51%, achieving optimal daylight values of 250 lux.

Bakmohammadi et al. [65] introduced a parametric and optimization platform to determine the best classroom layout and glazing strategy for the climate conditions in Tehran, Iran. Using Grasshopper as the main parametric platform, and Ladybug and Honeybee as environmental analysis engines for daylight and energy simulation, the study iterated parameters such as window-to-wall ratio, glazing number, wall angle, and building rotation. This research identified the best layout solution and demonstrated a potential reduction of 47.92 kWh/m² in energy consumption.

Kim and Clayton [16,66] introduced parametric behavior maps (PBMs) to evaluate the energy performance of climate-adaptive building envelopes (CABEs), enabling designers to conduct building energy and daylight simulations and analyses. Applying origami-like shading in a small office in Houston, Texas, the study found that both dynamic and static shading methods contributed to optimal CABE performance. The proposed system supported architects and designers in the decision-making process through well-informed dynamic scenarios.

Cachat et al. [67–69] combined computational simulation, optimization, and field measurements to investigate the impact of PV integrated shading devices on daylighting and energy strategies for Norway's Nordic climate. The research found that smaller shading devices performed better and suggested the potential for reducing energy consumption by up to 47.92 kWh/m². Elbeltagi et al. [70] used a parametric approach to visualize and predict energy consumption for a simulated residential building in Cairo, Egypt. The study concluded that this visualization could significantly aid designers in analyzing energy consumption data and provide more accurate energy predictions.

Chapter 3. Methodology

3.1. **Software**

Figure 3.1 illustrates the software used in this study and their respective purposes. The primary work is conducted on Rhino, with foundational modeling completed using the Grasshopper platform within Rhino. Ladybug and Honeybee are then employed for solar and energy analysis. The Octopus plugin is used to perform multiple simulations and genetic iterations. Data generated in Rhino is exported to Excel via the Colibri plugin. Subsequently, the data is transferred from Excel to Origin and IBM SPSS for visualization and analysis.

3.1.1. Rhinoceros 3D

Rhinoceros, commonly known as Rhino, is a 3D computer graphics and computer-aided design (CAD) software developed by Robert McNeel & Associates. Rhino excels in creating complex and precise models due to its NURBS-based modeling system, which allows for the creation of accurate and detailed surfaces. Rhino is a commercial software, but it offers a free trial version. It is widely used in architecture, industrial design, and marine design due to its versatility and powerful modeling capabilities.

3.1.2. Grasshopper for Rhino

Grasshopper is a visual programming language and environment that operates within Rhino. Developed by Robert McNeel & Associates, it enables users to create complex parametric designs through an intuitive graphical interface. Grasshopper is included with Rhino and provides powerful tools for algorithmic and generative design, making it indispensable for architects and designers. It allows for the manipulation of geometric data and the creation of intricate design patterns and structures, facilitating a high degree of creativity and customization.

3.1.3. Ladybug & Honeybee

Ladybug Tools, including Ladybug and Honeybee, are free and open-source applications that support environmental design and sustainability in architecture. Developed by Chris Mackey and Mostapha Sadeghipour Roudsari, these tools integrate with Rhino and Grasshopper to offer comprehensive climate analysis, daylighting, and energy modeling capabilities. Ladybug is used for climate analysis and visualization, while Honeybee connects with simulation engines like EnergyPlus and Radiance for detailed energy and daylighting simulations. Together, they help architects and engineers make informed decisions about building performance and environmental impact.

3.1.4. Octopus

Octopus is a plugin for Grasshopper designed to facilitate multi-objective optimization using evolutionary algorithms. Developed by Robert Vierlinger, Octopus allows for the optimization of complex design problems based on multiple criteria. It is an open-source tool that helps designers explore a wide range of design solutions, balancing various performance aspects such as energy efficiency, structural integrity, and visual comfort. Octopus is particularly useful for iterative design processes where multiple objectives must be considered simultaneously.

3.1.5. Colibri

Colibri is part of the TT Toolbox developed by Thornton Tomasetti. It works within the Grasshopper environment to streamline the generation and evaluation of multiple design iterations. Colibri is free to use and aids in managing large sets of design options, making it easier to compare and optimize design solutions. It is particularly useful in parametric studies and design explorations where numerous variations need to be analyzed and evaluated efficiently.

3.1.6. Excel

Microsoft Excel is a spreadsheet software developed by Microsoft. It is a part of the Microsoft Office suite and is available both as a standalone product and as part of Office subscriptions. Excel is widely used for data analysis, financial modeling, and statistical analysis. It offers a wide range of functionalities, including pivot tables, graphing tools, and the use of formulas and functions to perform complex calculations. Excel supports VBA (Visual Basic for Applications) scripting, allowing users to automate repetitive tasks and create custom functions. While Excel is a commercial software, it is available on a subscription basis through Microsoft 365, and there are also free versions with limited functionality available online.

3.1.7. Origin

Origin is a proprietary data analysis and graphing software developed by OriginLab Corporation. It is widely used in scientific research, engineering, and data analysis fields for its robust tools for data visualization and analysis. Origin allows users to create publication-quality graphs and perform complex statistical analyses. It is commercial software, known for its user-friendly interface and powerful analytical capabilities, making it a popular choice among researchers and engineers.

3.1.8. IBM SPSS

IBM SPSS (Statistical Package for the Social Sciences) is a comprehensive software package used for statistical analysis. Originally developed by SPSS Inc. and later acquired by IBM, SPSS offers extensive tools for data management, statistical analysis, and reporting. It is commercial software widely used in social sciences, business, and health sciences for its ease of use and powerful statistical functions. SPSS is essential for conducting sophisticated data analyses and generating detailed reports, making it a staple in many research and business environments.

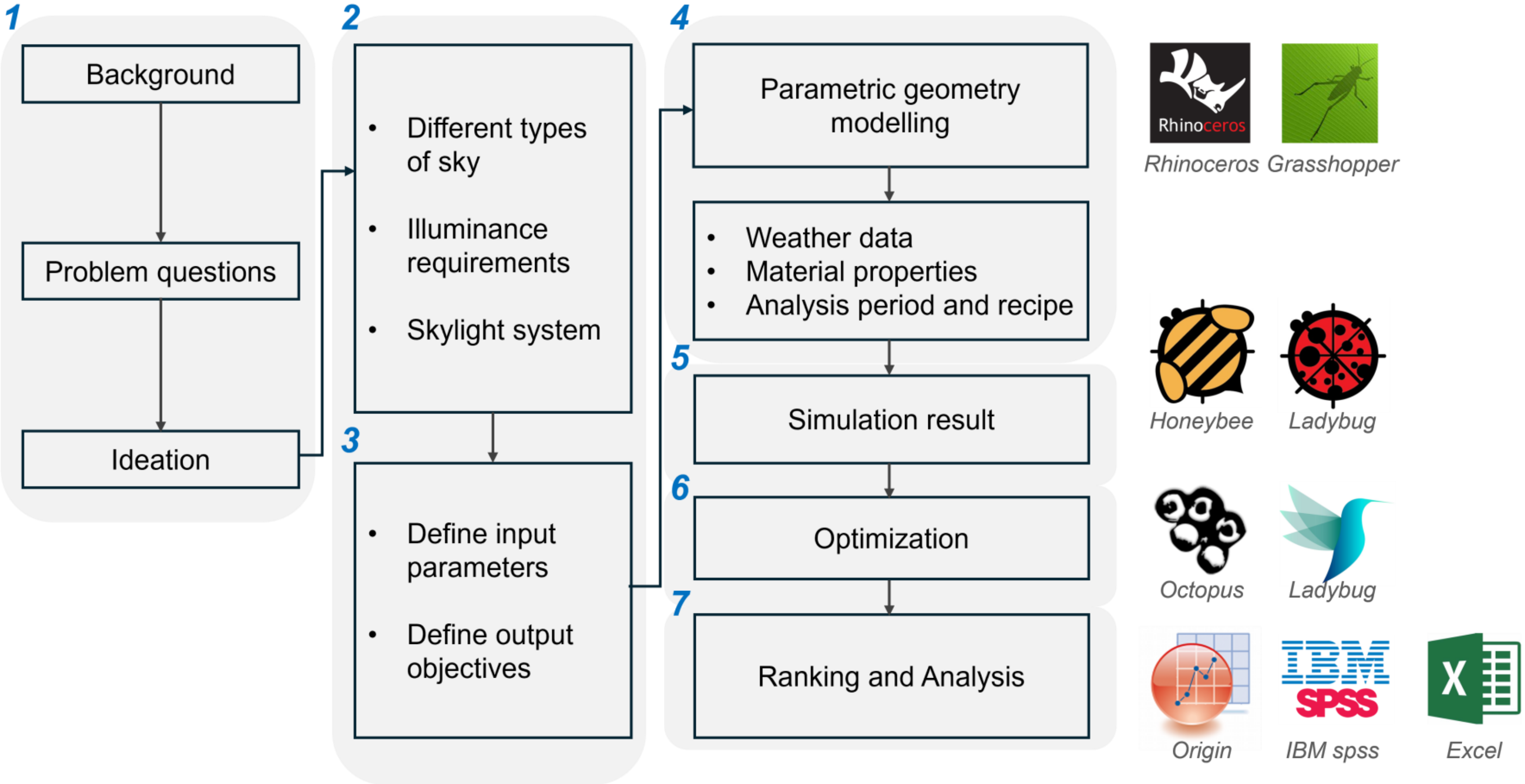

Figure 3.1 Tools used in this thesis

3.2. **Parametric definition arrangement**

This chapter explains the general overview of the methodology used in this thesis, which will be implemented in more detail in the dedicated chapters according to each specific case. Based on the pragmatism research philosophy, where knowledge is constantly questioned and interpreted rather than fixed, this process is classified as a computer simulation research methodology, specifically using parametric [50] and generative algorithm [44] deductive or quantitative approaches. This is due to the fact that the experiment involves a large number of calculations and design configurations that are only possible in the virtual world rather than in real measurements because of the high cost and time consumption.

The process begins with the ideation phase, which aims to respond to the issues raised in a specific context and answer the research question. The first phase is ideation, where the problem is formulated. In this phase, the information and background behind each experiment are collected. The ideation phase aims to respond to the research goals and answer the questions in the first step of the scenario. The ideation process leads to the production of the experimental scheme or experimental design. The ideation process concludes with the decision on what type of simulation to arrange and which parameters and design goals to use.

Following the ideation process, the next phase is the process of defining the design parameters and performance objectives of each research idea. Each process starts by precisely defining the design parameters and design goals along with their metrics. After the parameters and objectives are decided, the next step is arranging the parametric geometry modeling. In this phase, the layout and dynamic parameters are first established on the parametric platform.

3.2.1. Environmental simulations

A weather file contains detailed climate data for a specific location, including temperature, humidity, solar radiation, wind speed, and direction. These files are essential for accurate environmental simulations in building design, particularly for daylight and energy analysis. By using weather files, architects and engineers can simulate how a building will perform under realistic climatic conditions throughout the year. Weather files provide the necessary climate data to conduct accurate simulations for daylighting, energy consumption, and thermal comfort. These simulations help in predicting building performance, optimizing design for energy efficiency, and ensuring occupant comfort. Without weather files, simulations would lack the context of real-world environmental conditions, leading to inaccurate results.

EnergyPlus Weather (EPW) files are standardized weather files used with the EnergyPlus simulation engine. Developed by the U.S. Department of Energy, these files contain hourly weather data for various global locations. EPW files are widely used in building performance simulations due to their comprehensive data and compatibility with various simulation tools. To use an EPW file, it is typically imported into the simulation software, where it provides the necessary climatic inputs for analysis.

When conducting environmental simulations, the selected weather file is imported into the simulation software, such as Rhino with Grasshopper, Ladybug, and Honeybee. The software then uses this data to simulate daylight, energy usage, and thermal conditions throughout the year. This process helps in optimizing the building design by evaluating different scenarios and making data-driven decisions to improve energy efficiency and occupant comfort.

3.2.2. Computational exploration and optimization

From Figure 3.1, it can be seen that in phase 5, automation generates single design solutions for each parameter change, along with embedded parameter combinations and design objective values. Each single value produced by each experiment generally becomes a data point or individual in the optimization process in phase 6. In phase 6, iterations use two different systems: exploration and genetic optimization. The first is a genetic algorithm for multi-objective optimization (MOO) using Octopus, and the second is design exploration using Colibri. In phases 6 and 7, statistical analysis and manual observation are conducted to identify the best solutions from the filtering process. The final results produced in the last phase will be compared with the research objectives and research questions.

3.3. Data collection and analysis method

3.3.1. Observation of the best design solutions

The environmental and structural simulation parameters and data inputs are processed on a parametric platform, producing a series of rough numerical data. Each experiment generates a series of numbers, recorded during the optimization and exploration processes into Excel or comma-separated values files. Initial visualizations in the software yield various plots. Data from Octopus appears in 3D population fields, while exploration data may form parallel coordinate plots. These rough data files are further processed, visualized, and analyzed manually and statistically to examine parameter relationships and the roles of each parameter.

To find the best design solution through iterative processes, observations are conducted in multiple ways. The first method involves manual observation during optimization and exploration. For multi-objective optimization results, Octopus's reinstate solution function is used, while Colibri allows manual observation by highlighting desired objective value wires.

3.3.2. Solution ranking by fitness function

After observing the data, rank the Pareto front solutions using the fitness function with MOO and Colibri. A "fitness function" is a function used in genetic algorithms and other evolutionary algorithms to evaluate and measure the quality of individual solutions, as applied in previous studies [14,71,72], calculated in Excel and implemented in Chapters 5 and 6.

In optimization problems, the fitness function calculates a fitness value for each candidate solution, reflecting how well it meets the problem's requirements. Based on the fitness values, the algorithm decides which individuals can be carried over to the next generation, and it selects, crosses, and mutates them to gradually approach the optimal solution.

Key features of a fitness function include:

- Evaluation Criteria: The fitness function defines the criteria for evaluating individual solutions, which can be a single objective function or multiple objective functions.
- Numerical Representation: Fitness values are usually represented numerically; the higher (or lower, depending on the optimization goal) the value, the better the quality of the solution.
- Selection Basis: Genetic algorithms select superior individuals based on fitness values for reproduction and eliminate inferior ones.
- Evolutionary Drive: Through multiple generations of iteration, the fitness function drives the population to gradually evolve towards the optimal solution.

In different optimization problems, the specific form and calculation method of the fitness function vary, depending on the nature of the problem and the optimization goals. Each case's formulation is tailored to its specific data, parameter conditions, and design objectives.

The main difference between manual observation and fitness function calculation lies in the ranking process, where desired solutions are objectively presented in series. Manual observation relies on human visual assessment, while fitness function results are quantitatively generated, allowing for objective observation and justification through numerical values.

3.3.3. Sensitivity analysis

To identify the most influential parameter driving the design objectives, sensitivity analysis is performed. Knowing which parameters have the greatest impact allows designers to focus on these parameters to achieve more optimized design objectives.

The sensitivity analysis uses Standardized Regression Coefficients (SRC) to measure t-tests, examining the role of each parameter on objective values and evaluating variable relevance. This analysis is conducted using SPSS software, employing the fit-model command to estimate parameters, with standardized objectives as role variables and standardized parameters as construct model effects.

Results are presented in tornado plots, displaying SRC values along a horizontal axis to indicate positive or negative impacts. Each bar represents the influence of a parameter on the objective. This method provides a deeper understanding of parameter-objective correlations, allowing for more detailed identification and focus.

3.3.4. Tendency observation

Tendency observation is used to understand the relationship between design parameters and objectives within the context of multi-objective optimization (MOO). This type of observation helps designers identify parameter ranges that lead to desired objective values. It involves manually adjusting a parallel coordinate plot filled with lines connecting parameter and objective combinations, as seen in previous studies [73–76].

The parallel coordinate plot is generated using Origin. The data, derived from the optimization process, is distributed based on the maximum and minimum values of each parameter and objective axis. Manual observation focuses on the density of these lines, showing the distribution of solutions. By adjusting control points on the vertical axes of the plots, designers can isolate dense areas, allowing for analysis of tendencies within these regions.

Chapter 4. Preliminary Study

4.1. Some basic concepts of daylight

Daylight can be classified into two categories: direct and indirect. Direct daylight includes light from the diffuse skylight in the Earth's atmosphere and direct sunlight. Indirect daylight comes from light reflected off surfaces, such as pavement or walls facing windows.

4.1.1. Reflectance and transmittance

When light encounters a surface, it can be reflected, transmitted, or absorbed. The reflectance factor, which ranges from 0 to 1, represents the "ratio of reflected flux to incident flux" and determines the proportion of light that is reflected. Transmittance quantifies the fraction of light passing through a surface, while absorbance measures how much light is absorbed and converted to heat.

All surfaces reflect some amount of light. For instance, a white surface has a reflectance factor of 0.85, whereas a black surface has a value of 0.5. This factor indicates the amount of light reflected but does not specify how it is reflected. The surface characteristics determine the reflection type: smooth, polished surfaces create specular reflections, while matte surfaces scatter light, resulting in diffuse reflections. Choosing surfaces with high reflectance and low specular values (to reduce glare) will aid in directing light deep into the building. Furthermore, the quantity of light in these adjacent areas depends on the percentage of light transmitted through the glazing [8,77].

4.1.2. Illuminance and luminance

The overall light output from a source is referred to as luminous flux and is measured in lumens (lm). The strength of the light emitted in a specific direction, known as luminous intensity, is measured in candela (cd). When this intensity is measured over a surface, it is called illuminance, which indicates the amount of light energy at a specific point on a defined surface area and is measured in lux.

Illuminance represents light traveling through space and is not visible to the naked eye unless it hits a surface or is viewed directly at the source. The portion of light that is visible on a surface is termed luminance, defined as "the amount of visible light leaving a point on a surface in a particular direction," and is measured in cd/m^2. Thus, luminance indicates the perceived brightness by an observer, while illuminance signifies the presence of light in a given space [8,77,78].

4.1.3. Qualitative and quantitative aspects of daylight

A successful daylighting strategy should prioritize both the quality and quantity of light in a space [79]. Metrics like illuminance, daylight factor, and various daylight autonomy hybrids measure daylight quantity, while qualitative metrics define the luminous environment, shaping how we perceive light in a space. Factors such as color, contrast, and light temperature, as well as uniformity, significantly impact occupant comfort in daylit spaces.

Calleja et al.'s (2011) paper [80], "Conditions Required for Visual Comfort," discusses various aspects of the luminous environment. One key factor is the color of light, which significantly influences how people experience light in a space. The color and temperature of light should be maintained at comfortable levels to avoid eye strain for occupants performing tasks. The paper highlights that the color appearance of illumination depends on both light color and luminous intensity. A diagram in the paper shows a relationship between visual comfort and different levels of illumination and color temperature, with comfortable levels typically above 4000 kelvin (K), known as neutral white, and around 6000 K, known as daylight white.

Light contrast within a room is also crucial, representing the ratio of background light (ambient light) to foreground light (task light). Good quality contrast is achieved when ambient light levels are between one-half and two-thirds of task light. Mathematically, contrast is the difference between maximum and minimum luminance divided by the lower value [78].

Maintaining light uniformity is equally important. Uniformity is the ratio between minimum and average illuminance over a horizontal working plane. Good uniformity involves reducing high-intensity daylight zones and preventing dark zones, especially at the back of a room. High-intensity zones, whether on the workplane, floor, walls, or ceiling, can cause discomfort, known as glare [81]. Glare is defined as a condition where vision discomfort or reduced ability to see details is caused by an unsuitable distribution or range of luminance or extreme contrasts. Properly implemented shading devices can control glare, ensuring they do not create light patches over the workplane that could irritate occupants.

4.2. Different types of sky

4.2.1. The Impact of Different Weather Conditions on Sky and Indoor Illuminance

Understanding the different types of sky conditions is crucial for accurate daylight simulation in architectural design. Sky conditions such as clear (sunny), overcast (cloudy), and partly cloudy have significant impacts on both indoor lighting and the overall brightness of the sky.

Clear skies provide direct sunlight, resulting in strong illumination and sharp shadows. This condition enhances visibility but can cause glare and increase cooling loads due to higher thermal gains. The brightness is highest near the sun and decreases with distance. The sky's luminance is anisotropic, meaning it varies with direction. For instance, under a clear sky, the sun can produce illuminance levels up to 100,000 lux, making it essential to incorporate shading devices in architectural design to control glare and excessive light.

Overcast conditions diffuse sunlight evenly, providing uniform but lower light levels. This minimizes glare and shadows, creating a softer, more even illumination which is beneficial for visual comfort. Brightness is more uniform, with the highest luminance at the zenith (directly overhead) and decreasing towards the horizon. Typically, under overcast skies, the illuminance levels are around 5,000 to 20,000 lux. The uniform light distribution is ideal for spaces requiring consistent lighting without the harsh contrasts produced by direct sunlight.

Partly cloudy skies offer a mix of direct sunlight and diffuse light. This creates varying light intensities and can result in fluctuating indoor illumination levels throughout the day. Brightness levels fluctuate depending on cloud cover, with varying patterns of luminance due to the mix of direct and diffused sunlight. On partly cloudy days, illuminance can vary widely, from 10,000 lux to over 70,000 lux, depending on cloud density and the position of the sun. This variability can pose challenges for maintaining consistent indoor lighting conditions, necessitating adaptive lighting solutions.

Accurate simulation of these sky conditions is essential for designing energy-efficient buildings that optimize natural light use while ensuring occupant comfort. By understanding how different sky conditions affect light distribution, architects can better plan window placements, shading devices, and interior layouts to enhance natural lighting, reduce energy consumption, and improve the overall indoor environment.

4.2.2. Comparison of Sky Brightness Variations

In the realm of architectural design and environmental studies, understanding the dynamics of natural light is crucial.

Figure 4.1 offers a practical example of how different weather conditions and times of day can affect the distribution and intensity of natural light. The use of panoramic photography allows for a comprehensive view of the sky, capturing the subtle variations in light that occur due to the sun's position and cloud cover.

In the first image, taken during the late afternoon, the brightness gradient is pronounced. The area around the sun is significantly brighter, while the zenith and eastern horizon are dimmer. This indicates the angle of the sun and its lower position in the sky as it approaches sunset. The higher brightness near the sun can lead to increased glare, which is a critical factor to consider in museum design to protect exhibits and ensure visitor comfort.

The second image, taken around midday, shows the sun at its highest point, resulting in the brightest sky near the sun with a gradual decrease in brightness towards the zenith and horizon. This image highlights the need for effective shading solutions to mitigate the intense midday sun, which can cause overheating and excessive illumination inside buildings.

The third image, captured on an overcast day, presents a more uniform distribution of light. The cloud cover diffuses the sunlight, reducing the intensity and creating a softer light environment. This uniformity is beneficial in reducing glare and creating a more stable lighting condition, which is particularly advantageous in settings like museums and libraries where consistent lighting is essential for both preservation and usability.

By employing panoramic photography, this study offers a visual and analytical tool to better understand the behavior of natural light under different conditions. These insights are invaluable for architects and designers aiming to optimize natural light use in buildings, enhancing both energy efficiency and occupant comfort. This method allows for a detailed examination of how light interacts with different architectural elements and environmental conditions, paving the way for more informed design decisions.

East

West

Weather: Clear day Location: Nagasaki Time: 17:36

East

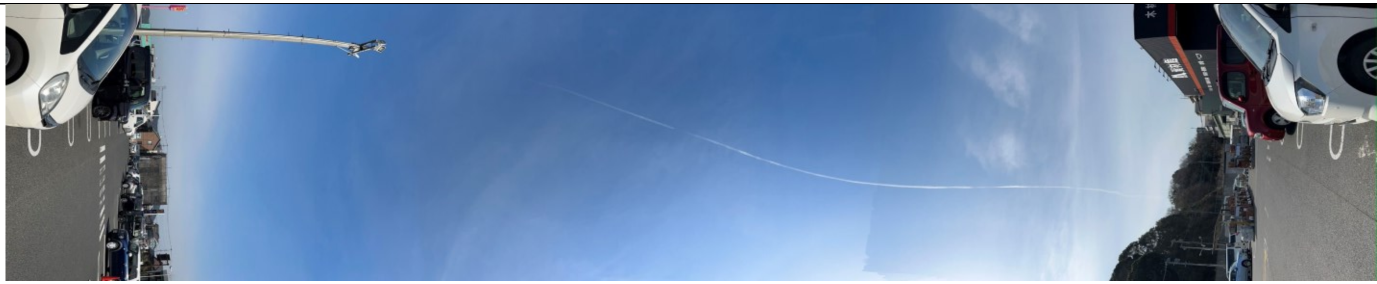

West

Weather: Clear day Location: Kitakyushu Time: 12:54

East

West

Weather: Overcast day Location: Kitakyushu Time: 15:48

Figure 4.1 Different types of skies

4.2.3. CIE Standard Sky

Natural light entering a building comes from three main sources: direct sunlight from the sun, diffused daylight from the Earth's atmosphere, and light reflected off the ground or other surfaces (also referred to as daylight). It is a common misconception that sunlight and skylight are interchangeable terms, but they are distinct due to their unique physical properties and varying impacts on skylight roofing systems. These differences manifest in intensity, diffusion (scatter), and color. When evaluating these types, it is crucial to consider two factors: luminance and illuminance.

Sky luminance fluctuates based on weather conditions, seasons, and time of day, making it challenging to standardize. However, the CIE provided a calculated method (International Recommendations for the Calculation of Natural Daylight, 1970) [82] using a set of curves to determine the periods during which daylight can meet a building's lighting needs as shown in Figure 4.2. This method estimates the percentage of necessary exterior illumination on a horizontal plane approximately from 07:00 to 17:00 hours at various latitudes. It should be noted that this method does not account for specific site conditions, such as shading by hills, trees, buildings, neighboring surfaces, or the building's design itself. [82]

The Commission Internationale de l'Eclairage (CIE), or the International Commission on Illumination, is a professional organization dedicated to worldwide cooperation and information exchange in all fields related to light and lighting, color and vision, photobiology, and image technology. Established in 1913, the CIE is the globally recognized authority on light and lighting, known for its scientific contributions and standards.

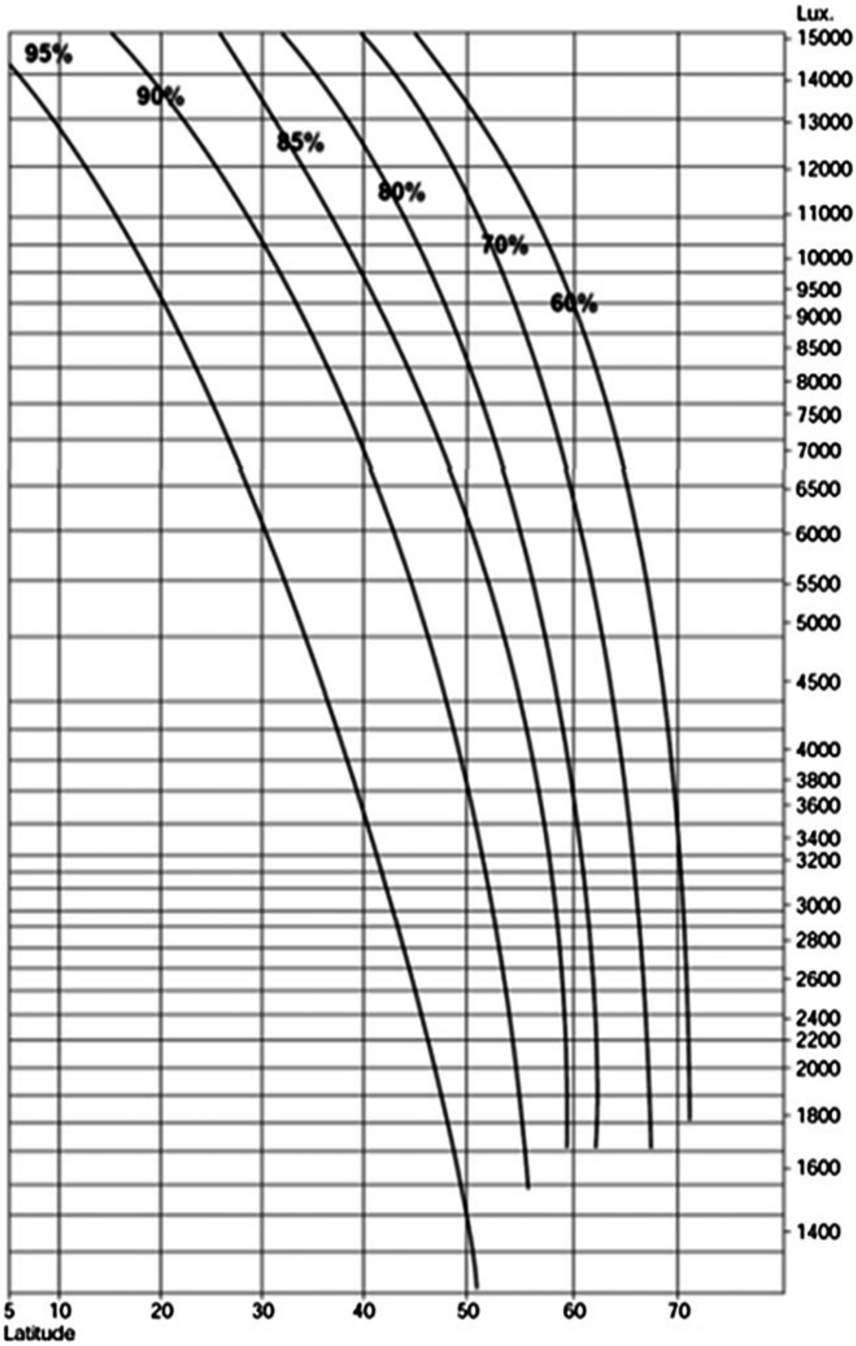

Figure 4.2 CIE calculation method that employs a set of curves to identify the amount of lux in a time period. [26]

CIE sky models are widely applied in various fields. In daylighting analysis, they evaluate how natural light enters and illuminates interior spaces. For energy efficiency studies, they assess the impact of daylighting on building energy consumption. Visual comfort assessments use these models to understand the effects of lighting conditions on occupant comfort and performance. In architectural design, CIE sky models guide the placement and sizing of windows, skylights, and other daylighting elements to optimize natural light use.

The CIE has successfully developed model skies that serve as valuable tools for anyone working with daylighting. These models can be broadly categorized into four types: Clear Sky, Intermediate Sky, Overcast Sky, and Uniform Sky. Figure 4.3 reflects examples of these four CIE standardized generic sky types. The primary simulations conducted in this thesis encompassed a diverse array of sky conditions based on the annual weather profile of the selected location, with the exception of the static simulations, which utilized the CIE standard overcast sky. To provide an understanding of the variations between different sky types, a brief overview of the main sky models is presented:

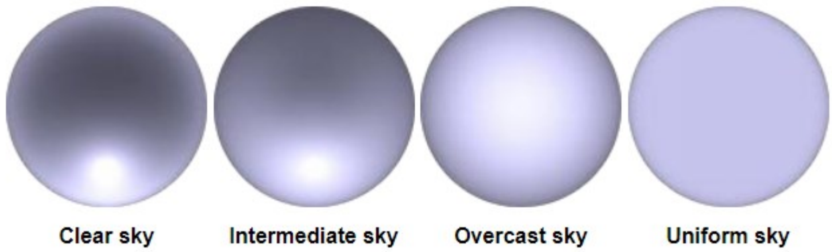

Figure 4.3 Examples of the 4 CIE standard general sky types

Clear sky
A clear sky is characterized by 0–30% cloud cover. It typically has higher radiation levels and brightness compared to other sky types, resulting in more pronounced shadows. The sky's luminance is highest near the sun, and at the horizon, it is approximately three times brighter than at the zenith when looking away from the sun. The CIE standard clear sky has no cloud cover [78,83].

The CIE Clear Sky model represents a completely clear sky with direct sunlight. It is characterized by high luminance near the sun, which decreases with distance, exhibiting anisotropic luminance where brightness varies with direction. This model is ideal for simulating environments with strong direct sunlight and clear conditions.

Intermediate Sky

This type of sky fluctuates between being mostly cloudy with some clear areas to being mostly clear with a few clouds, making it challenging to predict. It is characterized by having 30–70% cloud cover, representing the intermediate condition between overcast and clear skies [78,83].

The CIE Intermediate Sky model represents partly cloudy conditions. It features a mix of direct sunlight and diffuse light from clouds, capturing the variability of partly cloudy skies. This model is useful for simulations where conditions fluctuate between clear and overcast.

Overcast Sky

A sky with 70–100% cloud cover is considered overcast. Overcast skies typically have lower luminance and radiation levels, producing weaker shadows and more diffused light compared to clearer skies. The sky is approximately three times brighter at the zenith than at the horizon. The CIE standard for an overcast sky indicates a sky fully covered by clouds [78,83].

The CIE Overcast Sky model represents a completely overcast sky with no direct sunlight. It has a uniform luminance distribution, with the highest brightness at the zenith decreasing towards the horizon. The light is diffuse and soft, making this model suitable for scenarios requiring even, diffuse lighting, minimizing glare and harsh shadows.

Uniform Sky

This standard sky type harks back to the era when calculations were performed manually or using tables. It is defined by a consistent luminance that remains unchanged regardless of altitude or azimuth. Commonly referred to as the 16th CIE sky type, it is rarely used today due to its uniform luminance distribution.

The CIE Uniform Sky model is a theoretical representation of an idealized sky with completely uniform luminance. It features equal brightness across the entire sky dome. Although it rarely occurs in nature, this model is useful for specific analytical purposes where uniform lighting is assumed.

Generally, the luminance distribution of a clear sky is uneven. The brightness peaks where the sun is located, but significantly decreases in other areas. In contrast, the luminance of an overcast sky is more uniform and is less affected by the position of the sun. The sky distributions shown in Figure 4.4 were created using the RADIANCE synthetic imaging system. It was assumed that the sun was positioned at an altitude of 60º directly south. The sky luminance was mapped from the southern (0º) to the northern (180º) horizon, passing through the zenith (90º). It is important to note that these graphs should not be compared directly; for instance, it is incorrect to assume that uniform and overcast skies always exhibit the same zenith brightness.

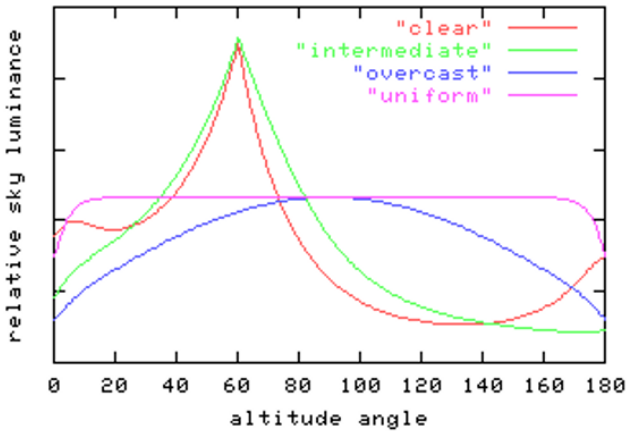

Figure 4.4 sky distributions

CIE sky models are used to simulate various natural sky conditions for accurate daylighting analysis. The models represent the distribution of luminance across the sky dome, which is crucial for simulating how daylight interacts with architectural spaces. The fundamental principle involves mathematically defining the luminance distribution based on empirical data and theoretical considerations.

Andrew Marsh [84] developed a web program for interactively experimenting with the latest Perez all-weather sky model. This is essentially a mathematical model used to calculate the representative spatial distribution of daylight across the sky dome, capable of functionally simulating a range of different weather conditions. Figure 4.5 [84] shows examples of the more detailed 16 types of CIE standard general skies.

CIE sky models use mathematical functions to describe the spatial distribution of sky luminance. These models are based on empirical observations and theoretical formulations that capture the variations in brightness and color due to atmospheric conditions, solar position, and scattering effects. The luminance data are then used in daylighting simulation software to predict the distribution and intensity of natural light within a given space, aiding in the design and analysis of architectural environments. Figure 4.6 [84] shows examples of real-world sky conditions and their simulated daylight distribution.

Understanding and simulating different sky conditions enable architects to design buildings that maximize natural light, enhance energy efficiency, and improve occupant comfort. Accurate daylight simulation informed by these studies leads to better-performing and more sustainable buildings.

4.2.4. Different types of natural light

In real-world conditions, sunlight and daylight exhibit distinctly different characteristics. Sunlight is a highly directional point source of light, often referred to as a beam. This concentrated beam casts sharp shadows and can provide illumination levels ranging from 50,000 to over 100,000 lux. The intensity of sunlight varies based on geographic location and time of year, being extremely intense at noon in tropical regions or at high altitudes with thin air, and less intense in the Arctic due to the low angle of the sun.

Conversely, daylight is diffused and scattered in all directions, producing no shadows. It consists of light from both cloudy and clear blue skies. Interestingly, cloudy skies are often brighter than clear blue skies, with the brightness depending on cloud thickness and color. Generally, complete cloud cover results in a very uniform lighting condition, whereas a clear blue sky is highly variable, being brightest around the sun and darkest 90° away from the sun's position [27]. These differences also affect color temperature, with clear blue skies delivering a cool color temperature of approximately 10,000 °K (9726 °C), and cloudy skies providing a warmer color temperature of around 7500 °K (7226 °C). Understanding these properties at specific locations helps in estimating the amount of illumination available for skylighting [28] (Table 4.2.1).

Climate conditions have a direct impact on daylight levels, necessitating an understanding of environmental factors that influence the quality and quantity of daylight to select the appropriate system. Table 4.2.2 summarizes key issues related to natural light as highlighted in the studies by Ruck and Aschehoug [27] and Phillips [5].

Table 4.2.1 Daylight characteristics. [28]

Types of daylight	Light direction	Illumination fc	Brightness cd/m2	Colour temp.	Colour description
Sun at midday	Beam	8000-10,000	1,600,000,000	5500 K	Neutral
Sun at horizon	Beam	3000–8000	6,000,000	2000 K	Warm
Clear sky	Diffuse	1000–2000	8000	10,000 K	Bluish
Cloudy sky	Diffuse and Beam	500–5000	2000	7500 K	Cool

Table 4.2.2 Important issues related to design with natural light.

Factors	Description
Change/varity	Daylight change from day to night, changes associated with variations in the weather (from bright sunny days to dark and cloudy or rainy days) as well as season. Daylight direction on overcast and cloudy days remains changeable, although the light is more diffused than that on a clear day. On overcast days, daylight is uniform but varies in absolute brightness from sunrise to sunset.
Orientation	The orientation of sunlight during a year is changeable. For instance, in Malaysia, January with its low inclination in the south is different from April, which is overhead, and June, which has low inclination in the north. The characteristic of each month is unique because every period in a year reflects a specific sun path.
Sunlight effect	The effect of sunlight in hot climates varies according to cloud cover and weather conditions and influences the distribution of solar radiation as direct or diffuse, which is changeable in a day and a year.

Colour	Daylight colour varies from morning to evening and with variations in weather patterns and sky conditions. The sun at midday provides 5500 K neutral colour temperature, whilst the sun at the horizon provides 2000 K warmth. Vision is improved with good contrast, and the natural colour of daylight increases contrast.

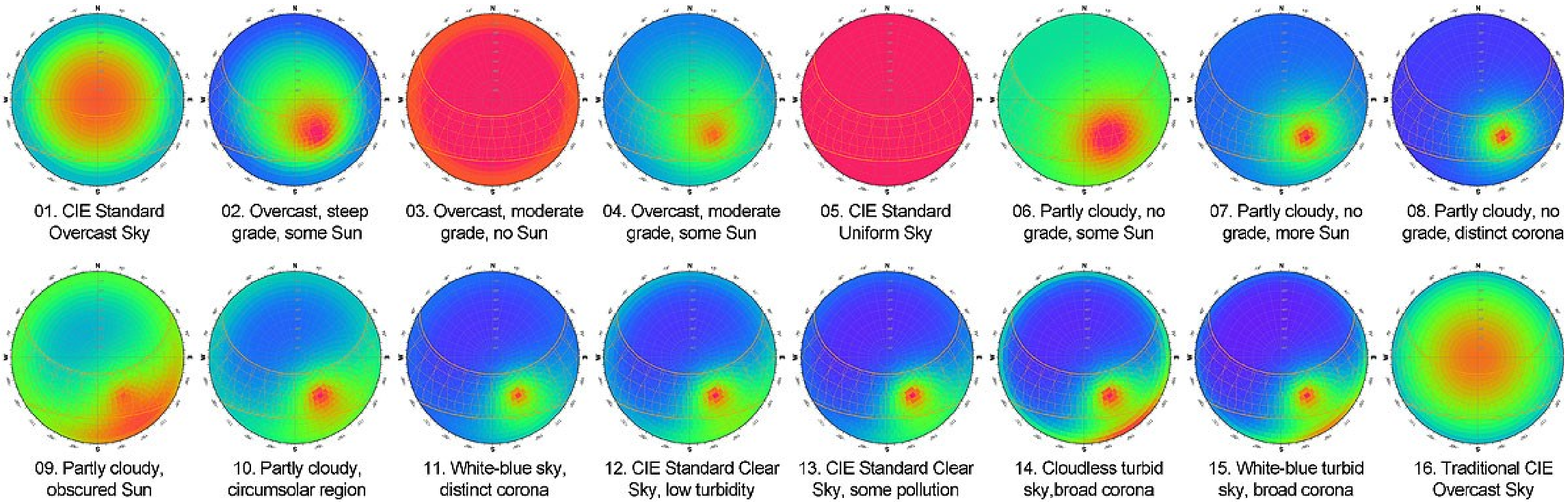

Figure 4.5 Examples of the 16 CIE standard general sky types.

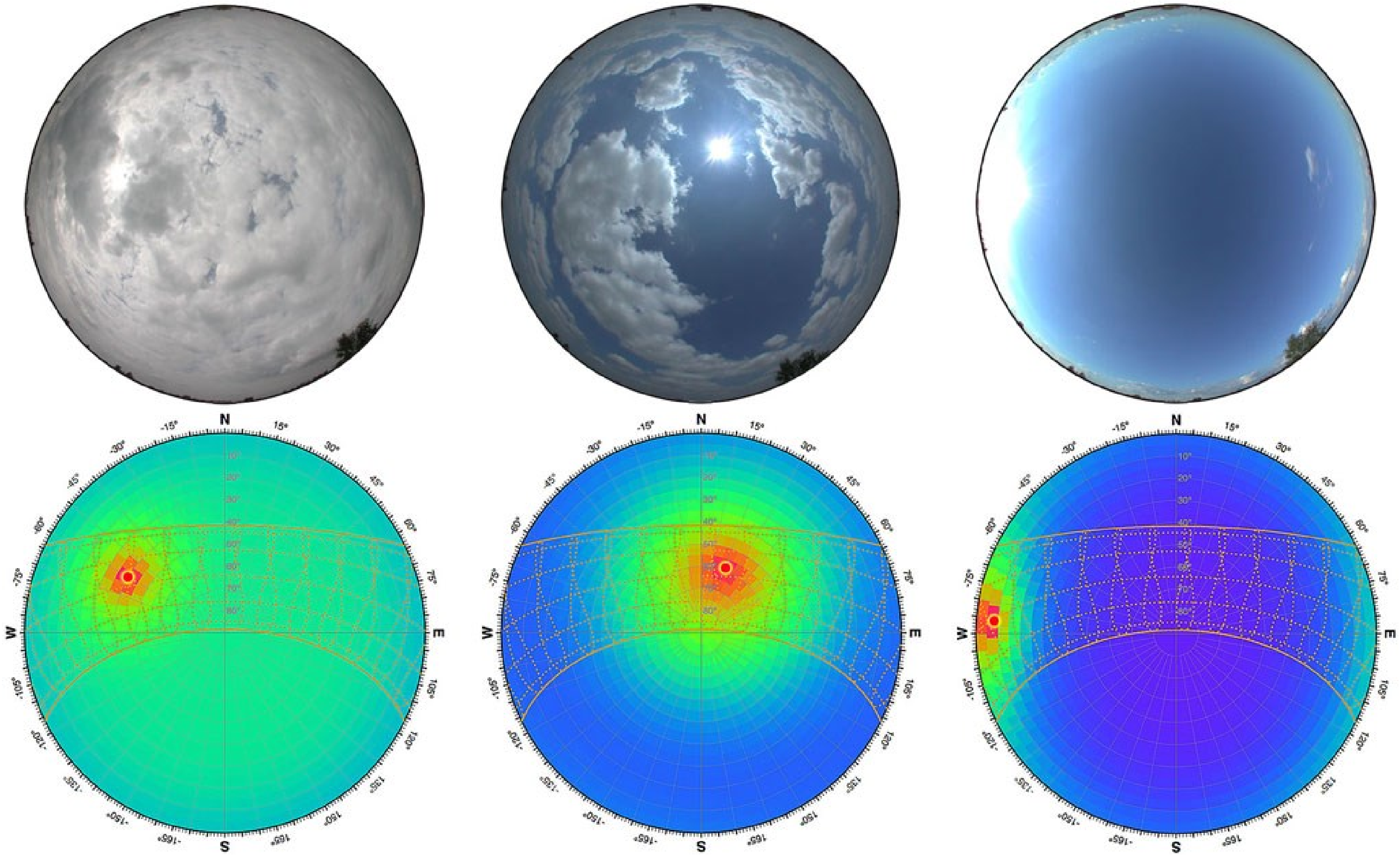

Figure 4.6 Some example real sky conditions and their modelled daylight distributions.

4.3. **Types, Materials, and Display Methods of Exhibits in Art Galleries**

Art galleries exhibit a diversity of artworks that reflect the richness of artistic expressions and the variability of visual effects. Sculptures and paintings are the most common types of exhibits, showcasing not only the beauty of the artworks themselves but also the artistry and science of display techniques. Below, we explore the materials and display methods of these exhibits in detail. Figure 4.7 [85] shows the layout of sculptures and paintings in a typical art museum. Table 4.3.1displays the types of museum exhibits, materials, and display methods.

Figure 4.7 The layout of sculptures and paintings [85]

Table 4.3.1 The types of museum exhibits, materials, and display methods.

Type	Material	Display method

Sculpture	Ceramics, glass, stone and metals, wood, horn, bone, ivory, minerals	Platform (Vertical)
Painting	linen, cotton, or wood, pigment, paper	Wall (Horizontal)

4.3.1. Display techniques and materials of sculpture.

Sculptures, as a three-dimensional art form, use a variety of materials including stone, metal, wood, and synthetic materials. Each material offers unique textures and expressive possibilities.

Stone sculptures are one of the most traditional and classic forms. Common stones like marble and granite are widely used due to their durability and fine texture. According to Cone [86], marble is often used for sculptures representing human beauty due to its white sheen and delicate texture, while granite, known for its hardness and color variety, is used for monuments and large public artworks. Stone sculptures are typically placed in central locations or courtyards of art galleries to emphasize their historical significance and artistic value, allowing viewers to appreciate their details and textures up close.

Metal plays a significant role in modern sculpture. Common metals include copper and iron. Martin [87] highlighted the role of metals in modern sculpture, noting that copper is favored for its malleability and resistance to corrosion, allowing for intricate and delicate art forms, while iron is valued for its strength and industrial aesthetic. Metal sculptures often have a reflective and refractive quality that draws viewers’ attention. They are typically displayed in well-lit galleries or outdoor spaces to showcase their material properties and the artist's creative intent.

Synthetic materials like resin and glass are increasingly used in contemporary sculpture creation. Resin is favored for its lightweight and moldable properties, making it ideal for abstract or modernist sculptures. Glass, with its transparency and vibrant colors, is often used to create stunning light and shadow effects. Hall [88] emphasizes in his study that the use of these materials adds a modern touch to exhibitions, providing a rich visual experience with their diverse colors and shapes.

The display of sculptures typically considers their spatial relationship with the environment and the interaction between the viewer and the artwork. Large sculptures are often placed in open spaces, allowing viewers to walk around and appreciate the three-dimensional aspects of the work. Smaller or more detailed sculptures might be placed in more intimate settings with specific lighting effects to guide viewers in closely examining the craftsmanship.

4.3.2. Display techniques and materials of paintings.

As a representative form of flat art, paintings are typically exhibited by hanging them on walls. The diversity of painting materials and techniques determines the variety of display methods.

Oil painting is one of the most common forms of painting, primarily using oil paints and canvases. Common canvases include linen and cotton, with the former being durable and suitable for large works, while the latter is less expensive and suitable for studies. Due to its thick texture and depth of color, oil paint can express complex themes and emotions. Omar et al. [89] studied the impact of lighting on the display effect of oil paintings and found that suitable lighting can highlight the layering and details of the paintings. Therefore, oil paintings are usually hung on walls with even lighting and highlighted using adjustable spotlights to enhance their visual effect.

Watercolor paintings, characterized by their light and transparent nature, are uniquely suited to expressing soft scenes and delicate emotions. The primary materials for watercolor paintings are watercolor paper and paints, with the former needing to be absorbent and resilient. Jeanneret et al. [90] researched the best lighting conditions for displaying watercolor paintings, suggesting avoiding direct strong light to prevent colors from becoming flat or losing detail. Typically, even diffused lighting is used to present the best color effect and depth of the paintings.

Prints and drawings are another important category of paintings, often used to showcase details and techniques. Prints use carving knives and plates, while drawings employ pencils, charcoal, and other tools. Clark and Barger [91] noted that when displaying these works, explanatory labels or digital information points are often used to enhance their educational value and viewing experience. To protect these works, the exhibition environment needs to control temperature and humidity to prevent paper deformation or pigment fading. The height and spacing of the display also need careful design to ensure viewing comfort and overall aesthetic appeal.

4.3.3. Exhibition Environment and Protective Measures

In art museums, controlling the exhibition environment is crucial to ensuring the best display effect of artworks. For both sculptures and paintings, stability of temperature and humidity, uniformity of lighting, and intensity control are essential considerations. These measures not only protect the artworks from physical and chemical damage but also enhance the viewing experience for the audience. Huang, Wei, and Zhu [92] studied the impact of daylight on exhibition hall display effects and provided practical suggestions on how to effectively utilize natural light to improve display effects and protection conditions.

In summary, sculptures and paintings, as the main exhibits in art museums, each have unique materials and display methods. Through thoughtful exhibition design and environmental control, museums can not only showcase the beauty of the artworks but also enhance the viewing experience for visitors, ensuring that the artworks are presented in the best possible environment.

4.4. Types of Light Sources in Museums

Museum exhibit displays are typically classified into four groups: flat displays on vertical surfaces, display cases, three-dimensional objects, and realistic environments. Each category presents unique challenges and creative opportunities for lighting designers.

4.4.1. Flat Displays on Vertical Surfaces

Achieving uniform illumination for large vertical displays, such as paintings, prints, documents, and explanatory labels, is a common challenge in museums. The use of acrylic or glass to protect artifacts can complicate lighting due to reflections. Specular surfaces combined with poorly positioned lights can cause glare and obscure the artifacts. Studies, such as those by Loe et al. [93], have explored preferences for different lighting distributions. Generally, lighting should provide uniform illumination across the entire surface. Positioning luminaires with the beam center axis at a 30° angle from the vertical can minimize shadows and glare, allowing visitors to closely approach artifacts without casting shadows.

Wall Wash: Using wall-wash luminaires is an effective method to achieve even illumination over large vertical surfaces. Many manufacturers provide charts showing the distribution of light from these luminaires on the wall.

Spotlights: For smaller to medium-sized pictures or label panels mounted on a wall, spotlights are typically used. The mounting position can be adjusted to avoid shadows from oversized frames by following specific guidelines, such as those in Figure 4.8**.** Increase or decrease "X" as required to avoid shadows from oversize frames on paintings. Compute the angle of incidence/reflection to avoid glare to viewer. Optical projectors can frame objects but might create an artificial appearance. Additional soft lighting may be needed to avoid making paintings look like transparencies. Allowing some spill light around the area can soften the overall effect. Separate picture labels should be placed in the spill-light area to avoid frame shadows.

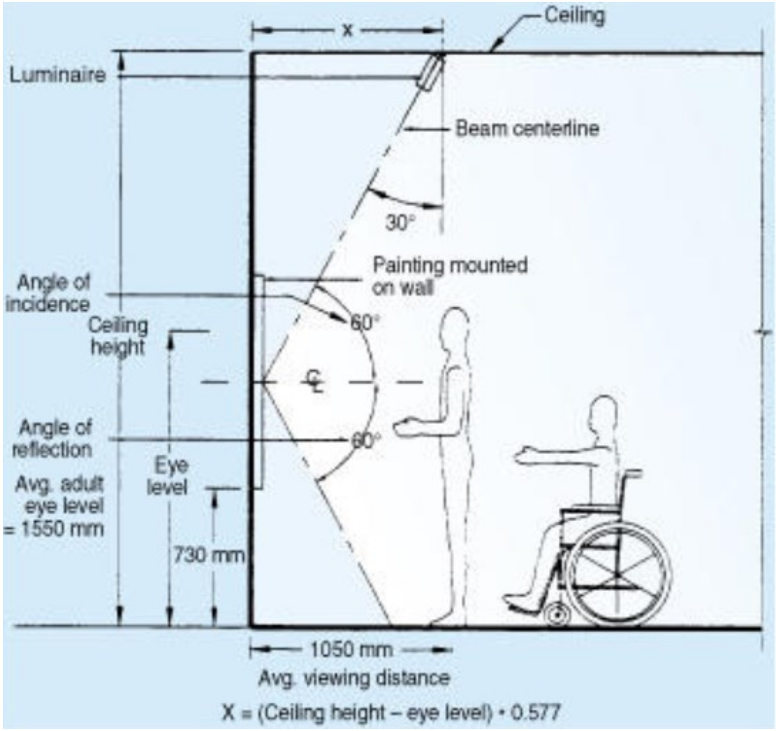

Figure 4.8 Guidelines for luminaire mounting position for flat displays on vertical surface. Use the formula as a guide. [94]

4.4.2. Exhibit Cases

Museum exhibit cases serve to allow visitors a close view of rare and delicate artifacts while protecting them from degradation, vandalism, or theft. These cases typically house small, fragile, and valuable items and can range from small acrylic cubes for jewels to large cubes for rare clothing. They may have either corner mullions or clear acrylic or tempered glass panels glued at the edges.

These cases can feature internal or external lighting, with lamp types ranging from low-voltage incandescent to fluorescent to high-intensity discharge. Challenges in lighting display cases include reflections in the glass, shadows from visitors or objects, and heat buildup. As shown in Figure 4.9 and Figure 4.10, a transparent or translucent barrier between the light source and the artifact helps mitigate unwanted heat.

Minimizing Reflections: Reflections are particularly problematic in display cases with dark interiors. Solutions include positioning cases against black walls, using angled or specially curved glass to direct reflections away, eliminating glass barriers in favor of railings or motion sensors, and creating a high luminance ratio between the interior and exterior of the case.

External Lighting: When lighting is external, the lights should be above the front of the case and directed straight down to minimize shadows. Diffusing materials can reduce harsh shadows, though they may cause reflections on the ceiling. Heat buildup can be managed with dichroic reflector lamps and heat filters.

Internal Lighting: Freestanding or built-in display cases often feature overhead light attics or light boxes for concealed and customized illumination. Partial light attics suit cases viewed from one direction and can contain fluorescent or incandescent lamps. Full light attics are needed for cases viewed from all sides, providing soft, uniform illumination.

Supplementary Lighting: Lighting from the side, back, or bottom enhances the texture and shape of three-dimensional objects, improving the display of ceramics, glass, and polished metals.

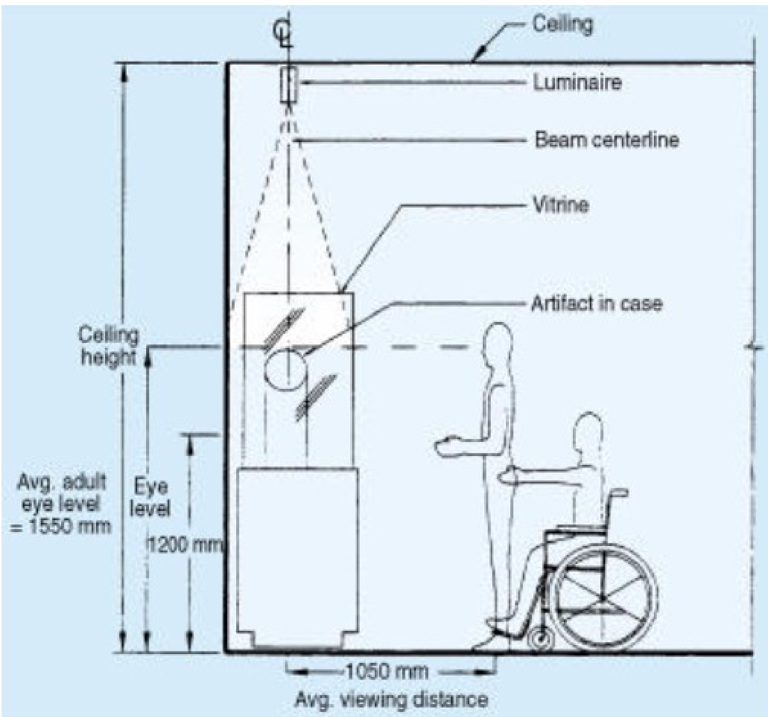

Figure 4.9 Guidelines for luminaire mounting position for a display case, with the luminaire outside the case. [94]

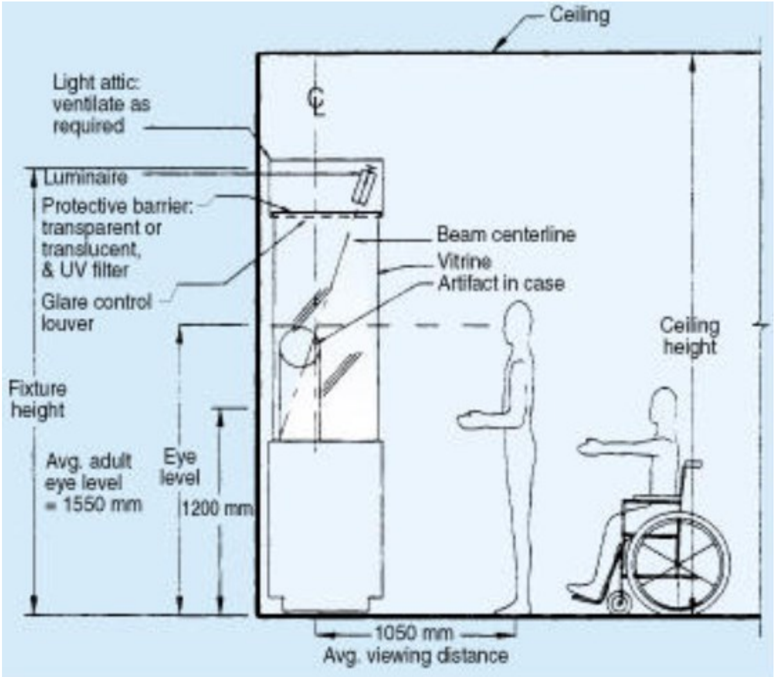

Figure 4.10 Guidelines for luminaire mounting position for a display case, with the luminaire inside a full light attic. [94]

4.4.3. Three-Dimensional Objects

No matter the size, a three-dimensional artifact should be illuminated from multiple angles. Lighting from different directions shapes a sculpture, highlighting some areas and casting shadows on others to create a sense of depth. Take, for instance, a bronze statue with a patina in shades of light blue, green, and gray. Illuminating from various angles enhances these colors with varying emphasis.

Highlights and Shadows: Highlights offer clear visual cues about surfaces, but it's crucial to ensure they don't become overly bright or monotonously repetitive. Shadows can effectively indicate surface forms and textures, as long as they aren't too strong to obscure important details.

Reducing Glare: For objects at eye level or below, lighting from all sides with luminaires positioned where the beam's center axis is 30° or less from the vertical minimizes viewer issues. For small, low objects, steeply angled lighting reduces glare for viewers across from the display. With taller objects, light may overshoot and cause glare for viewers looking up. As shown in Figure 4.11 and Figure 4.12, Solutions include:

- Sharply angling lights downward and using a high-reflectance pedestal to soften shadows.
- Keeping light beams within the object's display area.
- Illuminating from below without distorting appearances.
- Using soft, overall lighting (fill light) for visibility and focusing a narrow beam (key light) on key parts.
- Lighting the background behind the artifact.

Outdoor sculptures and monuments require similar lighting principles but need different equipment due to their size, placement, weather, and vandalism risks. Efforts should be made to minimize light pollution and trespass.

(a) Thoroughly diffused overhead illumination.

(b) Flow of light from right, due to a large diffusing light source.

(c) Flow of light from right, due to a compact, directional light source.

(d) Multiple compact sources.

Figure 4.11 Effects of lighting upon the appearance of a group of four objects: two black and two white, and two glossy and two matt. [95]

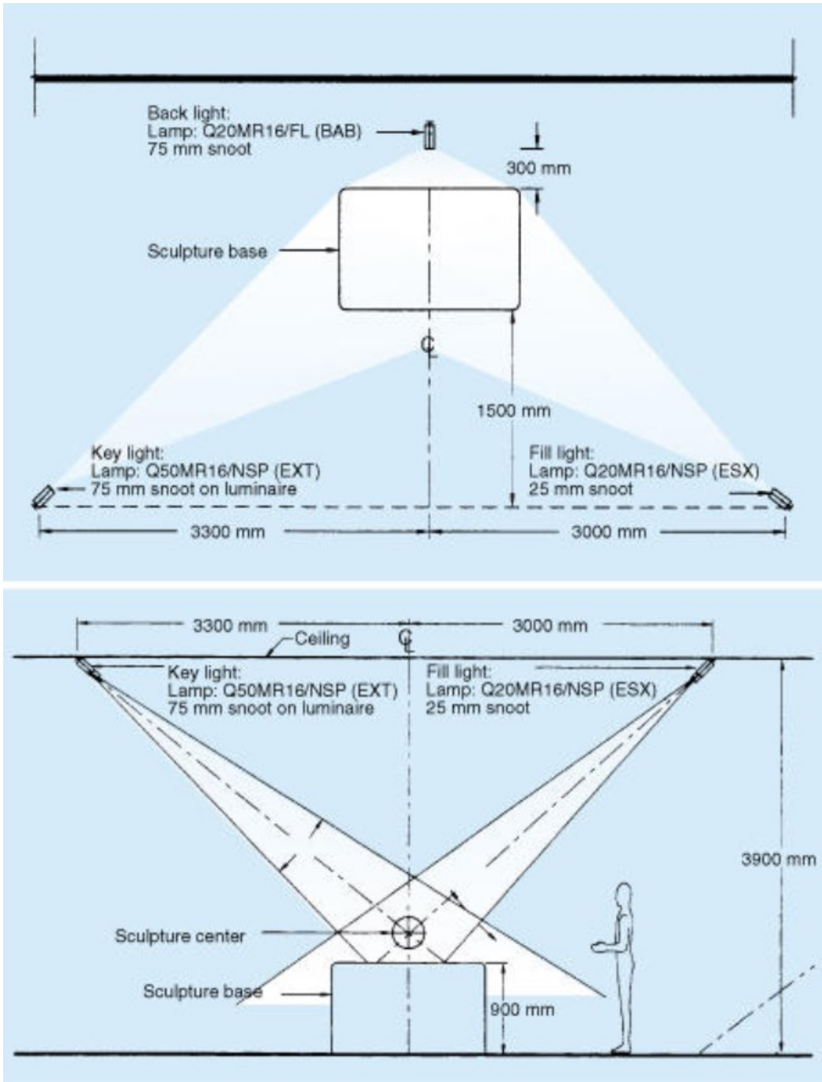

Figure 4.12 Sculpture lighting [94]

4.4.4. Realistic Environments

Museums often craft realistic environments where the space itself communicates a message. Examples include period rooms, outdoor scenes, and historical houses. Achieving lighting that reflects the original purpose of these spaces is ideal, but must be balanced with practical considerations. For instance, the Museum of Science and Industry in Chicago features a simulated "coal mine." Real miners, accustomed to helmet lamps, require minimal lighting, but replicating such conditions would compromise visitor safety and the effectiveness of the exhibit's message.

Realistic exhibit spaces often necessitate compromises. Lighting designers can use two primary techniques to achieve authentic lighting effects: concealed lighting positions and dual lighting systems.

Concealed Lighting: Concealed lighting positions require clearly defined viewing areas, highlighted display features, and sufficient illumination for visitor safety.

Dual Lighting: A dual lighting system utilizes control equipment to switch, either automatically or manually, between realistic lighting and optimal display lighting. The display lighting should harmonize with the realistic lighting in style and color. To ensure safety and preservation, electric lighting replaces original flame sources (candles, gas jets, etc.). Real flames would introduce unwanted soot and water vapor into the exhibit. Electric lighting that subtly transitions between the glow of a gas jet and sufficient brightness for easy viewing can be very effective. Recreating realistic lighting requires thorough research and careful observation by the designer.

4.5. Architectural aspects and daylight

Analyzing the architectural forms and the influence of daylight on lighting in museums and art galleries is essential to understand their effects on adaptation, orientation, and artifact preservation. Six key factors determine the final luminance produced by architectural surfaces and daylight:

- The ratio of operative glazing to floor area.
- Room dimensions, particularly ceiling height and room depth.
- Placement and spacing of available glazing.
- Site location, including longitude, latitude, and direction.
- Obstructions, both external and internal.

- Reflective characteristics of interior surfaces.

4.5.1. Adaptation, Orientation, and Artifact Preservation

The human visual system can comfortably perceive only a narrow range of brightness at one time. Generally, the exhibit illuminance should be no more than five times the surrounding area's illuminance (5:1) [94].

Transitional Spaces: The time required to adapt to changes in retinal illumination depends on several factors, including the magnitude and direction of change, transition time, and the visitor's age. Typically, adaptation occurs within 1 second for luminance changes within a 100:1 range. Larger changes (greater than 1000:1) necessitate photochemical adaptation. Changes to higher luminance levels occur faster than to lower levels. Cone photoreceptors adapt within minutes, while transitions involving rod photoreceptors may take tens of minutes. Older individuals generally require more time to adapt compared to younger ones [94].

Preservation: North-facing window walls (in the northern hemisphere) should only transmit visible light, eliminating wavelengths below 400 nm. The room's illuminance should adhere to the guidelines in Table 4.5.1, potentially resulting in less than five percent visible and solar energy transmittance. Galleries should have a method to completely block daylight when closed to the public, ensuring no direct sunlight strikes sensitive artifacts.

Table 4.5.1 Recommended Total Exposure Limits in Terms of Illuminance Hours per Year [94]

Types of Materials	Maximum Illuminance	Lux-Hours Per Year*
Highly susceptible displayed materials: textiles, cotton, natural fibers, furs, silk, writing inks, paper documents, lace, fugitive dyes, watercolors, wool, some minerals	50 lux	50,000 lux

Moderately susceptible displayed materials: textiles with stable dyes, oil paintings, wood finishes, leather, some plastics	200 lux	480,000 lux
Least susceptible displayed materials: metal, stone, glass, ceramic, most minerals	Depends on exhibition situation	

Note: All UV radiation (400 nm and below) should be eliminated. The visible spectrum is defined as extending from 380 nm to 760 nm. Museum conservators treat all wavelengths shorter than 400 nm as UV; the damage potential is high below this wavelength and the visual effect is very small.

*These values follow the reciprocity principle, and therefore the maximum illuminance values can be altered for different annual exposure times.

4.5.2. Sample of Architectural Features

Light Wells: Skylights with light wells can introduce daylight without degrading artifacts. These wells should be splayed with side walls tilted at 30° to the vertical, finished in matte white.

Electrically Controlled Glazings: These glazings contain electrically charged particles that align when voltage is applied, making the glass translucent. Removing the charge randomizes the particles, turning the glass transparent. This technology has significant potential for museum applications.

Low-Emissivity Glazings: These glasses and plastics reduce brightness as their transmittance decreases, reflecting most UV rays responsible for fabric fading. Low-emissivity windows typically consist of a clear outer pane, a space, and a low-emissivity coating on the airgap side of the inner pane.

4.5.3. Natural light in museum

Natural light is crucial in the design of various building types, optimizing both their functionality and the well-being of their occupants. This section explores the specific daylight requirements for museums, detailing the necessity, intensity, duration of exposure, and providing references from existing research to support these standards.

Museums require carefully controlled natural light to prevent damage to exhibits and to enhance the visitor experience. Light-sensitive artifacts need limited exposure to prevent degradation, typically no more than 50 lux for the most sensitive materials [94]. However, controlled daylight can also bring out the true colors and details of exhibits, making them more appealing.

The integration of natural light into architectural designs is not only a matter of aesthetic enhancement but a well-researched approach to improving functionality, energy efficiency, and occupant well-being across various building types. Each setting demands specific considerations for intensity and duration of light exposure, guided by both empirical research and established industry standards.

Understanding and studying the illuminance requirements of buildings is crucial for several reasons. The quality of lighting, often referred to as "good lighting," is determined by the visual tasks that the human eye needs to perform. Different visual tasks, such as reading or viewing light-sensitive artworks or sculptures, require varying lighting qualities. Good lighting is defined by three fundamental quality features, which are weighted differently depending on the specific space and its lighting needs. Table 4.5.2 illustrates the standard definition of quality characteristics that determine the quality of a lighting system.

In 1979, the Illuminating Engineering Society of North America (IESNA) established nine illuminance categories, ranging from "A," the lowest recommended illuminance level, to "I," the highest. Each category provides general descriptions of visual tasks without specific application context. Table 4.5.3 [94] provides detailed explanations of these categories.

Table 4.5.2 Standard definition of quality characteristics that determine the quality of a lighting system

Visual comfort	Visual performance	Visual ambience

• Color rendering • Harmonious brightness distribution	• Lighting level • Glare limitation	• Modeling • Light color • Direction of light

Firstly, adequate lighting is essential for creating comfortable and functional spaces that meet the needs of occupants. Proper illuminance ensures that activities such as reading, working, and viewing exhibits can be performed efficiently and comfortably, reducing eye strain and enhancing productivity.

Secondly, knowing the illuminance requirements informs the daylight simulation and design process. By understanding the specific lighting needs of different spaces within a building, designers can optimize natural light usage, thereby reducing the reliance on artificial lighting. This optimization not only enhances energy efficiency but also promotes sustainability by lowering the building's overall energy consumption.

Furthermore, accurate daylight simulations help in predicting how natural light will interact with the architectural elements of a building. This prediction is vital for achieving balanced and aesthetically pleasing lighting conditions, which can significantly improve the visual appeal and comfort of the spaces. Ultimately, comprehending illuminance requirements allows for the creation of better-designed buildings that offer improved well-being and productivity for their occupants.

Table 4.5.3 Determination of Illuminance Categories [94]

Orientation and simple visual tasks. Visual performance is largely unimportant. These tasks are found in public spaces where reading and visual inspection are only occasionally performed. Higher levels are recommended for tasks where visual performance is occasionally important.		
A	• Public spaces	30 lx (3 fc)
B	• Simple orientation for short visits	50 lx (5 fc)
C	• Working spaces where simple visual tasks are performed	100 lx (10 fc)

Common visual tasks. Visual performance is important. These tasks are found in commercial, industrial and residential applications. Recommended illuminance levels differ because of the characteristics of the visual task being illuminated. Higher levels are recommended for visual tasks with critical elements of low contrast or small size.			
D	•	Performance of visual tasks of high contrast and large size	300 lx (30 fc)
E	•	Performance of visual tasks of high contrast and small size, or visual tasks of low contrast and large size	500 lx (50 fc)
F	•	Performance of visual tasks of low contrast and small size	1000 lx (100 fc)
Special visual tasks. Visual performance is of critical importance. These tasks are very specialized, including those with very small or very low contrast critical elements. Recommended illuminance levels should be achieved with supplementary task lighting. Higher recommended levels are often achieved by moving the light source closer to the task.			
G	•	Performance of visual tasks near threshold	3000 to 10,000 lx (300 to 1000 fc)

**To account for both uncertainty in photometric measurements and uncertainty in space reflections, measured illuminances should be within ± 10% of the recommended value. It should be noted, however, that the final illuminance may deviate from these recommended values due to other lighting design criteria.*

4.5.4. Illuminance requirement of museum

Collections are most vulnerable to light damage while on display. The duration of exposure and the intensity of light are the two primary factors to consider for their protection. The Illuminating Engineering Society of North America (IESNA) [94] advises that artifacts should be adequately visible when displayed. Insufficient lighting that prevents visibility is pointless as it does not fulfill the purpose of displaying the artifact. Institutions must determine the acceptable amount of light damage over time, considering the desired lifespan of the artifacts. It is crucial for institutions to assess and understand the sensitivity of each artifact or group of artifacts as precisely as possible.

Radiant heat increases an object's surface temperature, which can lead to discoloration, cracking, and deterioration. Photochemical reactions alter the object at the molecular level, resulting in embrittlement. Daylight consists of visible light (400–760 nm), ultraviolet (UV) radiation (wavelengths shorter than 400 nm), and infrared (IR) radiation (wavelengths longer than 760 nm). Light-sensitive materials will always be affected by light exposure, regardless of how minimal the exposure might be. However, the risk of light damage can be mitigated. Strategies to reduce light damage include:

- Reducing the amount of visible light an object receives – lowering the illuminance or light intensity
- Reducing the time an object is exposed to visible light – lowering the cumulative effect
- Eliminating all invisible radiation – blocking ultraviolet and infrared radiation

Although daylight intensity varies, the damage caused by light exposure is a combination of both the intensity of the light and the duration of exposure. Exposure to light (radiant energy) can cause cumulative and permanent damage to light-sensitive objects. This energy induces irreversible changes, either through radiant heating or photochemical reactions. Therefore, it is essential to control the exposure time of museum objects by minimizing their total annual light exposure. Annual exposure hours are determined based on the standard museum's annual opening hours. To preserve light-sensitive materials, it is crucial to identify the light sensitivity of each displayed object. Table 4.5.1 provides recommendations for maximum illuminance levels for specific materials. Table 4.5.4 shows the relationship between time and fading in materials sensitive to light exposure.

The human eye needs at least 50 lux to properly perceive the shape and color of an object. Consequently, art conservation experts recommend a maximum illumination level of 50 lux for very delicate materials. For moderately sensitive items, the maximum recommended level is 200 lux. While materials that are insensitive to light are not affected by the light intensity, it is advisable to keep the light levels below 300 lux. This is to prevent difficulties for the human eye in adjusting to significant differences in light levels between different gallery spaces.

Table 4.5.4 Time until Fading in Materials Sensitive to Light

Illuminance	Damage	Low sensitivity	Medium sensitivity	High sensitivity
50 lux	Just noticeable fade	300 yr – 7,000 yr	20 yr – 700 yr	1.5 yr – 20 yr
	Almost total fade	10,000 yr – 200,000 yr	700 yr – 20,000 yr	50 yr – 600 yr
150 lux	Just noticeable fade	100 yr – 2,000 yr	7 yr – 200 yr	6 mo – 7 yr
	Almost total fade	3,000 yr – 70,000 yr	200 yr – 7,000 yr	15 yr – 200 yr
500 lux	Just noticeable fade	30 yr – 700 yr	2 yr – 70 yr	6 mo – 2 yr
	Almost total fade	1,000 yr – 20,000 yr	70 yr – 2,000 yr	5 yr – 60 yr
5,000 lux window or study lamp	Just noticeable fade	3 yr – 70 yr	2 mo – 7 yr	5 d – 2 mo
	Almost total fade	100 yr – 2,000 yr	7 yr – 200 yr	6 mo – 6 yr
30,000 lux Average dalight	Just noticeable fade	2 mo – 10 yr	2 wk – 1 yr	1 d – 2 wk
	Almost total fade	20 yr – 300 yr	1 yr – 30 yr	1 mo – 1 yr

The annual cumulative daylight illuminance for medium sensitive materials should be kept above 50,000 lux-hours but should not exceed 480,000 lux-hours. Medium to highly sensitive objects should be illuminated with minimal light (50 lux) and, due to their faster rate of damage, their exposure time should be limited. Since daylight exposure is cumulative, it is crucial to limit the total annual lux-hours and not just focus on the maximum illuminance. Additionally, glazing should be used to eliminate all ultraviolet radiation (wavelengths of 400 nm and below).

4.6. Skylight system

The shading system plays a pivotal role in the design of natural light harvesting systems. On one hand, it mitigates direct exposure to high-intensity sunlight during summer, lowers indoor heat load, and diminishes the reliance on air conditioning systems [96]; on the other hand, it ensures the provision of soft and uniform natural light, enhancing occupant comfort [97]. To accommodate varying sky conditions, shading devices exhibit diverse morphologies, ranging from static or fixed [98] to adjustable or kinetic configurations [99,100]. Passive shading strategies, devoid of mechanical systems or controllers, demand significantly less maintenance and offer greater energy savings compared to active mechanical shading systems [101].

4.6.1. Materials and light

Light and materials are interdependent, with materials directly affecting both the quantity and quality of light. Two critical properties of materials are color and surface texture. Reflective materials and glossy surfaces act like mirrors, reflecting light and showing the reflected images of the light source on their surfaces. Matte surfaces, such as natural stone, wood, and plaster, scatter light evenly in all directions. Light is characterized by hue, reflectance value, and intensity. The reflectance value determines the proportion of light that is absorbed versus reflected. For instance, a white wall reflects about 80% of the incident light, whereas a dark wall reflects around 10%. Additionally, colored surfaces impart some of their color to the reflected light.

Skylight configurations can be classified into Light Shelves, Wall Wash Toplighting, Central Toplighting, Linear Toplighting, Tubular Skylights, among others [102]. Irrespective of the configuration, two essential aspects must be addressed: light transmission and light distribution. Light transmission largely depends on the glass composition of the skylight system, with various types of glass including clear, tinted, low-emissivity, plexiglass, and other commonly utilized glasses exhibiting different spectral transmittance rates. Light distribution refers to the manner in which natural light, reflected by opaque materials, permeates the surrounding environment. Reflective materials and glossy surfaces act as mirrors, projecting reflected images of the light source onto surfaces, whereas matte surfaces such as natural stone, wood, and plaster distribute light uniformly in all directions. In addition to facilitating the ingress of natural light, skylight designs must also consider factors such as indoor ultraviolet transmission, solar heat gain, and thermal transmission, among others [95].

4.6.2. Location of the Daylight Source

In museums, daylighting is generally achieved through two main concepts: lighting through side windows and lighting through roof openings and skylights. Skylights are often paired with light-guiding systems and light-scattering, UV-filtering glass ceilings, which permit only diffused daylight to enter while blocking direct sunlight. Light-guiding systems, including light-directing devices in the roof area and light-reflecting ceiling cavities, redirect daylight via multiple reflections into the exhibition space, distributing it evenly through light-diffusing glass ceilings.

These systems can be categorized into rigid, non-adaptable elements and mobile systems that dynamically modulate daylight and also serve as thermal sunscreens. Generally, light-guiding and shading systems are classified based on their function: sun protection (e.g., shading by external louvers), glare protection (contrast and direct light beams), light filtering (adjustment of illuminance), and light scattering (luminance distribution). Lateral windows in exhibition rooms are practical only if the displayed objects are not shaded by people or other objects and if indirect light is filtered through the facade. This can be achieved by arranging high lateral skylights or by orienting the facade to the north, allowing consistent daylight to enter the exhibition space [103].

4.6.3. Shading design strategies

Shading systems play a critical role in the design of natural light harvesting systems in buildings. These systems are essential not only for improving energy efficiency but also for enhancing occupant comfort. There are various types of shading systems, including static or fixed configurations and adjustable or kinetic designs. Each type has its specific applications and benefits depending on the building type and its requirements.

Shading systems are vital for several reasons. They significantly reduce the need for artificial cooling by minimizing solar heat gain, leading to substantial energy savings as buildings consume less electricity for air conditioning. According to a study by the National Renewable Energy Laboratory (NREL), effective shading can reduce a building's cooling energy use by up to 60% [104]. Additionally, properly designed shading systems provide a comfortable indoor environment by reducing glare and controlling indoor temperatures, thereby improving the well-being and productivity of building occupants. The American Society of Heating, Refrigerating and Air-Conditioning Engineers (ASHRAE) highlights the importance of shading devices in managing daylight to enhance visual comfort [105].

Shading systems can be broadly categorized into static or fixed shading systems and adjustable or kinetic shading systems. Static or fixed shading systems, such as overhangs, louvers, and fins, are permanently installed and designed to block direct sunlight during peak hours while allowing diffuse daylight to penetrate the building. These systems require minimal maintenance and are highly durable. Adjustable or kinetic shading systems, such as retractable awnings, adjustable louvers, and dynamic facades, can be manually or automatically adjusted to respond to changing sunlight conditions. These systems provide greater control over the amount of light and heat entering the building, enhancing energy efficiency and occupant comfort.

Different types of buildings utilize shading systems tailored to their specific needs. In residential buildings, common shading devices include blinds, curtains, and external awnings, which help maintain comfortable indoor temperatures and protect interiors from UV damage. Commercial buildings often employ advanced shading systems like motorized blinds and dynamic facades, which adjust automatically based on the time of day and weather conditions to optimize natural light use while maintaining energy efficiency. Public buildings such as schools, hospitals, and libraries use shading systems to create comfortable learning and healing environments. For instance, libraries might use light shelves and fixed louvers to diffuse natural light throughout reading areas, reducing glare and enhancing visibility. Museums and galleries often require specialized shading systems to protect light-sensitive exhibits. Passive shading strategies, such as fixed louvers and overhangs, provide diffuse light and minimize UV exposure, thereby preserving artworks and artifacts.

4.6.4. Daylighting System Typologies

Contemporary museums employ passive lighting systems, which, according to the design of their lighting ceilings, can be broadly categorized into three distinct types: the Surface system, the Linear system, and the Point system, as elaborated in Table 4.6.1 [106]. In the Surface system, the gallery's entire ceiling consists of either a Daylight ceiling or a combination of a Daylight ceiling with a velarium. The Linear system features linear skylights, which may be positioned horizontally (as roof glass strips) or vertically (in a sawtooth pattern). Meanwhile, the Point system is characterized by a daylighting arrangement comprising individual skylights. Although the Linear system is prevalent, it necessitates a polar orientation of the building to mitigate excessive direct sunlight, and despite this orientation, it cannot fully prevent the ingress of direct sunlight [107]. Conversely, the Point system, consisting of multiple individual skylights, manages to circumvent orientation constraints and more effectively limit direct sunlight exposure. However, additional research into various parameters within skylight clusters is essential to further investigate the potential of such systems and to advance their practical implementation in engineering.

Table 4.6.1. Examples on the three types of skylights

Surface system	Linear system	Point system
• Daylight ceiling • Daylight ceiling with velarium	• Glazing strip • Sawtooth skylight	• Single skylights • Skylight cluster

Beyeler Foundation Museum

Broad Contemporary Art Museum

High Museum of Art Expansion

Daylight-diffusing skylights, such as glass roofs, linear horizontal skylights, and point skylights, capture a combination of direct sunlight, blue-sky light, and cloud-reflected light. These skylights modulate the light through translucent materials and louvers. Polar-oriented skylights (sawtooth skylights) use a northern orientation and external shading to prevent direct sunlight from entering the gallery space. The advantage of this setup is that the light source remains relatively constant throughout the day compared to direct sunlight. Since these skylights diffuse the sunlight, clear glazing can be used to allow occupants to observe the sky conditions.

A study conducted by the Collaborative for High Performance Schools [108] demonstrated the performance of the most common types of toplighting systems; such performance is shown in Table 4.6.2.

Table 4.6.2 Performance of the most common types of toplighting systems [108]

Design Criteria	View Windows	High Sidelight w/ Light Shelf	Wall Wash Toplighting	Central & Patterned Toplighting	Linear Toplighting	Tubular Skylights
Uniform Light Distribution	○○	●/○	●	●●	◉	◉
Low Glare	○	●	●	●	●	●/○
Reduced Energy Costs	○	●	●	●●	●	●
Cost Effectiveness	●	●	●	●	●	●●
Safety/Security Concerns	○	●/○	●	●	●	●●
Low Maintenance	○	●	●	●	●	●

●● Extremely good application ● Good application ○ Poor application ○○ Extremely poor application
◉ Depends on space layout and number and distribution of daylight apertures ●/○ Mixed benefits

Chapter 5. Optimizing Natural Lighting Effects in Non-Polar Oriented Museums: A Genetic Algorithm Approach for Sawtooth Skylight Design

5.1. **Introduction**

Natural lighting plays a crucial role in museum design, contributing to the overall ambiance and enhancing the visitor experience. The importance of natural lighting in museum design lies in its ability to create a pleasant and inviting exhibition environment. It provides soft and even distribution of light, making the space brighter, more comfortable, and accentuating the details and colors of the exhibits. Natural lighting creates a sense of connection with the artwork and cultural artifacts, enhancing visitors' emotional engagement.

In museum use, however, natural light can lead to constant changes in light intensity and direction, which can adversely affect exhibits and artifacts. Intense sunlight can lead to uneven lighting, reflections and solarization that can damage or fade exhibits. The ultraviolet radiation contained in natural light can damage exhibits and artwork made of delicate materials such as watercolors, silk and wool. Therefore, in the design of natural light in museums, it is necessary to consider the visual comfort of visitors on the one hand, and the protection of exhibits on the other.

There are several types of toplight system exist for museums, and sawtooth-shaped toplight (SST) is one of the most widely adapted. The sawtooth-shaped toplight system was originally adapted in industrial buildings of the late 19th and early 20th centuries. However, due to its unique ability to control sunlight entering the exhibition space, architects have recently begun using it in museums. The main benefit of sawtooth-shaped toplight is the abundance of natural light it provides. By splitting the top of the building into multiple vertical windows, light can be evenly distributed throughout the interior, reducing shadows and uneven lighting. Figure 5.1 shows the indoor and outdoor appearance of an example of a sawtooth-shaped toplight (SST).

(a) Outdoor appearance of SST (b) Indoor environment of SST

Figure 5.1 Example of Sawtooth-Shaped Toplight (SST)

For polar oriented museums, the light efficacy of sawtooth-shaped toplight can be best utilized. However, for non-polar oriented museums, the change in orientation of the building can result in more direct sunlight coming into the room from the east or west side, which can damage exhibits or create glare. This leads to the design of natural light in museums being largely limited by the orientation of the building.

In non-polar oriented museums, there are challenges associated with achieving adequate natural lighting. These museums face limitations in terms of the angle and intensity of sunlight due to their orientation, such as facing north. As a result, there may be over- or under-intensity in the exhibition space, which can be detrimental to the exhibits themselves or affect the visual comfort of the viewer [94].

Overcoming these challenges requires innovative design approaches and techniques. Designers and engineers can optimize the use of available natural light resources through thoughtful architectural layouts and skylight designs. The design of shading systems becomes particularly important, allowing control over the entry and distribution of light by adjusting the position and angle of shades or curtains to achieve desired lighting effects. Advanced lighting simulation software and tools like Octopus and Ladybug can assist in evaluating the impact of different skylight and shading configurations on light distribution, facilitating optimized designs. Optimization methods such as genetic algorithms can be applied to optimize the design of serrated skylights for improved natural lighting.

5.2. Daylight Metrics (Objectives)

According to the data listed by IESNA, there are significant differences in the sensitivity of different materials to light(Rea & Illuminating Engineering Society of North America, 2000). Because of their susceptibility to damage from natural light, highly sensitive materials such as silks, watercolors and wools typically require less than 50 lux of natural light. Moderately sensitive materials such as oil paintings and leather usually require less than 200 lux of natural light. Less sensitive materials such as metal and stone do not require as much natural light. Exhibits of moderately sensitive materials were used as the object of study. Figure 5.2 shows the research workflow of this study.

The selected daylight metrics and criteria were chosen based on recommendations from leading daylight researchers and the latest advancements in daylight measurement techniques. To ensure that accurate daylight values and assessments for occupant visual comfort were achieved, three specific daylight metrics were utilized. These metrics will be defined and their formulas explained in the following sections.

5.2.1. sUDI

sUDI stands for "Spatial Useful Daylight Illuminance", which is a metric used to evaluate the quality of natural daylighting in building interiors. sUDI considers both the level and duration of daylight, and it is calculated based on a specified illuminance threshold. In the referenced study, the illuminance threshold was set between 50 lux and 200 lux, and only the illuminance performance on the surrounding walls was considered. This parameter serves as one of the optimization objectives in multi-objective optimization (MOO). The formula for sUDI is as follows (Eq.(1)), where A_{UDI} is the area within the useful illuminance range (50 to 200 lux) during the specified occupancy time. A_{total} is the total area of the space considered.

$$sUDI = \frac{A_{UDI}}{A_{total}} \times 100 \tag{1}$$

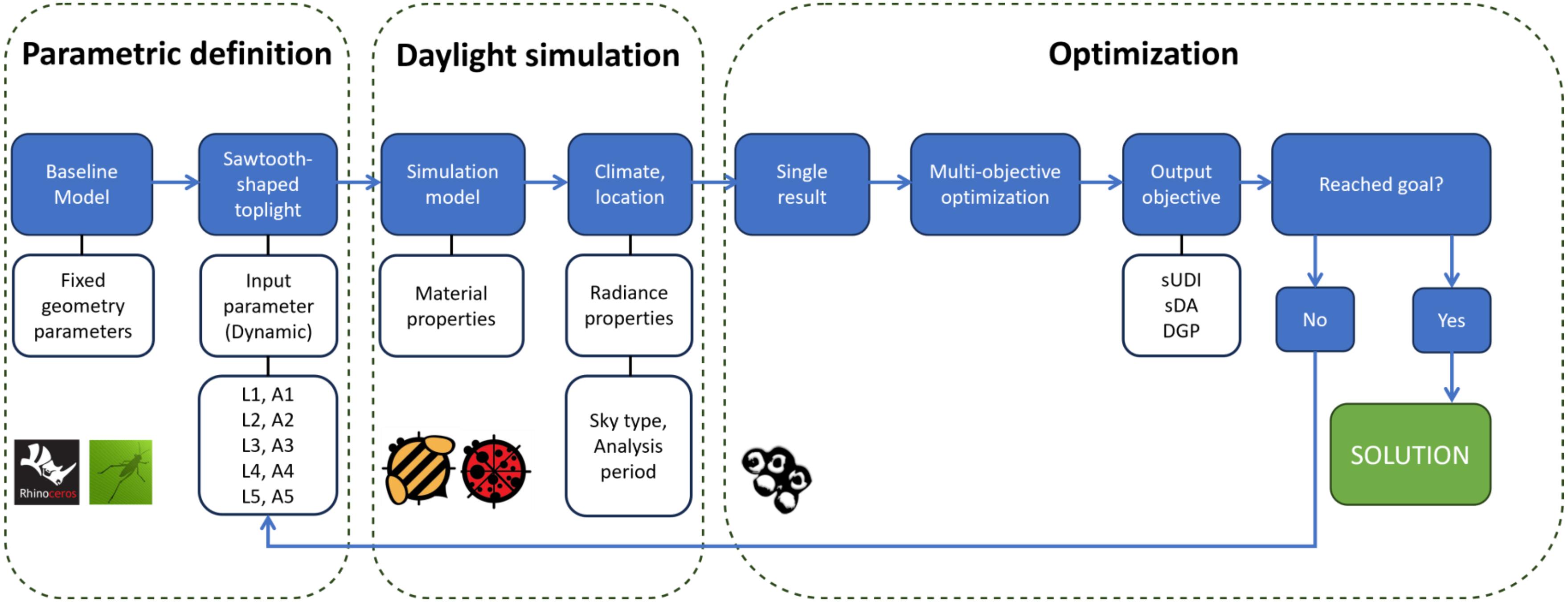

Figure 5.2 research workflow

5.2.2. sDA

Spatial Daylight Autonomy" (sDA) is a metric designed to assess the quality of natural daylight within building interiors. Initially introduced by Lisa Heschong in 2012, this index evaluates both the spatial and temporal aspects of daylight performance, making it a regional metric that reflects variations in natural light over time and space [109].

It measures the proportion of time within a certain period (typically a year) that the indoor space receives natural light that meets the desired illuminance levels. In the referenced study, the illuminance threshold was set at 300 lux or above, and only the illuminance performance on the floor was considered. This parameter serves as one of the optimization objectives in multi-objective optimization (MOO). The formula for sUDI is as follows (Eq.(2)), where A_{DA} is the area that receives illuminance levels of 300 lux or above during the specified occupancy time. A_{total} is the total area of the space considered.

$$sDA = \frac{A_{DA}}{A_{total}} \times 100 \tag{2}$$

Typically, the minimum threshold for daylight sufficiency is set at 50%, meaning that the value of x in the formula is replaced with 50. It's important to note that this relationship is expressed as a percentage. Designers utilize sDA to assess the daylighting performance of a space. A higher sDA percentage signifies greater daylight availability, which enhances occupant well-being and can significantly reduce the reliance on artificial lighting [110,111].

5.2.3. DGP

DGP stands for "Daylight Glare Probability", which is a metric used to evaluate the potential issue of glare from natural daylight in the interior of a building [112]. Glare should be assessed in areas where activities such as reading, writing, or screen viewing occur, and where it is not feasible to alter the user's position. This ensures that bothersome or intolerable glare is not experienced by the observer in these spaces. In this study, the objective is to minimize the annual DGP to the level of imperceptible glare, which is defined as being less than or equal to 0.35. This parameter serves as one of the optimization objectives in multi-objective optimization (MOO). The distribution of glare values is outlined in Table 5.2.1. The calculation formula for DGP is as follows (Eq.(3)):

$$DGP = a \cdot \left(\frac{L_b}{L_{b,ref}}\right) + b \cdot \left(\frac{L_s \cdot \omega_s}{L_b}\right)^{\log_{10}(L_s \cdot \omega_s)} + c \tag{3}$$

Where the parameters are defined as follows:

- L_b: Background luminance (cd/m^2)
- $L_{b,ref}$: Reference background luminance (cd/m^2)
- L_s: Source luminance (cd/m^2)
- ω_s: Solid angle of the source (sr, steradians)
- a,b,c: Empirical constants, typically determined from experimental data

By combining these parameters, the probability of glare for an observer in a given line of sight can be estimated. Optimizing design to minimize glare can enhance visual comfort.

Table 5.2.1 The range of DGP

Amount of glare	**Value of DGP**
Imperceptible glare	DGP ≥ 0.34
Perceptible glare	0.34 < DGP ≤ 0.38
Disturbing glare	0.38 < DGP ≤ 0.45
Intolerable glare	DGP > 0.45

5.2.4. ACI

ACI (Annual Cumulative Illuminance) is a metric used to assess the cumulative exposure to illuminance levels in a space over a specific time period, typically a year. It is a crucial metric in daylight analysis that quantifies the cumulative exposure to natural light across different seasons and times of the day. According to the Illuminating Engineering Society of North America (IESNA) [94], the recommended ACI for moderately sensitive materials, such as oil paintings and leather, ranges between 50,000 and 480,000 lux. It provides information about the distribution and consistency of illuminance levels throughout the year. In this study, ACI is not used as an optimization objective but solely for analyzing the variation of indoor illuminance intensity.

The formula for calculating ACI involves integrating the hourly illuminance values throughout the year. The calculation for ACI is given by the following equation (Eq.(4)), where 't' represents the total number of opening hours in a year for the museum, and 'Ei' denotes the illuminance recorded during the 'i-th' hour.

$$ACI = \sum_{i=1}^{t} E_i \tag{4}$$

5.3. Simulation tools

Computer simulations employed in this study utilized Rhinoceros, Grasshopper, Ladybug, Honeybee, and Octopus software. Rhinoceros served as the primary 3D modeling platform, enhanced by the parametric plugin Grasshopper for detailed modeling tasks. Grasshopper, integral to Rhinoceros, allowed for the adjustment of various skylight model shape parameters. The environmental analysis plugins Ladybug and Honeybee, integrated within Grasshopper, were used for processing and simulating architectural lighting models. Specifically, Ladybug facilitated the importation of EnergyPlus weather (EPW) data for analysis and visualization. Additionally, the genetic algorithm plugin Octopus was employed within Grasshopper to perform iterative processes, identifying the optimal solution set that balances lifecycle energy consumption and costs. The simulations and optimizations were conducted on a system equipped with an Intel (R) Core (TM) i9-10980XE (36 CPUs) 3.00 GHz processor, 128 GB RAM, and an NVIDIA GeForce RTX 3090 with 90 GB integrated RAMDAC GPU, running Windows 10 Pro 64-bit.

5.4. Parametric Modeling

As shown in Figure 5.3, all computer simulation models are based on a room that is 9.6 meters long, 9.6 meters wide, and 5.25 meters high. The baseline-01 model has a room orientation in the north-south direction and features a conventional sawtooth skylight design. The baseline-02 model has the room rotated 45 degrees in the horizontal plane and utilizes the same skylight design as baseline-01. The reason for the 45-degree angle is that it is the worst angle for the sawtooth-shaped toplight at which it is most likely to receive direct sunlight, which can lead to damage to the illuminated exhibit. The Optimized model has a room with the same orientation as baseline-02 and incorporates an optimized skylight design. Given that Ladybug and Honeybee do not fully support spline curve and spline surface, all curved surfaces must be transformed into planar surfaces.

Figure 5.4 illustrates the dynamic characteristics of the input parameters for the skylight system shape. The skylight shape is divided into four equal sections along the longer edge, with A1, A2, A3, A4, and A5 representing the angles between these five division points and the horizontal plane. L1, L2, L3, L4, and L5 represent the lengths that the skylight system extends from their corresponding angles. Finally, these five lines are lofted together to form a complete surface as the simulated generated skylight shape. Table 5.4.1 describes the dynamic range of all the input parameters.

Table 5.4.1 Dynamic-parameter range value

Parameter	Min	Max	Unit	Movement
L1	1.2	1.8	m	7
L2	1.2	1.8	m	7
L3	1.2	1.8	m	7
L4	1.2	1.8	m	7
L5	1.2	1.8	m	7
A1	0	5	degree	6
A2	0	5	degree	6
A3	0	5	degree	6
A4	0	5	degree	6
A5	0	5	degree	6

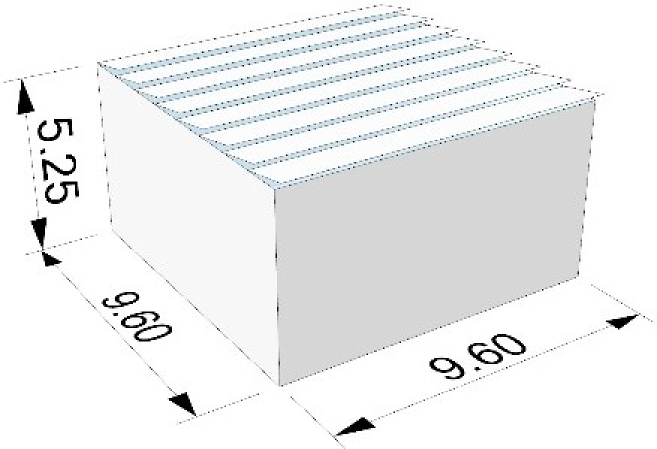

(a) Dimension of simulating room

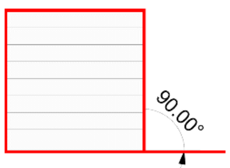

(b) Orientation of baseline-01.

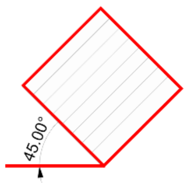

(c) Orientation of baseline-02

Figure 5.3 Dimension and orientation

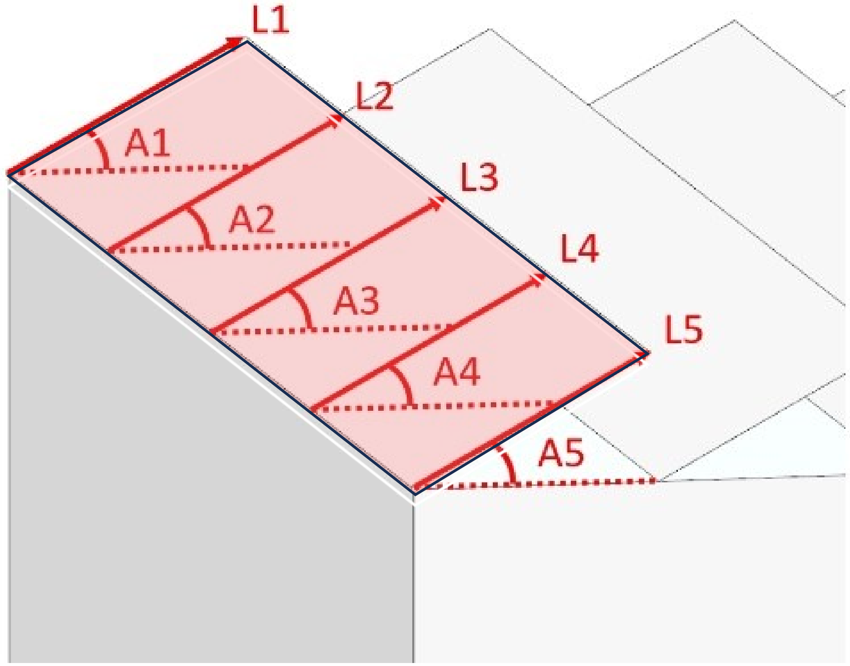

Figure 5.4 Dynamic parameters of shading.

5.5. Daylight simulation

5.5.1. Climate and Location

In this study, the simulation model was targeted at Kitakyushu, Fukuoka, Japan, located at 33°52'59.9916" N latitude and 130°52'59.9916" E longitude. Kitakyushu is situated in the southern part of Japan and experiences a moderate climate with no dry season and hot summers, classified under the Köppen climate classification as Cfa (Humid Subtropical Climate). Museum operating hours are set from 8 a.m. to 6 p.m. Tuesday through Sunday. For this simulation, the EPW file selected represents data from Fukuoka Airport, approximately 50 km from Kitakyushu. This EPW file, identified as a TMY3 (Typical Meteorological Year) file, contains meteorological data spanning from 1990 to 2010. The coordinates for this dataset are 33°35' N latitude and 130°27' E longitude, providing a close approximation of the climatic conditions at the museum's location.

5.5.2. Run daylighting simulation

The Ladybug plugin is specialized for daylight simulation. sUDI, sDA, and DGP simulations are utilized in a grid-based analysis to propagate daylight values. According to IESNA [94] standards, the average adult eye height in a museum is 1550mm, and the typical viewing distance from the wall is 1050mm. Consequently, the range for sensors on the wall is set within 0mm to 3000mm from the floor.

In the Ladybug Lighting Analysis plugin, light sensors are configured to measure, simulate, and analyze light conditions in and around buildings. This setup helps evaluate design decisions, enhance lighting effects, increase indoor comfort, and save energy. In this study, as illustrated in Figure 5.5, 81 sensors were installed on the floor, and 27 sensors were placed on each of the four walls at a height range of 0 to 3 meters. The daylight simulation's operating hours are set from 8 a.m. to 6 p.m., six days a week. Given the previously mentioned computer configuration, each simulation run takes approximately one and a half minutes.

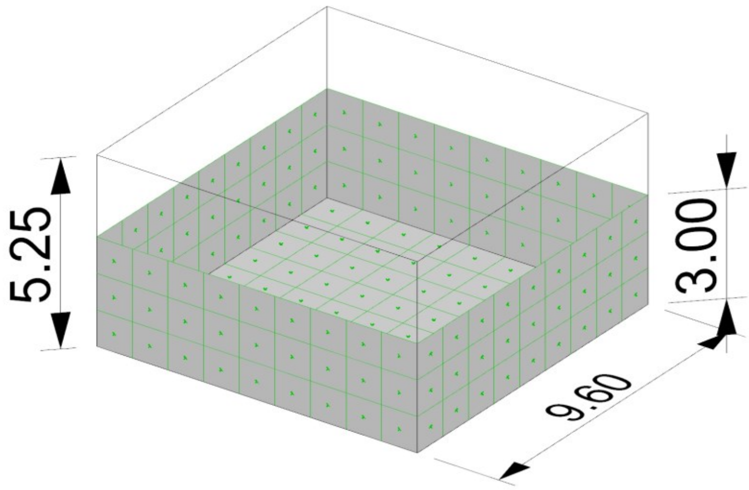

Figure 5.5 Sensor setting in the model.

5.6. Optimization Setting

5.6.1. Material properties

Before applying the established model to Ladybug and Honeybee for daylight simulation, it is necessary to set the materials for each component of the room. The materials primarily consider reflection, specularity, and transmission, as shown in Table 5.6.1 and Figure 5.6.

Table 5.6.1 Interior surface material properties

Surface	ρ	Specularity	Transmittance
Floor	0.379	0	
Wall	0.926	0	
Shading	0.8	0.9	
Glazing	0.5	0	0.5

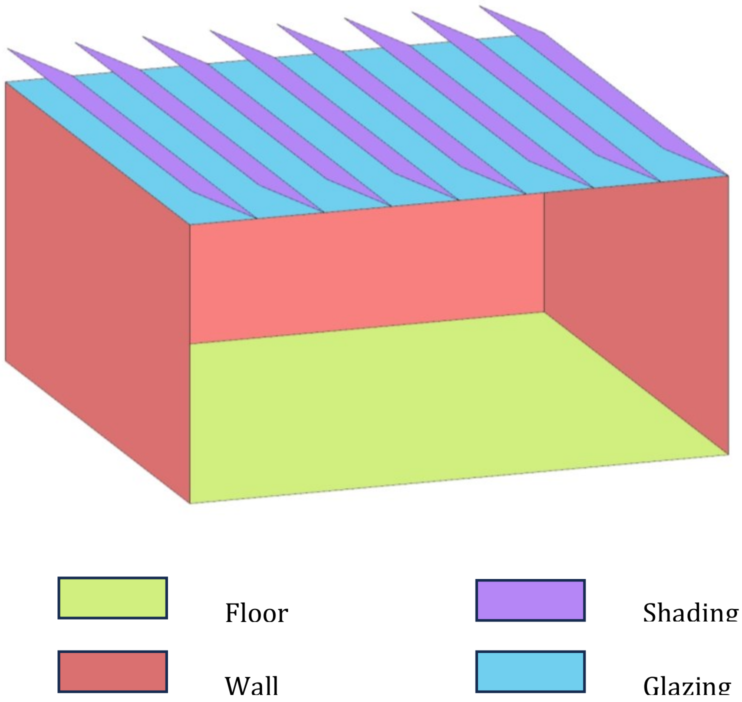

Figure 5.6 Interior surface material properties

5.6.2. Genetic algorithm and MOO

The Genetic Algorithm (GA) [113] is a robust computational optimization method that draws on the principles of natural selection and evolutionary biology. This technique utilizes computational processes such as replication, crossover, and mutation to iteratively evolve permutations and combinations of input parameters. The objective is to identify the most optimal solutions in an efficient manner, minimizing the number of iterations needed. GA excels at addressing complex optimization problems, particularly in situations where traditional methods may lack applicability or efficiency. One of the significant applications of Genetic Algorithms is in Multi-objective Optimization (MOO), which seeks to identify a spectrum of optimal solutions that balance conflicting objectives. By strategically adjusting these input parameters, MOO enables the harmonization of various interrelated design goals.

5.6.3. Daylight simulating setting

Even though the Honeybee Radiance plug-in detects light from multiple directions to obtain precise results, the use of diffuse indirect calculations and Monte Carlo sampling [114] can lead to slight variations in the results for each simulation test, even with identical genome group input parameters. Consequently, it is crucial to refine the daylighting simulation setup parameters to minimize result fluctuations. The settings for the annual daylighting simulation are detailed in Table 5.6.2.

Table 5.6.2 The annual daylight setting.

Parameter	Description	Value
-ab	ambient bounces	5
-ad	ambient divisions	15000
-as	ambient super-samples	2048
-dc	direct certainty	0.5
-dp	direct pretest density	256
-dr	direct relays	1
-ds	source substructuring	0.25
-dt	direct thresholding	0.25
-lr	limit reflection	6
-lw	limit weight	6.67E-07
-st	specular threshold	0.5

5.6.4. Octopus setting

Considering the multi-objective nature of this study, the mating between genomes in Octopus is highly complex. Therefore, Octopus needs to be configured to provide rapid feedback through building performance simulations and develop the most suitable design solutions. The interface settings for Octopus are described in Table 5.6.3.

Table 5.6.3 The Octopus Optimization setting

Parameter	Setting
Elitism	0.5
Mutation probability	0.2
Mutation rate	0.9

Crossover rate	0.8
Population size	100
Maximum generations	200
Record interval	1
Non-dominate ranking	HypE Reduction
Mutation strategies	HypE Reduction

5.6.5. Target value and fitness function

The aim of this study is to iteratively optimize the design variables (genomes) and correlate all outputs to potential solutions in a simultaneous discovery process. The results are then filtered based on the target values classified as the Pareto front. Octopus optimizes by minimizing each target value; thus, input numbers must be multiplied by minus one when a maximum value is desired as the optimization target. The primary objective is to maximize sUDI for all four walls in the room, while the other two objectives are to maximize sDA for the floor and minimize DGP for all four walls.

The following formula, shown in Eq.(5), is commonly used in research [14] to determine the fitness function value for each individual result in the Pareto front. Due to the involvement of multiple objectives, Multi-objective Optimization (MOO) often faces challenges in yielding a single optimal solution. Therefore, the fitness function can be used as a method to filter appropriate targets. These results are observed by identifying Pareto front individuals and grouping the specified regions on each axis.

$$
\begin{aligned}
FF_i &= (sUDI_i - sUDI_{min})C_1 - (sDA_i - sDA_{min})C_2 + (DGP_i - DGP_{min})C_3 \\
C_1 &= \frac{100}{sUDI_{max} - sUDI_{min}} \\
C_2 &= \frac{100}{sDA_{max} - sDA_{min}} \\
C_3 &= \frac{100}{DGP_{max} - DGP_{min}}
\end{aligned}
\tag{5}
$$

5.7. Analysis and Interpretation

Sensitivity analysis [115–118], widely adopted in numerous studies [57] concerning the built environment, was employed to identify the most influential variables. This analysis examines how changes in both quantitative and qualitative outputs can be attributed to different input parameters. By using sensitivity analysis, designers gain a deeper understanding of how each input parameter impacts the output objectives, enabling a more objective evaluation rather than relying solely on subjective judgments. The relationships between parameters and objectives are depicted using tornado plots and parallel coordinate plots.

5.8. Results

5.8.1. Optimization results

The sUDI, sDA, and DGP were measured and examined through daylight simulation and optimization. The optimization process concluded after 10 generations, resulting in 931 individuals, each characterized by embedded parameter values and objectives. The iteration results of individuals generated by Octopus are represented in a 3D scatter plot according to their corresponding objective values.

Figure 5.7 shows a three-axis 3D scatter plot filled with iteration results, depicting individuals developed in Octopus. These individuals are distributed as sequential points, positioned based on their objective values. The distribution in the graph illustrates the trend of optimal iteration movement, where individuals follow the search area of maximizing sUDI, maximizing sDA, and minimizing DGP. From Figure 5.7, it can be observed that the majority of the simulated results for sUDI are distributed within the range of 0% to 60%. The sDA values are distributed within the range of 0% to 100%, with a significant portion falling between 40% and 100%. Most of the DGP (Daylight Glare Probability) values are below 5%, while the remaining results with DGP values above 5% are not considered optimized results since their corresponding sUDI is 0. From this group of test results, a suitable optimization result is selected.

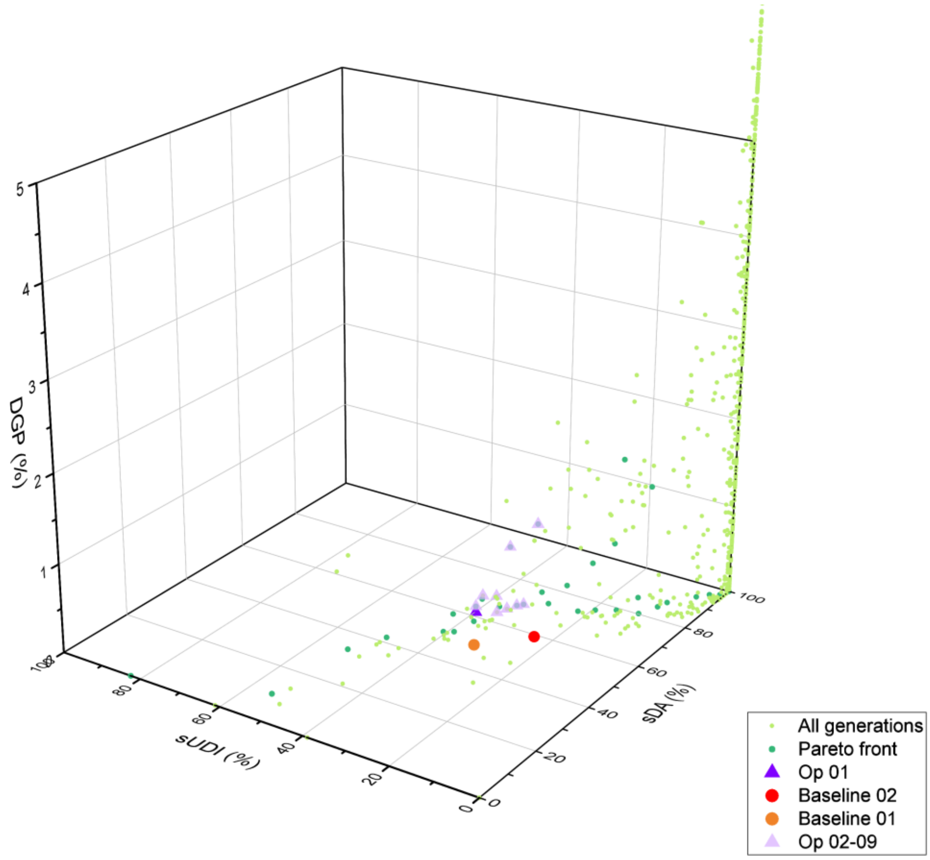

Figure 5.7 3D scatter plot based on the MOO

Figure 5.8, based on Figure 5.7, illustrates the relationship between each pair of objectives from three side views. In Figure 5.8 (a), as sUDI is maximized, sDA shows a decreasing trend. Figure 5.8 (b) shows that when sUDI is maximized, DGP exhibits a decreasing trend. In Figure 5.8 (c), as sDA increases, DGP also increases continuously. However, neither Figure 5.8 (b) nor (c) present a clear linear function relationship.

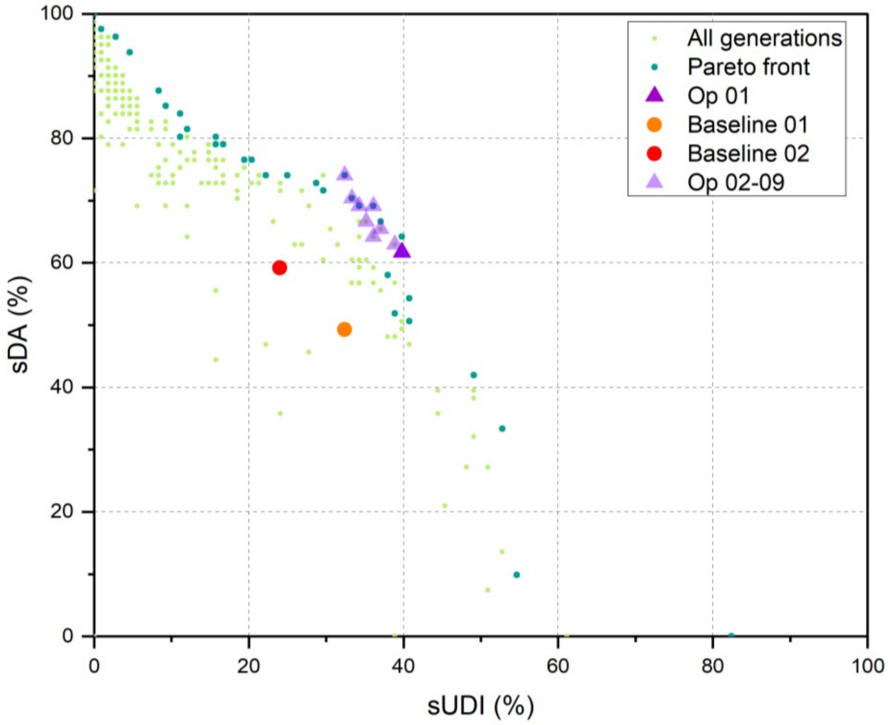

(a) sDA & sUDI

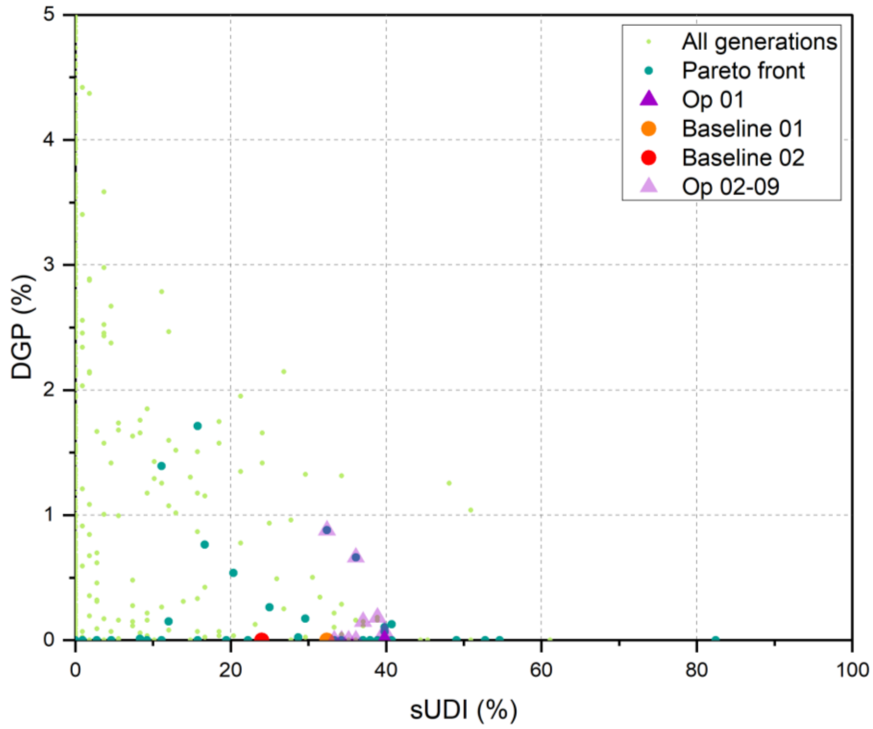

(b) DGP & sUDI

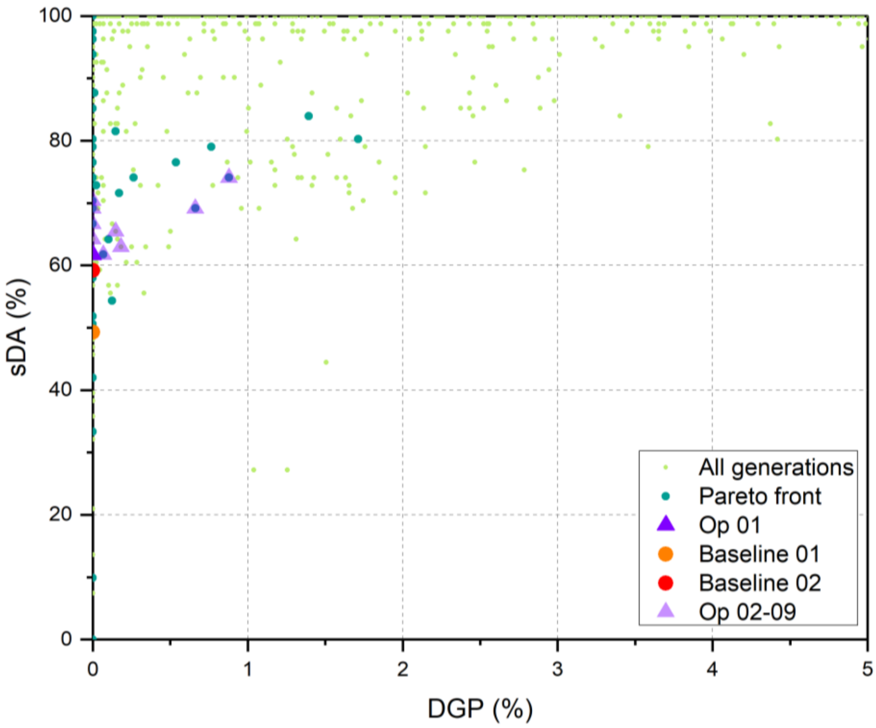

(c) sDA & DGP

Figure 5.8 Scatter plot showing the relationships among the objectives

5.8.2. Parameters to objectives (sensitivity analysis)

Investigating the impact of variations in different variables within the skylight system on the objectives is crucial. The aim is to identify key factors that require focused attention during the design phase to optimize daylight utilization. Figure 5.9 presents a Parallel Coordinate Plot of parameters versus objectives to illustrate how parameters are distributed when setting percentages for sUDI, sDA, and DGP. In this analysis, 53 valid results were selected, meeting the criteria of sUDI greater than 25%, sDA greater than 25%, and DGP less than 5%. These data are considered valid for further analysis. The color variation along the curves indicates sUDI values, with a lighter yellow shade representing higher sUDI values and a darker purple shade indicating lower sUDI values.

Regarding input parameters, among these valid results, the lengths L1, L2, L3, L4, and L5 almost covered the range between 1.2 and 1.8 meters. For angles A1, A2, A3, A4, and A5, input values within the range of 0 to 30 degrees are more likely to produce valid data. Notably, valid data is only generated when A1 and A5 are set to either 0 degrees or 10 degrees.

Sensitivity analysis was conducted using Linear Regression (LR). The Standardized Coefficients Beta test was utilized to assess the impact of each parameter on the target value and to evaluate the correlation among variables. LR uses the Fit Model command to estimate parameters, identifying each standardized target as a response variable and defining each standardized parameter as a factor influencing model construction.

Figure 5.10 shows the sensitivity ranking of design variables, highlighting the importance of each parameter relative to their respective targets. The absolute values of the sensitivity data indicate a positive relationship between parameters and objectives. The range is typically from 0 to 1, with values closer to 1 indicating higher sensitivity, meaning that minor adjustments to this parameter would lead to significant changes in the target value. According to the chart, for the optimization target sUDI, A5, A1, and A4 occupy the first, second, and third positions in sensitivity with values of -0.548, -0.271, and 0.202, respectively. L1, L3, and L5 occupy the last three positions in sensitivity with values of -0.026, 0.03, and 0.033, respectively. For the optimization target sDA, A5, A4, and A1 rank first, second, and third in sensitivity with values of 0.597, 0.301, and 0.251, respectively. L1, L3, and L4 rank last with values of -0.004, -0.008, and -0.021, respectively. For the optimization target DGP, A2, A1, and A3 rank first, second, and third with values of 0.589, 0.499, and 0.258, respectively. L4, L1, and L5 rank last with values of 0.009, -0.022, and -0.026, respectively.

Combining Figure 5.9 and Figure 5.10, it is evident that the angles A1, A2, A3, A4, and A5 of the skylight shading system are more sensitive to various parameters than the lengths L1, L2, L3, L4, and L5. Among them, A5 and A1 have the greatest impact on sDA and sUDI, with optimal effects at values of 0 degrees or 10 degrees. As the value of A5 increases, the value of sDA increases while the value of sUDI decreases. Although A2 does not have as significant an impact on sUDI and sDA as A5 and A1, it has the greatest impact on DGP.

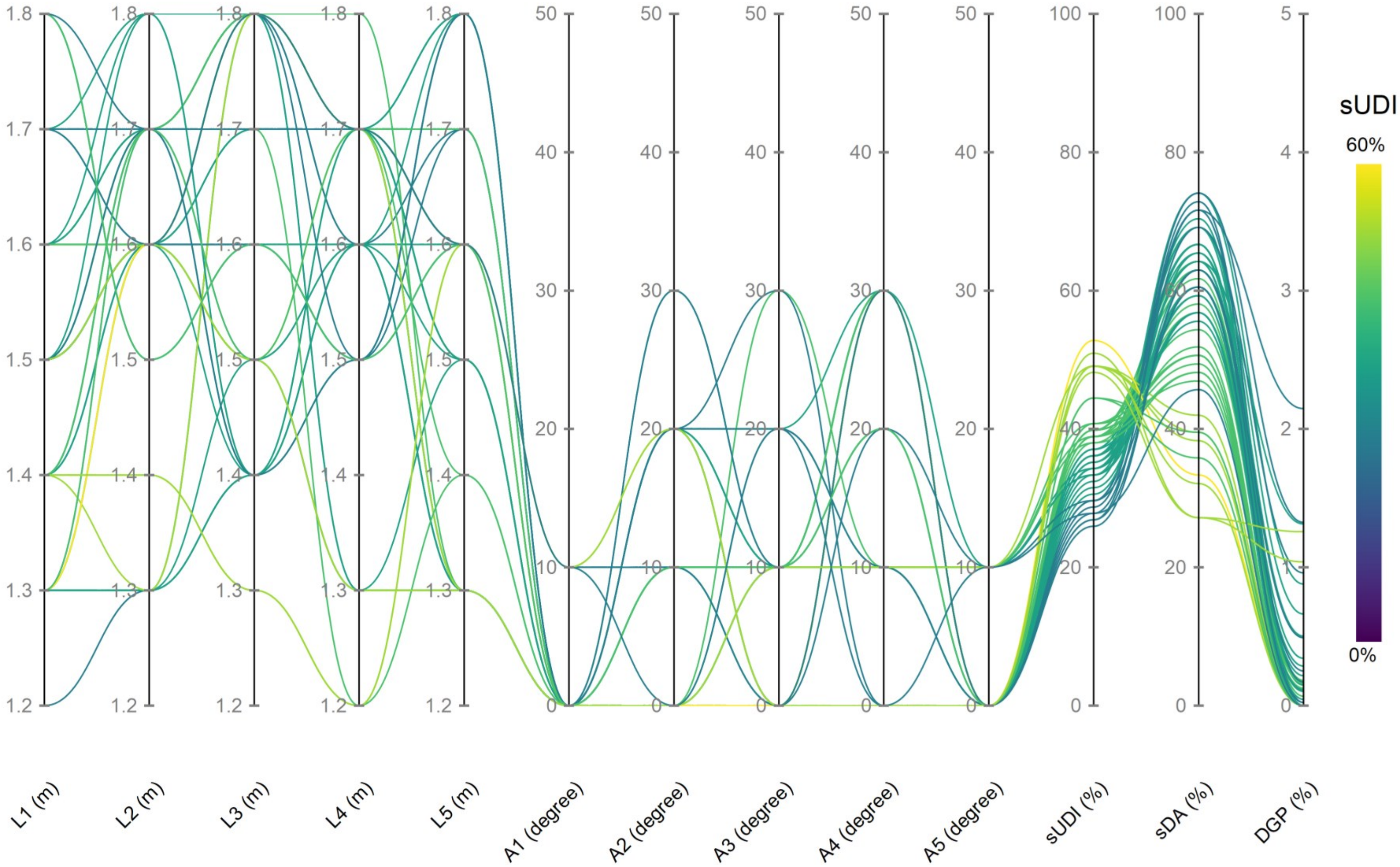

Figure 5.9 Parallel co-ordinate plot of the line of parameter values and objective values.

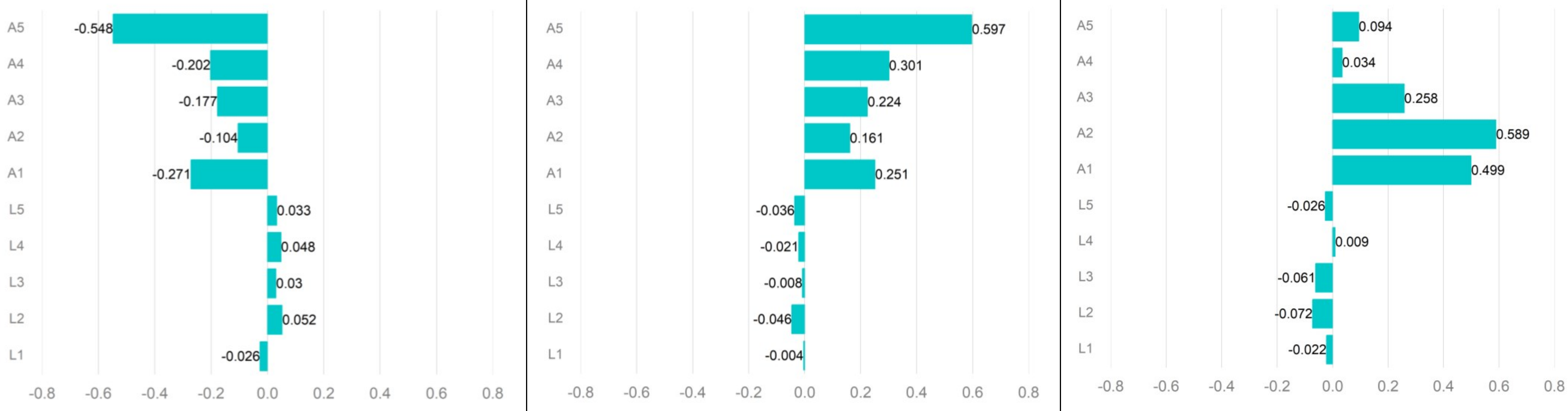

(a) Parameters for sUDI

(b) Parameters for sDA

(c) Parameters for DGP

Figure 5.10 Sensitivity analysis of the design variables.

5.8.3. Baseline-model simulation

Figure 5.11 shows the simulating results and the shapes of baseline-01, baseline-02, and Op-01. From Figure 5.11, it is evident that there are significant differences in daylighting between north-south orientation and non-north-south orientation under the same skylight shading system. In baseline-01, more daylight accumulates on the south-facing wall of the building. In baseline-02, more daylight accumulates on the east-facing wall of the building. In the ACI comparison, the indoor environment in baseline-02 experienced much higher year-round illumination than baseline-01. Consequently, the region meeting UDI requirements shifted from the north side in baseline-01 to the northwest side wall in baseline-02. The sUDI decreased from 32.4% to 24%, while the sDA increased from 49.3% to 59.2%. This indicates that the building's orientation has a significant impact on daylight performance under the same daylight environment and the same sawtooth skylight system, with north-south-oriented museums having better lighting conditions compared to non-north-south-oriented museums. This phenomenon may be due to the increased direct sunlight entering the building when its orientation is rotated. However, both baseline-01 and baseline-02 have a significant drawback in that the indoor illumination is not uniform, resulting in substantial differences in lighting conditions across different corners of the same building.

5.8.4. Optimal solutions

Figure 5.9 illustrates the morphology, sUDI, sDA, and DGP for baseline-01, baseline-02, and Optimized results. By comparing these three models, the patterns of lighting variations between them are identified and explored. To facilitate identification and comparison, the range of analytical chart legend values for the three scenarios is standardized. The ACI legend values range from 400,000 lux to 3,800,000 lux, and the UDI and DA legend values both range from 0 to 100%. From the figure, it can be seen that the sUDI and sDA values of the Optimized result are higher than the benchmark-01 and benchmark-02. Baseline-01 outperforms baseline-02 in sUDI; and underperforms baseline-02 in sDA.

Table 5.8.1 and Figure 5.12 show the attributes of the top 10 optimal solutions based on fitness function values. As shown in the table, the percentage range for the target sUDI among the top 10 solutions varies from 39.81% in model Op-01 to 33.33% in model Op-02. Although all ten results are below 50%, they show a significant improvement compared to baseline-01 and baseline-02. The percentage range for sDA spans from 74.07% in model Op-05 to 61.73% in model Op-07. All ten results are above 50%, marking a notable improvement over baseline-01 and baseline-02. The DGP percentage ranges from 0.88% in model Op-05 to 0% in models Op-01, Op-02, Op-03, Op-08, Op-09, and Op-10. All optimized models show significant improvements in DGP compared to baseline-01 and baseline-02.

Regarding the input parameter range, L1, L2, L4, and L5 did not show any concentrated distribution trends. However, L3 appeared seven times with a value of 1.8 meters. The values for A1, A2, A3, A4, and A5 exhibited more distinct distribution trends. A1 consistently had a value of 0 degrees. For A2, values ranged between 0 degrees and 20 degrees, with 20 degrees appearing five times, 10 degrees four times, and 0 degrees once. A3 values ranged between 0 degrees and 20 degrees, with 0 degrees appearing five times, 10 degrees four times, and 20 degrees once. A4 consistently had a value of 30 degrees. A5 consistently had a value of 0 degrees. This establishes clear guidelines for the angles of A1, A4, and A5 at 0 degrees, 30 degrees, and 0 degrees, respectively, providing specific direction for determining the shading panel angles.

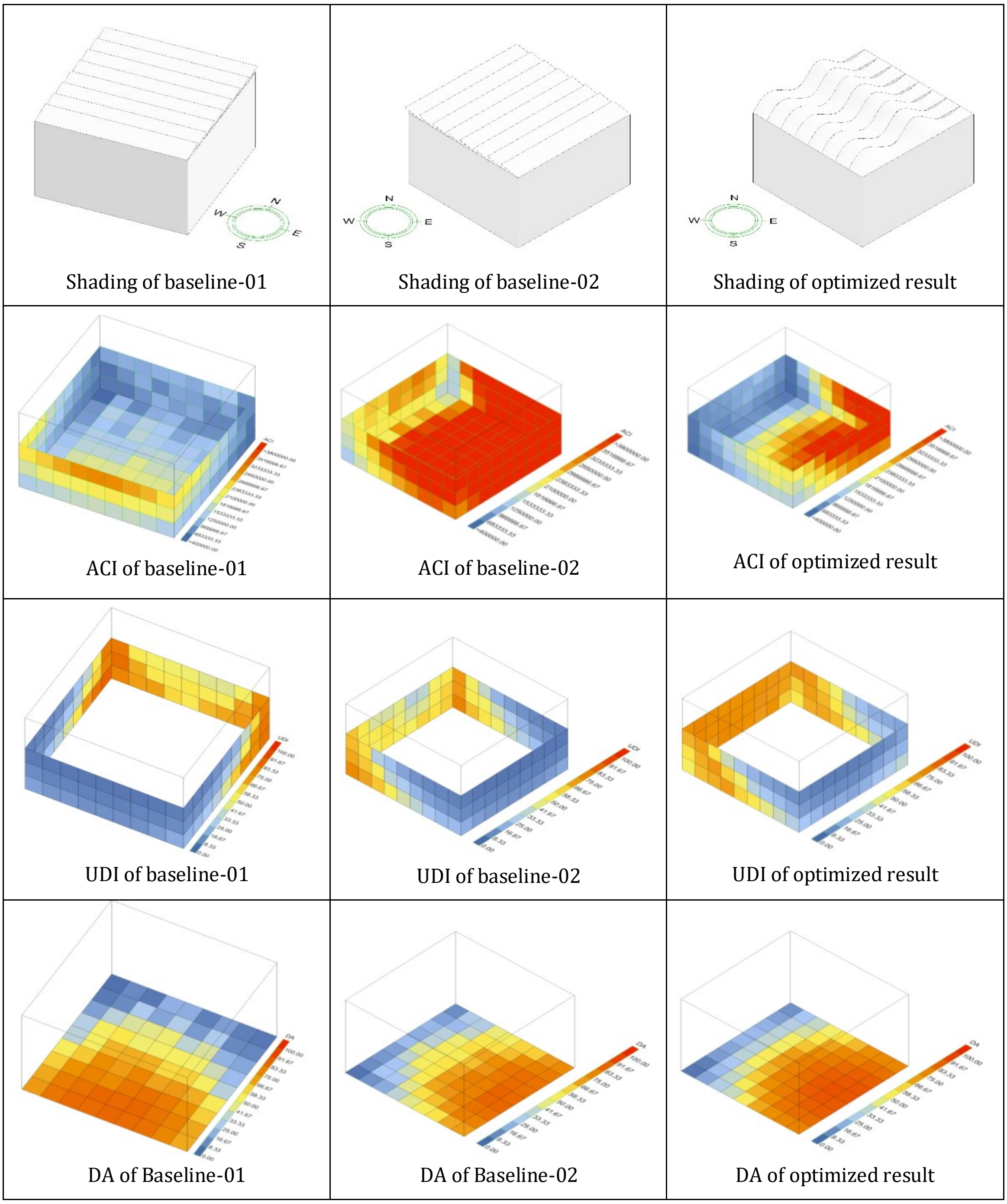

Shading of baseline-01 | Shading of baseline-02 | Shading of optimized result

ACI of baseline-01 | ACI of baseline-02 | ACI of optimized result

UDI of baseline-01 | UDI of baseline-02 | UDI of optimized result

DA of Baseline-01 | DA of Baseline-02 | DA of optimized result

Figure 5.11 The simulating result of baseline-01, baseline-02 and Op-01 result.

Table 5.8.1 Comparison of baseline models and optimized result parameters

Model	Input parameters										Output objectives		
	L1	L2	L3	L4	L5	A1	A2	A3	A4	A5	sUDI	sDA	DGP
Baseline-01	1.5	1.5	1.5	1.5	1.5	10	10	10	10	10	32.40%	49.30%	1.01%
Baseline-02	1.5	1.5	1.5	1.5	1.5	10	10	10	10	10	24.00%	59.20%	3.27%
Op-01	1.5	1.6	1.8	1.7	1.5	0	20	0	30	0	39.81%	64.20%	0.00%
Op-02	1.4	1.6	1.8	1.7	1.8	0	0	20	30	0	33.33%	70.37%	0.00%
Op-03	1.6	1.6	1.8	1.3	1.3	0	10	10	30	0	34.26%	69.14%	0.00%
Op-04	1.3	1.3	1.8	1.6	1.3	0	20	0	30	0	36.11%	69.14%	0.66%
Op-05	1.3	1.3	1.4	1.6	1.3	0	20	0	30	0	32.41%	74.07%	0.88%
Op-06	1.4	1.7	1.8	1.3	1.5	0	20	0	30	0	37.04%	65.43%	0.15%
Op-07	1.6	1.7	1.8	1.7	1.5	0	20	0	30	0	39.81%	61.73%	0.07%
Op-08	1.8	1.5	1.6	1.5	1.6	0	10	10	30	0	35.19%	66.67%	0.00%
Op-09	1.5	1.6	1.7	1.7	1.5	0	10	10	30	0	36.11%	65.20%	0.00%
Op-10	1.4	1.6	1.8	1.7	1.3	0	10	10	30	0	34.26%	65.97%	0.00%

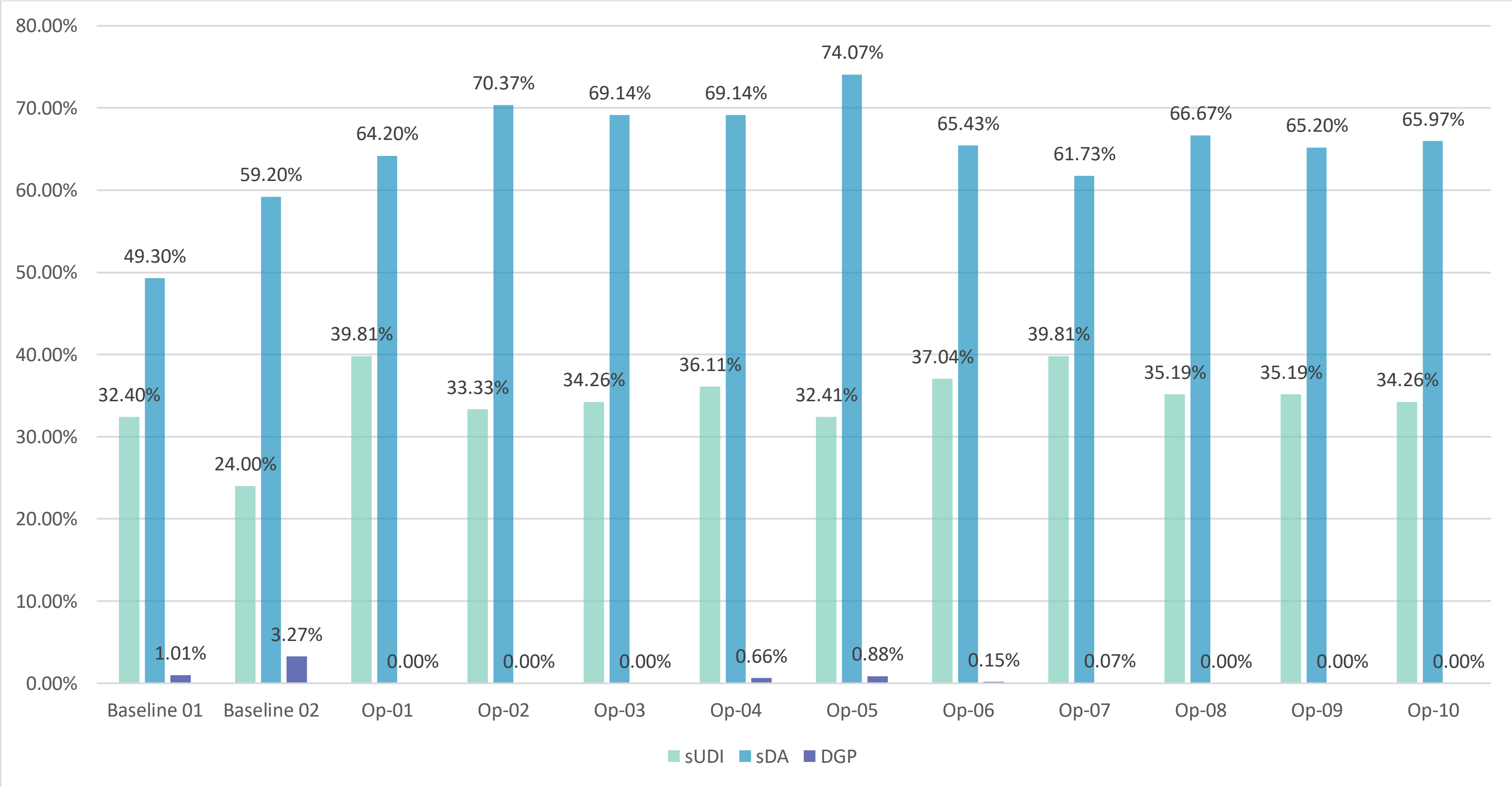

Figure 5.12 Comparison of sUDI, sDA, DGP.

5.8.5. Comparison of DGP

Figure 5.13 illustrates the annual distribution of daylight glare probability (DGP) on an hourly basis for the baseline-01, baseline-02, and Op-01 models scenario. In each chart, the X-axis represents the months (from January to December), and the Y-axis represents the hours of the day (from midnight to midnight, 24-hour format). Each chart corresponds to a different scenario: baseline-01, baseline-02, and Op-01. The different sections and colors in the chart represent the following information:

- Green: Imperceptible Glare.
- Light Green: Perceptible Glare.
- Yellow: Disturbing Glare.
- Red: Intolerable Glare.
- White: Night, indicating no daylight.

From Figure 5.13 (a), it can be seen that the instances of glare are concentrated between 4 PM and 6 PM from April to August. Figure 5.13 (b) shows that the instances of glare are concentrated between 2 PM and 4 PM from April to August. As the building orientation deviates from the north-south direction, the duration of glare and the frequency of intolerable glare significantly increase. In contrast, Figure 5.13 (c) demonstrates that with the optimization of the skylight shape, instances of glare are nearly eliminated.

From these three charts, we can derive the following insights and conclusions:

Across all three charts, most time periods are green or light green, indicating that for the majority of the time, the glare is either imperceptible or perceptible, thus having a minimal impact on users. Yellow and red areas are mainly concentrated around midday and during the summer months, suggesting that daylight glare is more severe during these times.

Baseline-01 and Baseline-02 exhibit a noticeable amount of yellow and red areas, especially around midday in the summer, indicating that glare during these periods can be disturbing or even intolerable for users. The Op-01 chart shows a significant reduction in yellow and red areas, demonstrating that the operational scenario is more effective in reducing daylight glare compared to the baseline scenarios.

All three charts show that during the winter months (from October to February), there is almost no yellow or red area, indicating minimal daylight glare. In the summer months (from April to September), particularly around midday, the glare problem is more pronounced.

The operational scenario Op-01 is significantly more effective in reducing both disturbing and intolerable glare compared to the baseline scenarios baseline-01 and baseline-02, especially during the peak times in summer and around midday. Therefore, Op-01 is a more suitable solution for mitigating the impact of daylight glare.

(a) Hourly plot of annual DGP of baseline-01

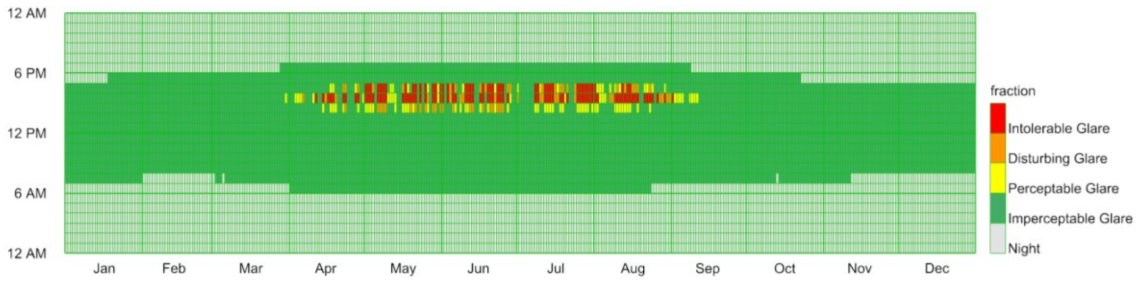

(b) Hourly plot of annual DGP of baseline-02

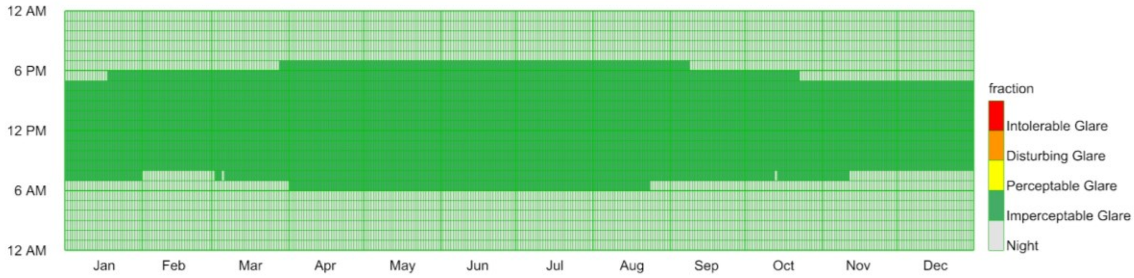

(c) Hourly plot of annual DGP of Op-01

Figure 5.13 Hourly plot of annual DGP of baseline-01, baseline-02 and Op-01.

5.8.6. Baseline-02 and Optimized Result

Under the same orientation, however, there is also a noticeable difference in daylight performance between baseline-02 and the Optimized result under different skylight system coverage. Although the higher ACI values are concentrated on the east-facing wall of the building in both models, the optimized scenario has significantly less year-round insolation than baseline-02. The UDI in the optimized results is significantly higher than the baseline -02 because of the significant decrease in the overall indoor ACI. The overall acceptable sUDI also increases from 24% in baseline-02 to 39.81% in the Optimized result. The optimization results in a slight increase in DA value from 52.20% in baseline-02 to 61.73%.

5.8.7. Baseline-01 and Optimized Result

These two comparisons have limited reference value because the skylight systems and orientations are different. After optimization of skylight system, it is speculated from the ACI perspective that the year-round light near the west wall is brighter than baseline-01 while the year-round light near the south wall is higher. The sUDI improved from 32.40% in baseline-01 to 39.81% after optimization. sDA improved from 49.30% before to 61.73% after optimization.

5.9. Discussion and Conclusion

This study addresses the natural light illumination effect of sawtooth-shaped toplight in a museum by simulating the daylighting situation and using genetic algorithms for multi-objective optimization and quickly determining the optimization results by using Grasshopper, Ladybug, Honeybee, Octopus and other software.
With the same daylighting environment and the same sawtooth skylight system, the orientation of the building has a significant impact on daylighting performance. The orientation of the opening of the sawtooth roof light is limited by the structure of the building itself. The indoor natural illumination of polar oriented museums is better than that of non-polar oriented buildings under the conventional sawtooth-shaped toplight. The glass openings in the skylights will be oriented in the same direction as the building. This results in sunlight entering the room through the openings of the sawtooth-shopped toplight when the building is oriented in a non-polar orientation. Therefore, a skylight with a non-polar orientation will reduce the light effect in the room.

The skylight design of the Sawtooth Rooflight significantly reduces glare in the room, thereby increasing the viewing comfort of the observer. At the same angle, the overall natural lighting of the interior can be significantly increased by optimizing the shape of the sunshade such as the wave form. Even for polar oriented museums, better lighting can be achieved by using similarly shaped skylight sunshades. Further experiments are needed to determine how to improve and optimize the skylight system and how much of an increase it can give.

Compared to the traditional approach, by iterating using a genetic algorithm, computer simulations can rapidly determine the optimal type of lighting to achieve the desired light harvesting goals, resulting in a significant improvement in interior lighting performance. The results of this study are expected to inform the design decision-making process based on design performance in the early stages of design.

Chapter 6. Parametric Design and Multi-Objective Optimization of Daylight Performance in Gallery Skylight Systems: A Case Study on the High Museum Expansion

6.1. **Introduction**

Museum buildings, serving as essential venues for the preservation, display, and transmission of cultural heritage, hold significant value in contemporary civilized society. Proper lighting design is pivotal in better presenting exhibits, enhancing visitor interest, and ensuring visual comfort. Compared to artificial lighting, natural light not only enriches the perception and experience of viewers [119], but also reduces the overall energy consumption and operational costs of buildings [120,121], and accurately reproduces the true colors and intricate details of objects [122]. However, in the realm of museum design, addressing the susceptibility of exhibits to ultraviolet and infrared radiation extends beyond enhancing visitor experience [123,124]. Various institutions and organizations have consolidated recommendations for crafting an optimal lighting environment suited to different types of exhibits, taking into account their material sensitivity [94].

In the early design stages, the design of shading systems can be facilitated through computer modeling, daylighting simulation, and Multi-objective Optimization (MOO). Many researchers have been utilizing parametric computation simulation and GA optimization to study the performance of shading devices, aiming to harness the potential of daylight and achieve high efficiency and optimization in visual comfort. Shirzadnia et al. [58] focused on the old boiler room of a factory in the Mazandaran historical textile factory in Iran, employing a novel design optimization approach that integrates manual methods with the SPEA-2 optimization algorithm to enhance the daylight efficiency of the study subject. El-Abd et al. [125] conducted research on a shopping center in Cairo, investigating different skylight design configurations and implementing multi-criteria optimization to reduce the area of excessive illumination by more than 50% inside the commercial space. Cabeza-Lainez et al. [126] optimized the original skylight performance of a school in Denmark, improving indoor daylight comfort. Laouadi et al. [127] developed a method for designing atrium skylights in cold climates through computer simulation, aimed at predicting and improving indoor environment caused by solar radiation. However, simulation studies on museum daylighting that concurrently consider the visual comfort and the lighting restrictions for protecting specific exhibits are currently limited.

This study delves into the potential of point skylight systems in museum design for enhancing visual comfort and protecting exhibits, utilizing computer modeling, daylighting simulation, and optimization through Genetic Algorithms. It exemplifies this through an analysis of the High Museum of Art expansion project designed by Renzo Piano in Atlanta.

The primary objectives of this research are threefold:

-To identify suitable skylight design combinations that ensure both the protection of wall-mounted exhibits and the comfort of viewing, by employing daylighting simulation and genetic algorithm optimization.

-To investigate the impact of various skylight parameters on the indoor lighting performance of galleries under specified conditions.

-To further explore, based on the optimization scheme, the impact of the optimized skylight on the changes in the gallery's indoor illumination environment.

6.2. Materials and Method

6.2.1. General overview

The research began with an initial phase focused on formulating the research problem and defining daylight metrics as the primary objectives. The second stage entailed the modeling process, which included developing both the baseline and the original building models, along with the parametric definition of the point-style skylight. In this phase, the functionality of the modeling components was integrated into a unified parametric definition framework. The third phase encompassed the development of a daylight and view simulation system. Models established in the preceding phase were transformed into simulated objects for daylighting simulation, incorporating the physical properties of the model, climatic data, and urban context. The fourth stage involved the optimization process, where the system generated a range of design alternatives, converging on a preferred alternative based on predefined optimization criteria. This iterative process explored various design possibilities by dynamically altering combinations of parameters, thereby influencing the configuration of the point skylight system. The final phase entailed a thorough analysis and interpretation of the data derived from the optimization processes, which involved close observation and a sensitivity analysis to elucidate the influence of each parameter. The basic workflow of the research is depicted in Figure 6.1.

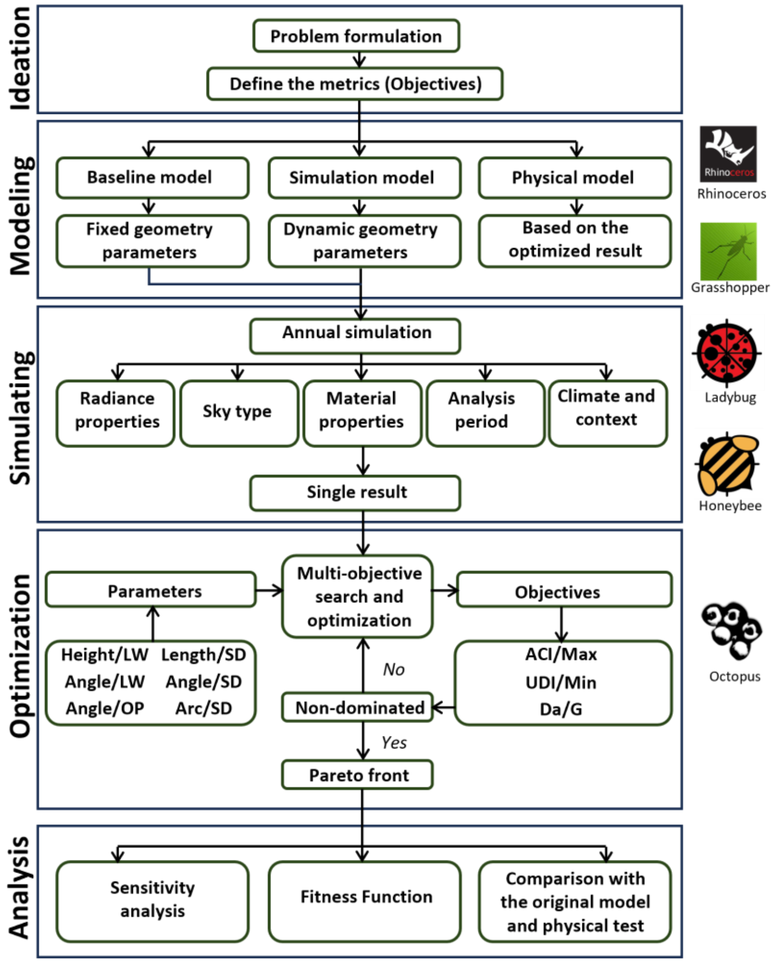

Figure 6.1 Research workflow

6.2.2. Case study

The High Museum of Art Expansion, designed by Renzo Piano and completed in 2005, is one of the most important museums in the United States. It is located in Atlanta at latitude 33.78 °N, Longitude -84.38 °W. This is a three-story building with a floor area of 29,000m². As shown in Figure 6.2, on the third floor of the exhibition hall, a grid of 1000 circular light scoops atop the ceiling provides ample natural light to illuminate the interior space. The skylight system, combined with the building's overall orientation and window placements, ensures that the interior spaces are bathed in a balanced light throughout the day. This careful orchestration of natural light transforms the museum into a dynamic space where the quality of light changes with the time of day and the seasons, creating a constantly evolving experience for visitors.

Renzo Piano’s design philosophy for the High Museum of Art Expansion also emphasizes sustainability. The extensive use of natural light reduces the need for artificial lighting, thereby lowering energy consumption and operational costs. This sustainable approach aligns with contemporary environmental standards and contributes to the building's LEED certification. The thoughtful integration of natural light into the museum’s design not only enhances the aesthetic appeal but also demonstrates a commitment to environmental stewardship. The approach to the High Museum of Art Expansion serves as a model for future museum designs, demonstrating how natural light can be harnessed to create visually stunning and environmentally sustainable spaces. The project highlights the potential for architectural innovation in achieving both aesthetic and functional goals, setting a new standard for museum design.

The combination of these advanced architectural features and the strategic use of natural light underscores the importance of considering environmental factors in the design process. By doing so, architects can create spaces that are not only beautiful and functional but also sustainable and energy-efficient.

Figure 6.2 The high museum of art expansion by Renzo Piano [128]

6.3. Ideation

6.3.1. Daylight metrics (Objectives)

The daylight metrics and criteria were selected based on the suggestions among daylight researchers and on recent advances in daylight measurement. Three daylight metrics are used to ensure that legitimate daylight values and assessments for occupant visual comfort were achieved. The definitions and formulas of these three metrics will be introduced next.

ACI

Annual Cumulative Illuminance (ACI), the first indicator, refers to the total amount of illuminance received over the course of a year at a specific location or within a particular space. It is a metric used in daylight analysis to quantify the cumulative exposure to natural light throughout different seasons and times of the day. According to IESNA [14], the required ACI for moderately sensitive materials, like oil painting and leather, is limited to between 50,000 and 480,000 Lux. The equation for calculating Annual Cumulative Illuminance (ACI) involves integrating the hourly illuminance values over the course of a year. The formula for ACI is as follows (Eq.(6)), where 't' is the total number of opening hours in a year for the museum. 'Ei' is the illuminance measured during the number 'i' hour.

$$ACI = \sum_{i=1}^{t} E_i \tag{6}$$

UDI

In addition to the ACI, which is used to assess annual light levels, the second metric known as the Useful Daylight Illuminance (UDI) introduced by Nabil and Mardaljevic [129] is used. The UDI is a modification of " Useful Daylight Illuminance " and is an annual time series of absolute values of predicted illuminance under real skies generated based on standard meteorological datasets.

The traditional daylight factor method's interpretive simplicity is retained in this metric, which uses the time-varying daylight illumination values over a full year to calculate UDI. UDI represents the percentage of occupied time annually when the internal horizontal illumination from daylight at a specific point falls within a designated comfort range. According to [130], UDI assesses both the occurrence of useful daylight levels and the frequency of excessive daylight levels that could cause discomfort for occupants.

In practice, UDI is employed to pinpoint an illuminance range that avoids being too dim or excessively bright [102], which is very important for museum daylight design and this research. Another approach to calculating this metric involves averaging all the measured points within the analyzed area to derive a final value, known as Average Useful Daylight Illuminance. The calculated range for average UDI typically falls between 50 and 200 lux for art gallery. The formula for UDI calculation aims to ensure that, on average, 50% of the occupied hours throughout the year have illuminances within the specified range. This target reflects a commitment to providing substantial useful daylight, promoting energy savings, occupant well-being, and sustainable building design.

The formula for the Useful Daylight Illuminance is delineated below (Eq.(7)). In this context, 't' signifies the aggregate number of hours the museum remains open to the public throughout the calendar year. The term '$E_{Lower\ limit}$' denotes the minimal threshold of illuminance deemed acceptable, whereas '$E_{Daylight}$' represents the cumulative illuminance recorded over the entire year. Additionally, '$E_{Upper\ limit}$' is indicative of the maximal threshold of illuminance beyond which conditions are considered excessively bright for the intended purposes.

$$UDI_{wall} = \frac{\sum_i wf_i \cdot t_i}{\sum_i t_i} \in [0,1]$$

$$UDI_{wall}\ with\ wf_i = \begin{cases} 1 & if\ E_{Lower\ limit} \le E_{Daylight} \le E_{Upper\ limit} \\ 0 & if\ E_{Daylight} < E_{Lower\ limit}\ \text{or}\ E_{Daylight} > E_{Upper\ limit} \end{cases} \quad (7)$$

DA

The third metric used for optimization is Daylight Autonomy (DA), which is a long-term and local index [102] defined as the percentage of the occupied hours of the illuminance of sole daylight is below the minimum threshold [131].

DLA is a simulation method that evaluates the daylight quantity associated with any given hour, geographic location, and sky condition on an annual basis [132,133].

The formulation for Daylight Autonomy (DA) is presented as follows (Eq.(8)), wherein 't' means the cumulative number of hours during which the museum is accessible to the public over the span of an annum. 'E_{Limit}' delineates the minimum threshold of illuminance that is considered acceptable, while '$E_{Daylight}$' constitutes the aggregate illuminance ascertained throughout the museum's operational hours over the course of the entire year.

$$DA_{floor} = \frac{\sum_i (wf_i \cdot ti)}{\sum_i ti} \in [0,1]$$
$$with \quad wf_i = \begin{cases} 1 & if \ E_{Daylight} \geq E_{Limit} \\ \frac{E_{Daylight}}{E_{Limit}} & if \ E_{Daylight} < E_{Limit} \end{cases} \tag{8}$$

6.3.2. Daylight standard and criteria

This study utilizes the IESNA [94] standards as the daylight target values for the annual daylight simulation, specifically tailored to the lighting conditions required by different materials, as shown in Table 6.3.1. The research sets the light threshold range using oil paintings made of medium-sensitive material as the subject. The ACI (Annual Cumulative Illuminance) is required to be below 480,000 lux, while the UDI (Useful Daylight Illuminance) and DA (Daylight Autonomy) need to be at least 50%. A summary table of the related limit values will be displayed in Table 6.3.2.

Table 6.3.1 Typical Categories of Light Sensitivity

Material/exhibit	Sensitivity	Recommended lux level
Most ceramics, glass, stone and metals	Low	200 lux or more

Oil and tempera paintings, undyed leather, lacquer, wood, horn, bone, ivory, minerals and modern black and white photographs	Medium	150–200 lux
Watercolor paintings, dyes, stamps, manuscripts, prints and drawings, vulnerable textiles, photographs, fur and feathers, miniatures, transparencies and unprimed thinly colored paintings on canvas	High	50 lux or less

Table 6.3.2. Limit values of daylight metrics

Name of daylight metrics	Minimal threshold	Maximal threshold
ACI	-	480000 lux
UDI	50 lux	200 lux
DA	300 lux	-

6.3.3. Simulation tools

Computer simulations utilized Rhinoceros, Grasshopper, Ladybug, Honeybee, and Octopus. This study employs Rhinoceros, a commercial software, as the 3D modeling platform, along with its parametric plugin Grasshopper for modeling. Grasshopper, a principal plugin of Rhinoceros, is used to adjust various shape parameters of the skylight model. The architectural lighting models are then processed and simulated using the Ladybug and Honeybee environmental analysis plugins within Grasshopper. The Ladybug plugin is utilized for importing EnergyPlus weather (EPW) data for data analysis and visualization. Furthermore, the genetic algorithm plugin Octopus is used within the Grasshopper platform for iteration to determine the optimal solution set that balances lifecycle energy consumption and lifecycle costs. Daylighting simulation and optimization were run on a platform equipped with an Intel (R) Core (TM) i9-10980XE (36 CPUs) 3.00 GHz processor, 128 GB RAM, and an NVIDIA GeForce RTX 3090 with 90 GB integrated RAMDAC GPU, on Windows 10 Pro 64-bit.

6.4. Parametric Modelling

6.4.1. The Baseline model and fixed parameters

The purpose of the baseline model is to assess the effect of the interior daylighting environment without a skylight system and with a skylight system of identical dimensions to the original case. It serves as a comparison for the results from subsequent optimizations. Baseline-01 is a virtual mock-up box measuring 9.6m in length, 9.6m in width, and 5.25m in height, designed as a workspace without a roof, oriented along the North-South axis with the façade facing south. This setup simulates year-round insolation without a roof. Building upon baseline-01, baseline-02 incorporates a skylight system based on the reference building's dimensions to evaluate how the original skylight system enhances daylighting in the room compared to baseline-01 [128]. The building's plan is illustrated in Figure 6.3 (a), and the detailed dimensions of baseline-01 and baseline-02 are depicted in Figure 6.3 (b). The dimensions of the models, including the height, length, and width of the baseline models, are fixed parameters. Given that Ladybug and Honeybee do not fully support spline curve and spline surface, all curved surfaces must be transformed into planar surfaces, as demonstrated in Figure 6.3 (c).

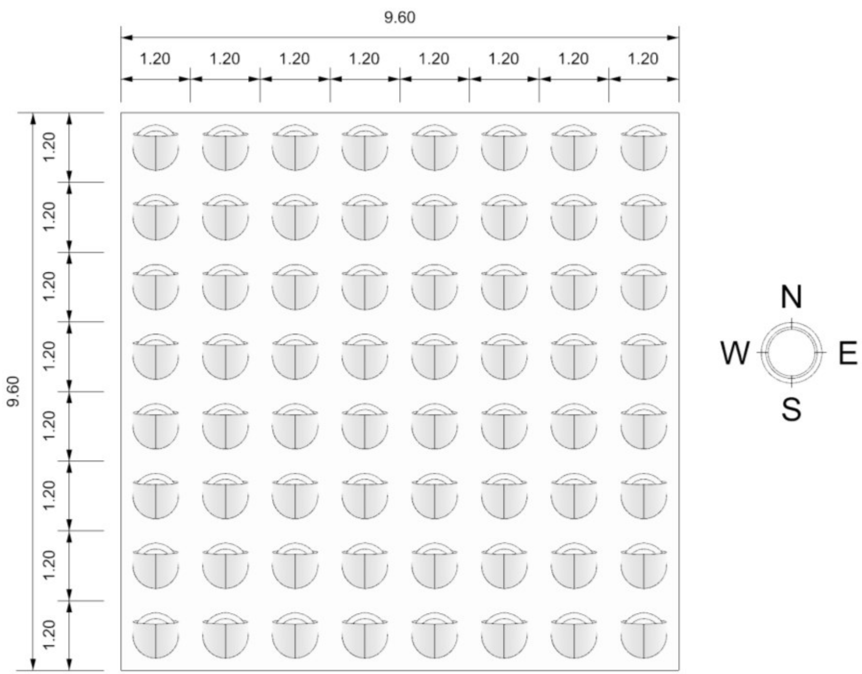

(a) Plan and orientation of the model

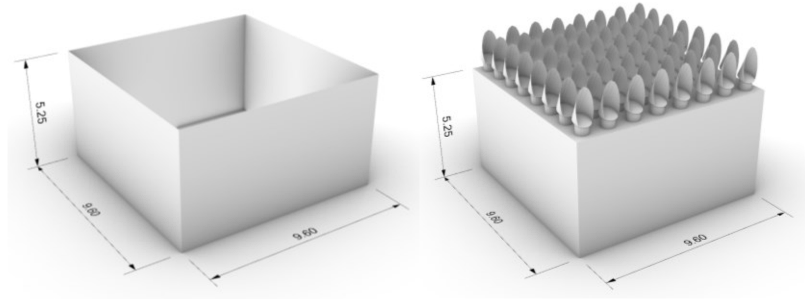

(b) Dimension of baseline-01 and baseline-02

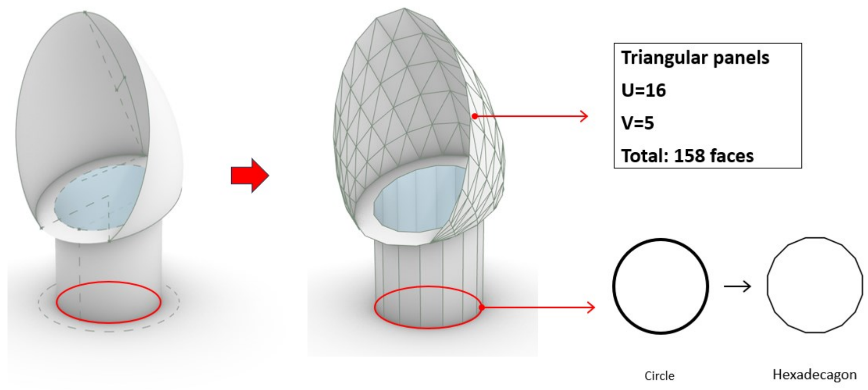

(c) Simplified logic of the model

Figure 6.3 Basic simulation modeling

6.4.2. Skylight shading and parameters

The skylight system consists of two parts, including the design of the ceiling below the roof, and the design of the shading system above the roof. This study simplifies the skylight system by examining only the design of the shading system above the roof while keeping the design of the ceiling below the roof unchanged.

Figure 6.4 (a) marks the portions of the skylight system that do not participate in optimization and have fixed dimensions in this study; while Figure 6.4 (b) displays the parts of the skylight system subject to optimization, highlighted with red lines and red text indicating the parameters to be optimized. Such a skylight system consists of six main components: the height of the light well Height/LW, the angle of the aperture at the top of the light well Angle/LW, the opening angle of the shading panel Angle/OP, the length of the shading panel Length/SD, the angle between the shading panel and the horizontal plane Angle/SD, and the curvature of the shading panel Arc/SD. In Ignacio Acosta's study, it is proposed that the curved shape results in an approximate 3.5% increase in average daylight factors compared to the rectangular shape [19].

Therefore, Arc/SD is an additional parameter set in this study to control the shape of shading and study on the natural light effect in the room. By moving the arc created by the midpoint of d in a direction perpendicular to d, the arc is used as a section to determine the curvature of the surface of the shading. To simplify the total possible iterations, the value range for each dynamic input parameter was set, as shown in Table 6.4.1.

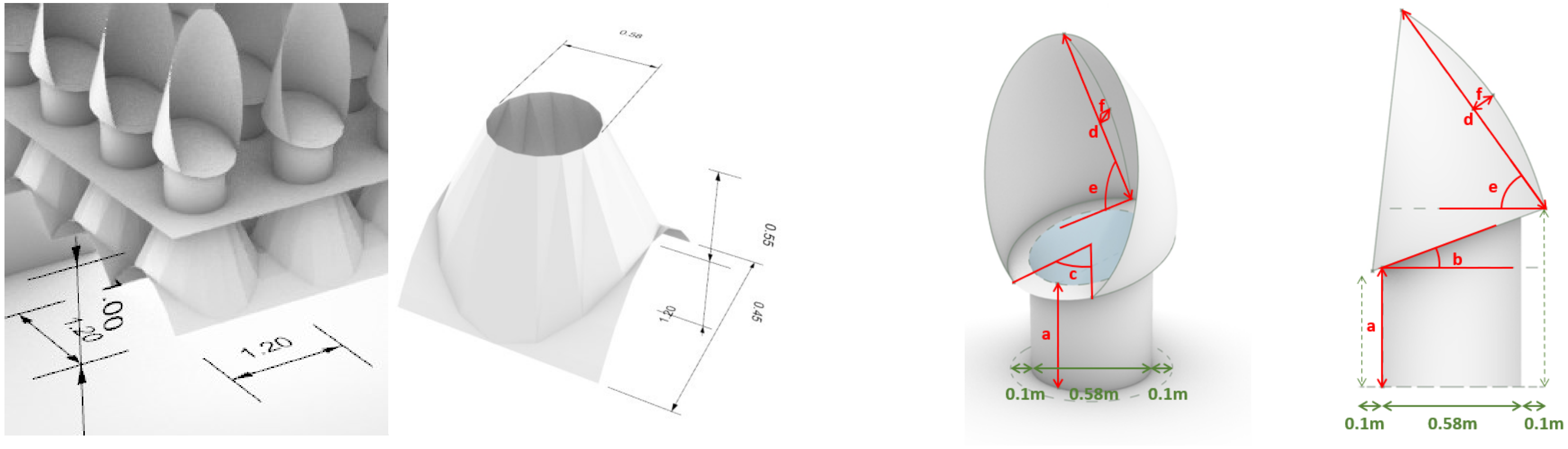

(a) Fixed dimension of skylight (b) Dynamic dimension of skylight

Figure 6.4 Dynamic and fixed dimension of skylight

Table 6.4.1 Dynamic-parameter range value

Name	Parameter	Min	Max	Unit	Movement
a	Height/LW	0.3	0.7	Meter	4
b	Angle/LW	0	40	Degree	4
c	Angle/OP	50	130	Degree	8
d	Length/SD	0.7	1.5	Meter	8
e	Angle/SD	40	90	Degree	10
f	Arc/SD	-0.3	0.3	Meter	6
	Total possible iteration				61440

Material properties and building programme

Radiance Material is necessary for the daylight calculation in Ladybug's tools. The Grasshopper geometry had to be concreted to a Honeybee surface and zone. The Radiance Color Picker offered by Jaloxa [134] and adopted in ref [135] is used to modify the surface model. Radiance Opaque Material and Radiance Glass Material were utilized to represent the geometric surface. The transmittance values used for all materials in the models are presented in Figure 6.5 and Table 6.4.2.

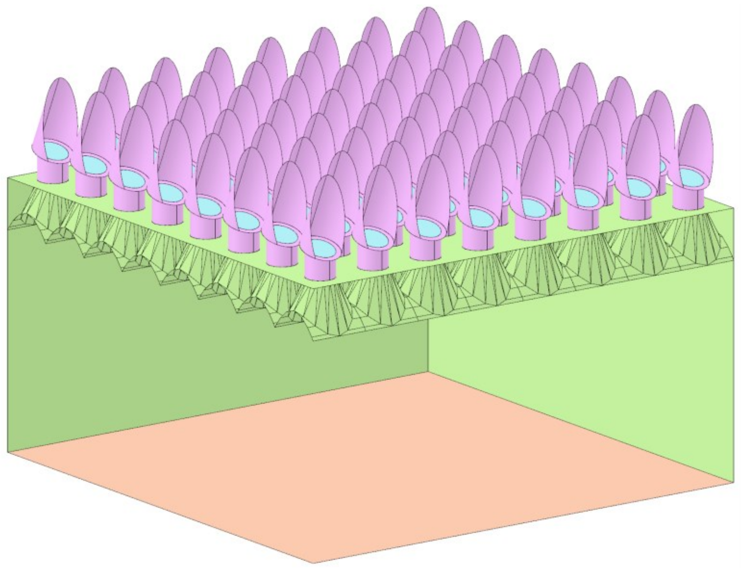

Figure 6.5 Materials of building

Table 6.4.2 Interior surface reflection and transmission properties.

Surface	ρ	ρR	ρG	ρB	Specular-ity	Roughness
Natural oak	0.379	0.379	0.379	0.379	0	0
SW 7757 white paint	0.926	0.926	0.926	0.926	0	0
Aluminium	0.8	0.8	0.8	0.8	0	0
Double pane low-e glass*	0.5	0.5	0.5	0.5	0	0

*For glass, the value should be read as transmittance τ

6.5. Daylight simulation

6.5.1. Climate and context

The "EPW" (EnergyPlus Weather) file format is specifically designed for use with the EnergyPlus simulation tool, but it can also be used with other building performance simulation software capable of reading EPW files. Although the proposed methodology can be applied anywhere EPW data is provide, in this research, the simulation model was intended to be located in Atlanta, Georgia, the United States at 33°44′ north latitude and 84°23′ west longitude, which is the city where the building was originally located. Atlanta is in the southeastern United States and has a Temperate, without dry season, Hot summer climate according to the Koppen climate classification system [136]. However, there was no EPW file located directly at the original building location, so Fulton County airport, 12km from the original address, was chosen. The selected EPW file is identified as a TMY3 file, embodying the Typical Meteorological Year data spanning from 1991 to 2005. The geographical coordinates for this dataset are positioned at a latitude of 33°44′ north and a longitude of 84°31′ west longitude.

6.5.2. Run daylighting simulation

The Ladybug plug-in is dedicated to simulating daylight. $ACI_{480000lx}$, $UDI_{50\text{-}200lx}$, DA_{300lx} simulations were used in a grid-based analysis to propagate daylight values. According to IESNA [94] requirements, the average adult eye height in a museum is 1550mm and the average viewing distance from the wall is 1050mm, so the range of sensors on the wall is set within a limited range of 800mm to 2300mm from the floor as shown in Figure 6.6. The hours of operation of the daylighting simulation are set at 8 a.m. to 6 p.m., six days a week. Based on the computer configuration environment previously mentioned, the duration of each simulation is approximately one and a half minutes.

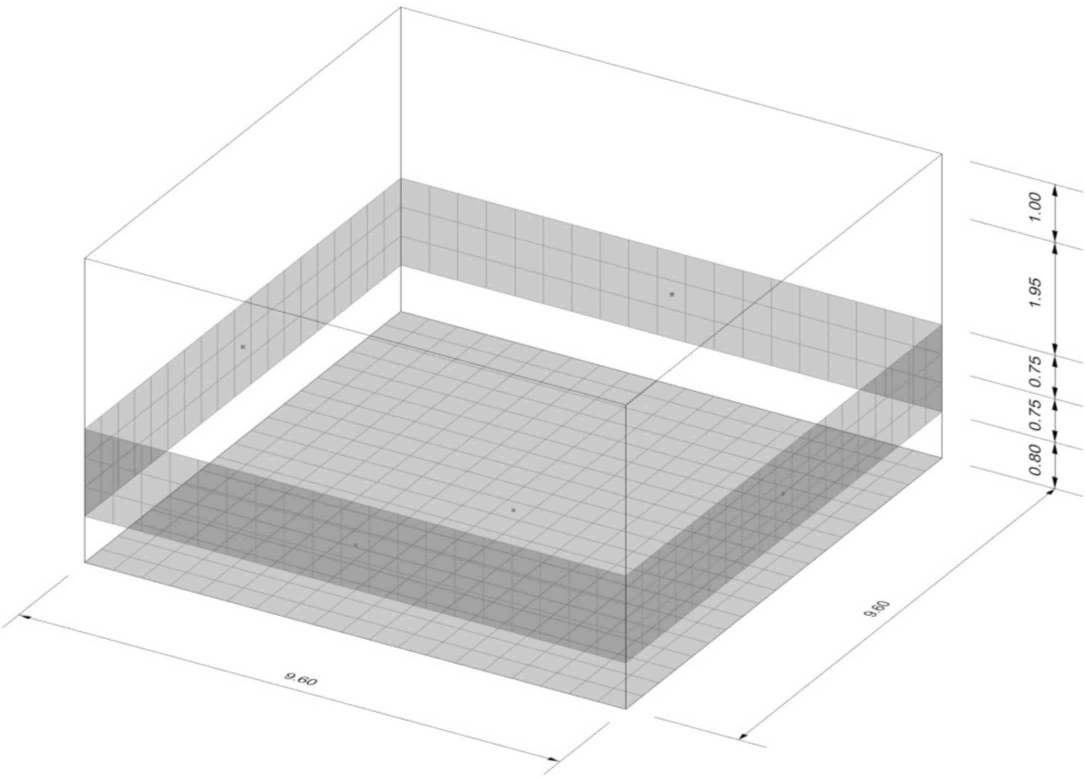

Figure 6.6 Sensors of simulating model

6.6. Optimization

6.6.1. GA and MOO

The Genetic Algorithm (GA) is a highly efficient computational optimization algorithm that draw inspiration from the concepts of natural selection and evolutionary biology [137]. By employing computational processes such as replication, crossover, and mutation to evolve the permutations and combinations of input parameters, the goal is to filter out the optimal results in the most effective manner with the fewest iterations [138]. GA is adept at tackling complex optimization challenges, particularly in scenarios where traditional methods may falter in terms of applicability or efficiency [139]. A prominent application of Genetic Algorithms lies in Multi-objective Optimization (MOO), which aims to uncover a range of optimal solutions that negotiate between conflicting objectives. Through strategic adjustment of these input parameters, MOO facilitates the synchronization of diverse, interrelated design objectives.

6.6.2. Optimization setting (Algorithm setting)

As a commonly used GA plugin, Octopus contains both the Strength Pareto Evolutionary Algorithm (SPEA-2) and the Hypervolume Estimation Algorithm (HypE) for its capacity to identify optimal solutions among a range of search objectives, making it a preferred tool for multi-objective optimization in building studies [14,51,66,67,72,140–146]. The study by Bader and Zitzler [147] demonstrates that the HypE algorithm surpasses other evolutionary algorithms in addressing multi-objective optimization challenges, thereby establishing it as the optimization method for this research. Khidmat's study of the multi-objective optimization effort informs the setup of the Octopus interface, as detailed in Table 6.6.1 [57].

Table 6.6.1 The Octopus optimization setting.

Parameter	Setting
Elitism	0.5
Mutation probability	0.2
Mutation rate	0.9
Crossover rate	0.8
Population size	100
Maximum generations	200
Record interval	1
Non-dominate ranking method	HypE Reduction
Mutation strategies	HypE Reduction

6.6.3. Target value and fitness function

The aim of this study is to optimize the process iteratively designing variables (genomes) and correspond all outputs to possible solutions in a simultaneous discovery process. The findings are then filtered according to the target values classified as Pareto front. octopus optimizes by dragging each target value to the minimum, so that the input numbers should be multiplied by minus one when a maximum value is required as the optimization target. The objective to be minimized is ACI_{MAX}, the maximum value of $ACI_{480000lx}$ for all four walls in the room, and other two objectives to be maximized are UDI_{MIN}, the minimum value of $UDI_{50\text{-}200lx}$ for all four walls, and DA_{300lx} for the floor.

The following formula shown in (Eq.(9)) is commonly used in the research [14,71,72] to determine the fitness function value for each individual result in the Pareto front. Due to the involvement of comparisons among multiple objectives, Multi-objective Optimization (MOO) often struggles to yield a singular optimal solution. Consequently, the Fitness function can serve as a method to help filter appropriate targets. Those results were observed by finding Pareto front result individuals and grouping the specified regions on each axis.

$$
\begin{aligned}
&FF_i = (UDI_i - UDI_{min})C_1 - (ACI_i - ACI_{min})C_2 + (DA_i - DA_{min})C_3 \\
&C_1 = \frac{100}{UDI_{max} - UDI_{min}} \\
&C_2 = \frac{100}{ACI_{max} - ACI_{min}} \\
&C_3 = \frac{100}{DA_{max} - DA_{min}}
\end{aligned}
\tag{9}
$$

Although the Honeybee Radiance plug-in detects light from multiple directions to obtain accurate results, due to the use of diffuse indirect calculations and Monte Carlo sampling [114],even if the input parameters of the genome group are the same, the results of each simulation test will show subtle differences. Therefore, it is important to improve the daylighting simulation setup parameters to reduce the fluctuation of the results. The setting of annual daylighting simulation is presented in Table 6.6.2**.**

Table 6.6.2 The annual daylight setting.

Parameter	Description	Value
-ab	ambient bounces	6
-ad	ambient divisions	25000
-as	ambient super-samples	4906
-dc	direct certainty	0.75
-dp	direct pretest density	512
-dr	direct relays	3
-ds	source substructuring	0.05

-dt	direct thresholding	0.15
-lr	limit reflection	8
-lw	limit weight	4.00E-07
-st	specular threshold	0.15

6.7. Analysis and Interpretation

Sensitivity analysis [115], adopted by several research [57,116,148,149] of the built environment, was utilised to find the most influential variable. Sensitivity analysis is the study of how output, for both quantitatively and qualitatively, changes are assigned [150]. Sensitivity analysis is used to understand how each input parameter affects the output objective, thus helping designers to evaluate more objectively rather than relying solely on subjective judgments. The data of relationship between parameters and objectives are presented in tornado plots and parallel co-ordinate.

6.8. Physical model test

Calibration and validation of computer simulation data will be conducted through testing a physical model constructed at a 1:12 scale based on the dimensions of the computer model. The purpose of fitness physical model is to evaluate the variation of wall illuminance within a room from morning to afternoon, essentially the capacity for daylight changes throughout the day. Since the material properties of the physical test and the computer simulation model differ, calibration and validation will focus on the trend or pattern of light changes rather than exact values.

Measurements will be taken from 9 AM to 4 PM on November 21, 2023, under clear sky conditions, with data recorded hourly. The location is in Kitakyushu City, Fukuoka Prefecture, Japan, with coordinates at 33°53'N 130°53'E, nearly identical in latitude to Atlanta. The same daylighting simulation will also be conducted on the computer model under identical climatic conditions, date, and time. The physical illuminance results obtained from the actual model will be compared with the light simulation results from the computer model to analyse the feasibility of the optimization approach.

As shown in Figure 6.7, the simulated room is presented at a 1:12 scale to the actual computer model, oriented north-south, and includes 25 designated test points. The model's skylight system is made of 3D-printed polylactic acid, with its shape determined by the final optimized results. The model's walls and floor are constructed from 3 mm thick styrene board, covered with opaque sheets to prevent light transmission through the surrounding styrene material. For onsite physical illuminance measurements, a TR-74Ui Illuminance UV Data Logger was used.

(a) Mock-up model

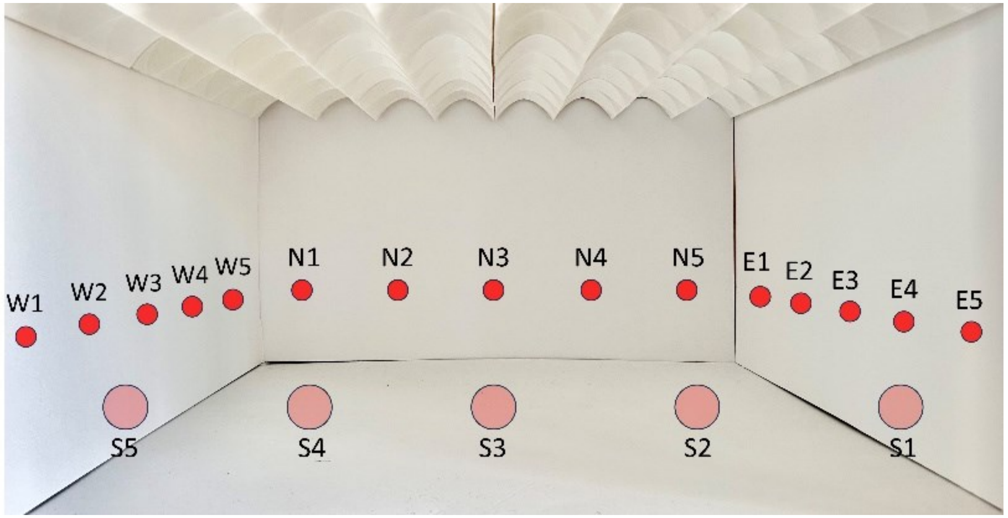

(b) Interior of model and sensors position

Figure 6.7 Mock-up room experimentation and on-site measurement

6.9. Results

6.9.1. Optimization results

$ACI_{480000lx}$, $UDI_{50\text{-}200lx}$, DA_{300lx} were measured and examined through daylighting simulation and optimization. The optimization process concluded after 49 generations, resulting in 4987 individuals, each characterized by embedded parameter values and objectives. The iteration results of individuals generated by Octopus are represented in a 3D scatter plot according to their corresponding objective values.

Figure 6.8 (a) presents a three-axis 3D scatter plot filled with iteration outcomes, depicting individuals developed in Octopus. These individuals are spread as sequential points, positioned based on their objective values. The distribution in this graph illustrates the trend of optimal iteration movement, where individuals follow the search area of UDI/Min maximum, DA/G maximum, and ACI/Max minimum. Figure 6.8 (b) displays Pareto front solutions derived from the latest generation of optimization processes. The global distribution was narrowed down to the maximum ACI/Max limit of 480,000 lux, the minimum UDI/Max limit of 50%, and the minimum DA/G limit of 50%.

Figure 6.9 illustrates the relationship between each pair of objectives from three side views, building upon Figure 6.8. In Figure 6.9 (a), as UDI/Min aims for maximization, DA/G decreases to around 50%; when DA/G increases or decreases based on a 50% criterion, UDI/Min significantly declines. Figure 6.9 (b) shows that ACI/Max is approximately 400,000 lux when UDI/Min is maximized; and UDI/Min significantly decreases as ACI/Max deviates from 400,000 lux. In Figure 6.9 (c), the relationship between ACI/Max and DA/G follows a pattern akin to an exponential function curve. The curve's slope escalates sharply within the 0 to 400,000 lux range for ACI/Max, coinciding with the maximum UDI/Min.

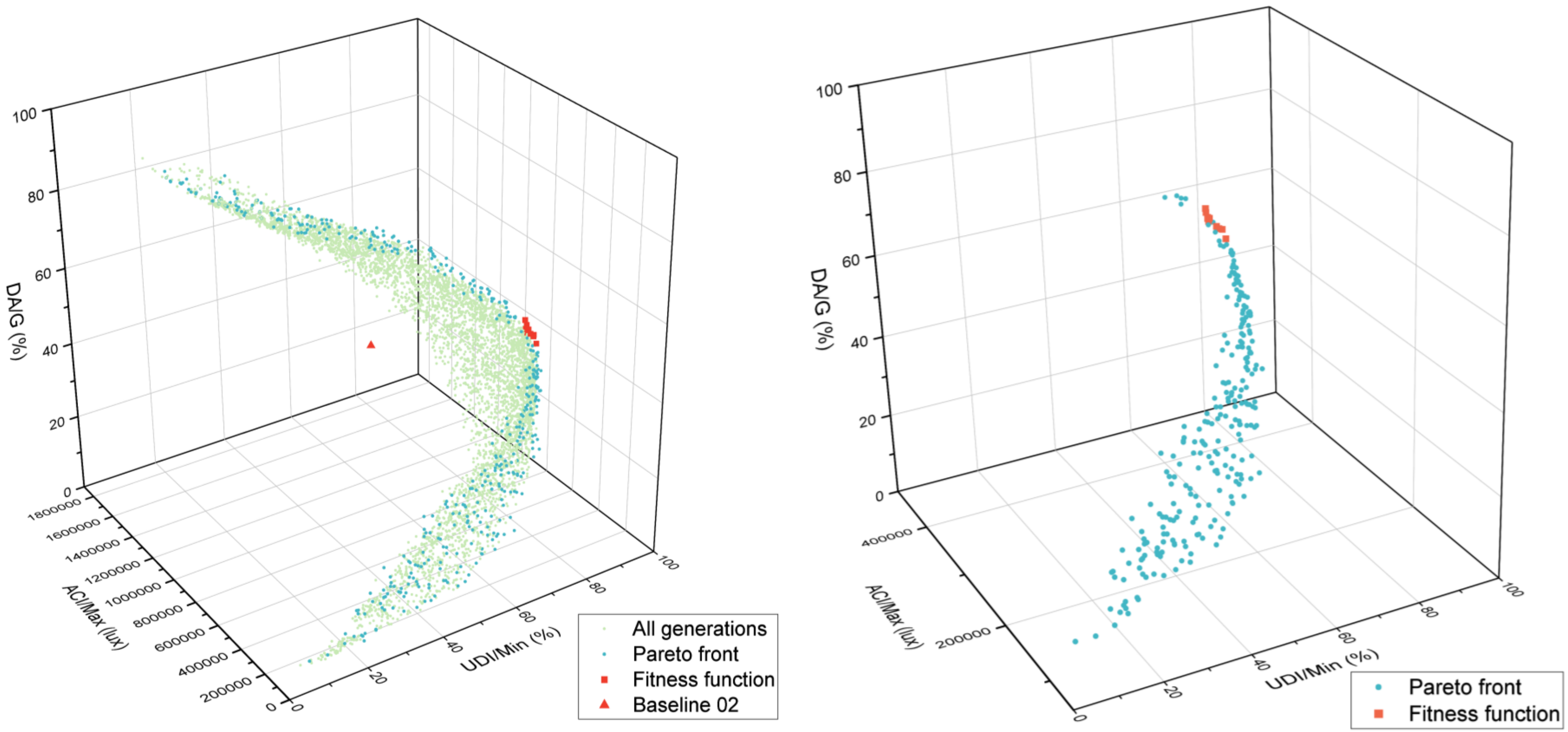

(a) All iteration outcomes

(b) Pareto frontiers

Figure 6.8 3D scatter plot of results.

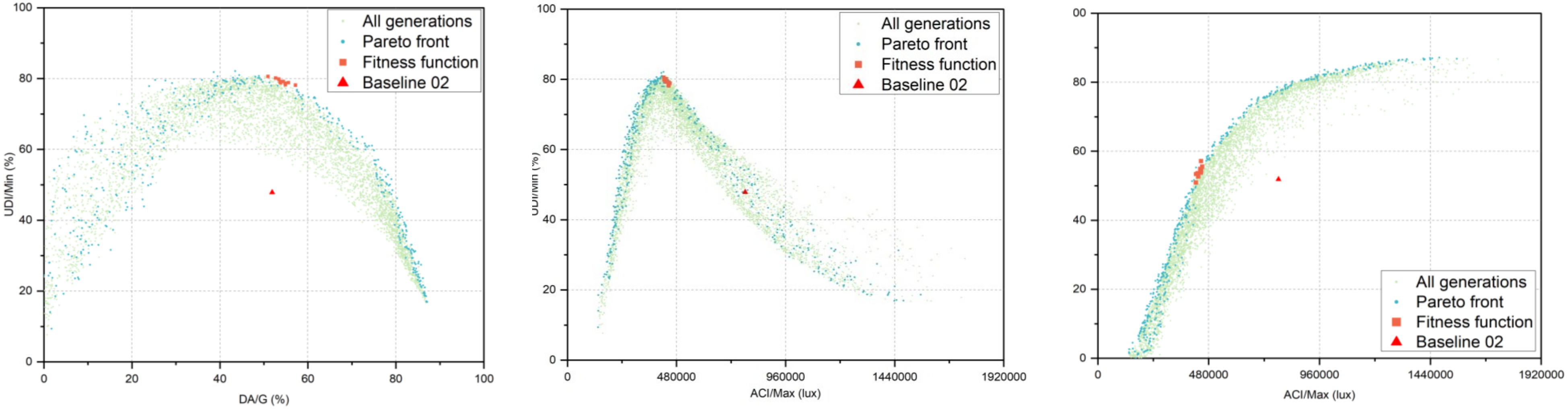

(a) DA/G & UDI/Min (b) ACI/Max & UDI/Min (c) ACI/Max & DA/G

Figure 6.9 Scatter plot showing the relationships among the objectives.

6.9.2. Parameters to objectives (sensitivity analysis)

Investigating the impact of variations in different variables within the skylight system on the objectives is crucial. This is aimed at identifying key factors that necessitate focused attention for daylight optimization during the design phase. Figure 6.10 showcases a Parallel Coordinate Plot of parameters versus objectives to illustrate how parameters are distributed when setting values and percentages for ACI, UDI, and DA. In this analysis, 183 results were selected, meeting the criteria of ACI below 480,000 lux and both UDI and DA exceeding 50%, considered valid data for further analysis. The color variation along the curves indicates ACI values, with a lighter yellow shade denoting higher ACI values and a darker purple shade indicating lower ACI values.

Regarding input parameters, among these valid results, the Height/LW dimension is primarily optimized with values of 0.6 and 0.7 meters. For Length/SD, input values within the range of 1.1 to 1.5 meters are more likely to produce valid data. In terms of Angle/SD, values ranging from 40 to 75 degrees are more conducive to yielding valid results. Notably, valid data is generated only when Arc/SD is set to -0.2 meters and -0.3 meters. Sensitivity analysis was conducted using the Standardized Regression Coefficient (SRC), a technique for linear regression analysis. The t-test was utilized to assess the impact of each parameter on the target value and to evaluate the correlation among variables. SRC uses the Fit Model command to estimate parameters, identifying each standardized target as a response variable and defining each standardized parameter as a factor influencing model construction.

Figure 6.11 presents the sensitivity ranking of design variables, highlighting the importance of each parameter in relation to the respective target objectives. The absolute values of the sensitivity data indicate a positive relationship between parameters and objectives. Generally ranging from 0 to 1, values closer to 1 indicate higher sensitivity, suggesting that minor adjustments to this parameter would lead to significant changes in the target value. According to the chart, the Height/LW parameter is most critical for the ACI/Max and UDI/Min target objectives and ranks second to Angle/SD for the DA/G target objective. The SRC values for Height/LW regarding ACI/Max, UDI/Min, and DA/G are -0.61, 0.047, and -0.56, respectively. Angle/SD is the second most important parameter, with its SRC values ranking second, third, and first for various target objectives. The third most influential parameter is Arc/SD, ranking third in SRC values for ACI/Max and DA/G, while its impact on UDI/Min is considered negligible. Angle/LW is second in impacting UDI/Min, with negligible effects on other target objectives. The influences of Angle/OP and Length/SD are deemed negligible.

By integrating Figure 6.10 and Figure 6.11, it is evident that the Height/LW parameter exhibits the most substantial impact on various target objectives, with optimal effects achieved at values of 0.7 and 0.6. The importance of Angle/SD is only slightly inferior to Height/LW, and appropriate lighting effects can be achieved within the range of 40 to 75 degrees. Although the impact of Arc/SD is less pronounced than the former two parameters, from Figure 6.11, it is apparent that optimal lighting effects can be attained when its values are between -0.2 and -0.3.

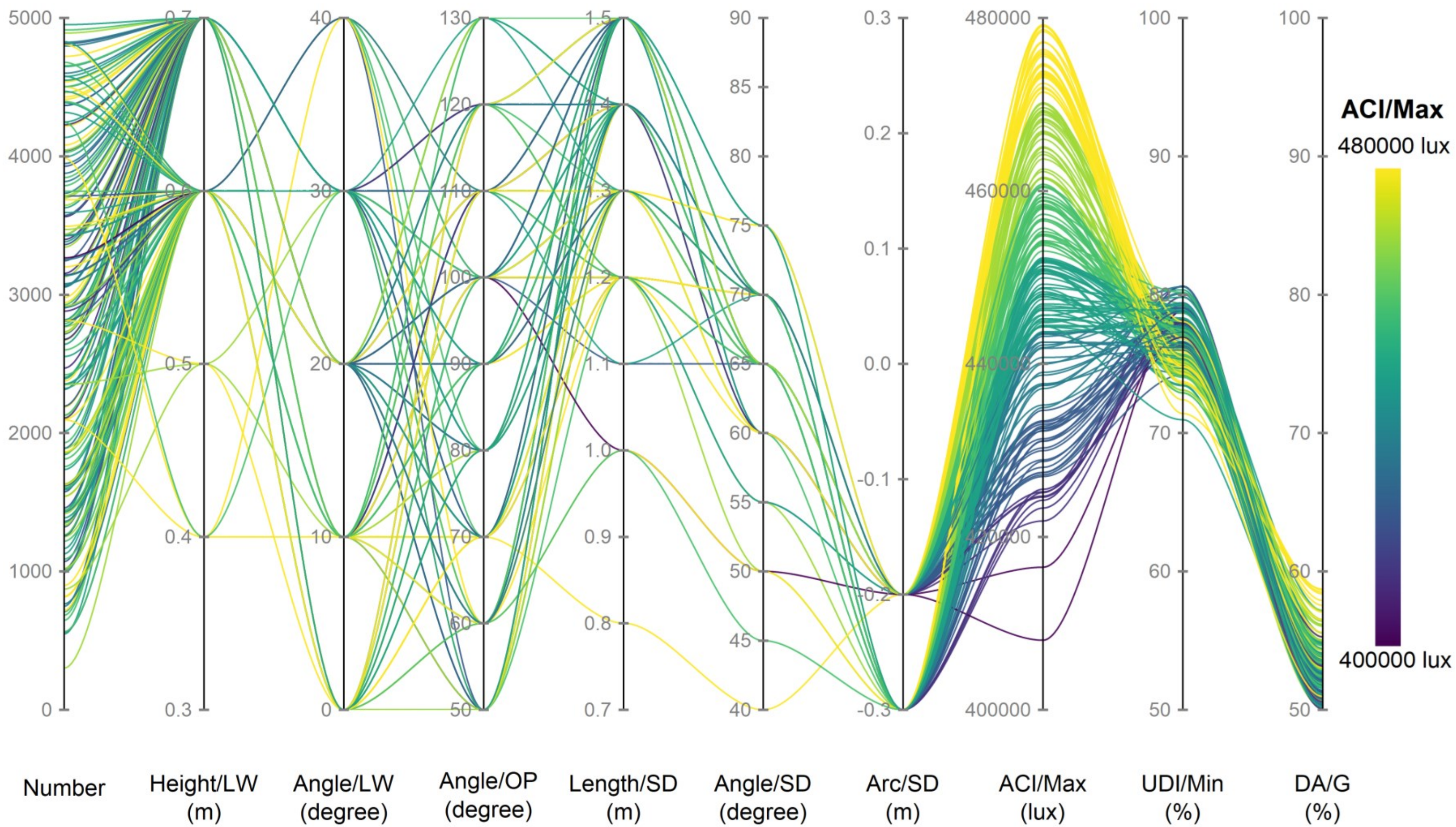

Figure 6.10 Parallel co-ordinate plot of the line of parameter values and objective values.

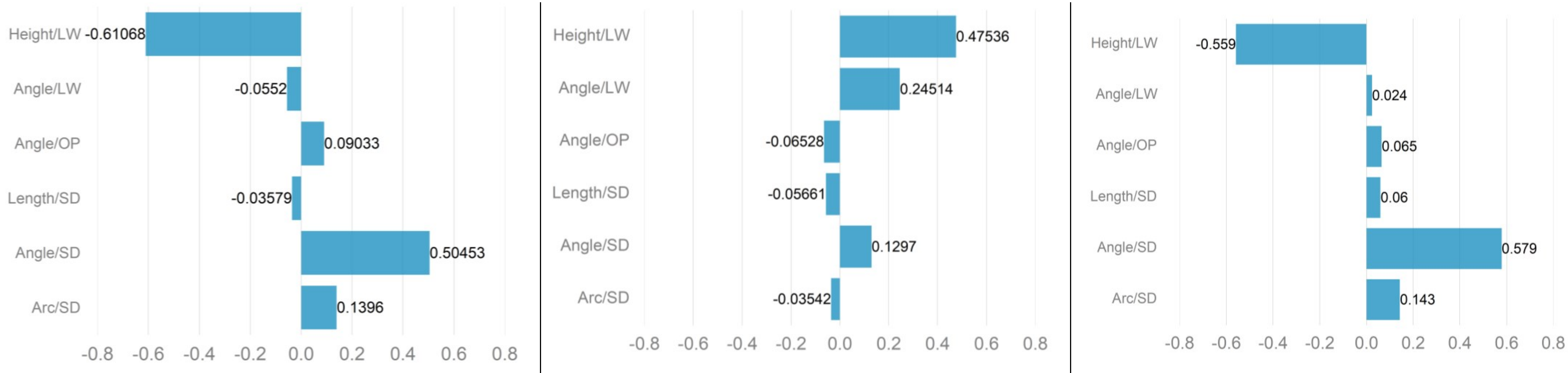

(a) Parameters for ACI/Max

(b) Parameters for UDI/Min

(c) Parameters for DA/G

Figure 6.11 Sensitivity analysis of the design variables.

6.9.3. The impact of different input parameters on three objectives

Based on the sensitivity analysis in the previous chapter, which evaluated the impact of various parameters on the objectives, it can be concluded that Height/LW, Angle/SD, and Arc/SD are the most influential factors. Therefore, in this chapter, box plots (Figure 6.12, Figure 6.13, Figure 6.14) are used for detailed analysis. By observing the distribution of each input parameter's values on the output objectives, a specific analysis is conducted on these three indicators. The following elements are explained in the box plots:

- Box (middle 50% of the data): Shows the data range from the first quartile to the third quartile.
- Whiskers: Show the upper and lower limits of all data, i.e., the maximum and minimum values.
- Median (thick line): Represents the middle value of the data.
- Mean (square): Represents the average value of the data.

Hight/LW

Figure 6.12 demonstrates the impact of skylight height (Height/LW) on annual cumulative illuminance (ACI/Max), useful daylight illuminance (UDI/Min), and daylight autonomy (DA/G). Overall, the three metrics exhibit different trends as the skylight height changes.

From Figure 6.12 (a), it is evident that as the Height/LW increases from 0.3 to 0.7, the annual cumulative illuminance (ACI/Max) shows a general downward trend. This indicates that as the skylight height increases, cumulative illuminance decreases. At Height/LW of 0.3, the data distribution range is the widest, showing high variability. At Height/LW of 0.7, the data distribution range is the narrowest, indicating more stable illuminance at this height. At Height/LW of 0.6 and 0.7, many data points are close to the target value of 480,000 lux, indicating that the annual cumulative illuminance at these heights is closer to the optimization target. At Height/LW of 0.3 and 0.4, most data points significantly exceed 480,000 lux, indicating excessively high illuminance at these heights. This suggests that higher skylight heights (0.6 and 0.7) are closer to the target value of 480,000 lux for annual cumulative illuminance, while lower heights (0.3 and 0.4) lead to excessively high illuminance.

From Figure 6.12 (b), it can be seen that useful daylight illuminance (UDI/Min) exhibits a trend of initially increasing and then decreasing as Height/LW increases. UDI/Min performs best at medium heights (0.5 and 0.6). At Height/LW of 0.3 and 0.4, the median and mean UDI/Min values are lower, and the data distribution range is wider. At Height/LW of 0.5 and 0.6, the median and mean UDI/Min values are higher, and the data distribution is more concentrated. At Height/LW of 0.5 and 0.6, most data points meet the requirement of being greater than 0.50, and some data points are close to or exceed 0.75. At Height/LW of 0.7, although the mean and median UDI/Min values are higher, the distribution range is larger. This indicates that medium skylight heights (0.5 and 0.6) perform best in terms of useful daylight illuminance, being more likely to meet the UDI/Min requirement of greater than 0.50, with some data points close to or exceeding 0.75.

From Figure 6.12 (c), it can be seen that daylight autonomy (DA/G) decreases as Height/LW increases. Lower skylight heights (0.3 and 0.4) have higher daylight autonomy, meaning these heights provide more daylight autonomy. At Height/LW of 0.3, the median and mean DA/G values are the highest, with most data points exceeding 0.75. This indicates higher autonomy at lower heights. At Height/LW of 0.3 and 0.4, most data points meet the requirement of being greater than 0.50, with many data points exceeding 0.75. As the height increases to 0.7, the median and mean DA/G values significantly decrease, with most data points below 0.50. This indicates that lower skylight heights (0.3 and 0.4) are more likely to meet and exceed the daylight autonomy optimization target (>0.75), while higher heights are less likely to meet this requirement.

In summary, it is recommended to choose higher skylight heights (0.6 and 0.7) because the annual cumulative illuminance at these heights is closer to the optimization target of 480,000 lux. Lower heights (0.3 and 0.4) provide more illuminance but are more likely to exceed the target value of 480,000 lux. Lower skylight heights (0.3 and 0.4) help to meet and exceed the daylight autonomy optimization target, providing higher daylight autonomy. If daylight autonomy is the main goal, lower skylight heights are recommended. Medium heights (0.5 and 0.6) perform best in terms of useful daylight illuminance, meeting the requirement of UDI/Min greater than 0.50, with some data close to or exceeding 0.75. Considering useful daylight illuminance, medium skylight heights are recommended.

Angle/SD

Figure 6.13 illustrate the impact of different skylight angles (Angle/SD) on three different lighting metrics: Annual Cumulative Illuminance (ACI/Max), Useful Daylight Illuminance (UDI/Min), and Daylight Autonomy (DA/G).

In Figure 6.13 (a), as the Angle/SD increases, ACI/Max generally rises. This indicates that larger skylight angles increase the annual cumulative illuminance. Both the mean and median values rise with increasing angles, and the distribution range also expands. The data distribution range becomes larger with the increase in angle, especially at higher angles (85 degrees and 90 degrees), showing more variability and extreme values. Lower skylight angles are closer to the target value of 480,000 lux, while higher angles result in excessively high annual cumulative illuminance.

From Figure 6.13 (b), UDI/Min does not show as clear an increasing trend as ACI/Max and DA/G with varying angles. Overall, higher UDI/Min values are observed at intermediate angles (55 degrees to 75 degrees). The data distribution range is relatively large at all angles, but the median and mean values are higher at intermediate angles, indicating that these angles might be the most effective range. Useful daylight illuminance (UDI/Min) performs better at moderate angles (55 degrees to 75 degrees), with lower performance at both ends of the angle spectrum. At low angles (40 degrees to 50 degrees) and high angles (80 degrees to 90 degrees), the median and mean UDI/Min values are lower. Skylight designs at intermediate angles are more likely to meet the UDI/Min requirement of greater than 0.50, though achieving a high standard of greater than 0.75 remains challenging.

In Figure 6.13 (c), DA/G increases with the increase of Angle/SD, indicating that larger skylight angles provide more daylight autonomy. At lower angles (40 degrees to 55 degrees), the data distribution range is larger, with lower median and mean values. At higher angles (70 degrees to 90 degrees), the data distribution range is smaller, with higher and more stable median and mean values. Higher skylight angles are favorable for achieving and exceeding the optimization goals of daylight autonomy.

Lower skylight angles (40 degrees to 55 degrees) are closer to the target of 480,000 lux, but higher angles may result in excessively high illuminance. Intermediate angles (55 degrees to 75 degrees) are more likely to meet the requirement of greater than 0.50, though achieving a high standard of greater than 0.75 is challenging. Higher skylight angles (70 degrees to 90 degrees) are beneficial for achieving and exceeding the optimization goals of daylight autonomy.

Arc/SD

These three box plots illustrate the impact of shading arc (Arc/SD) on annual cumulative illuminance (ACI/Max), useful daylight illuminance (UDI/Min), and daylight autonomy (DA/G). Overall, as Arc/SD changes, the three metrics exhibit different trends.

From Figure 6.14 (a), it can be seen that as Arc/SD varies from -0.3 to 0.3, there is no obvious monotonic trend in annual cumulative illuminance (ACI/Max). However, the mean and median values change significantly across different arcs. When Arc/SD is at -0.3 and 0.3, the data distribution range is narrow, while at intermediate arcs (-0.1 to 0.2), the data distribution range is wider. At these intermediate arcs, the annual cumulative illuminance is closer to the target value of 480,000 lux, while at other arcs, most data points exceed the target value. When Arc/SD is -0.3, the data distribution range is narrow, and both the median and mean are below the target value of 480,000 lux. When Arc/SD is -0.2 and -0.1, the data distribution range widens, and both the median and mean significantly exceed 480,000 lux. When Arc/SD is -0.2 and 0.3, despite the wide data distribution range, the median and mean are close to the target value of 480,000 lux, indicating good performance.

From Figure 6.14 (b), it is clear that daylight autonomy (DA/G) is lower when Arc/SD is -0.3, higher between -0.2 and 0.2, and then decreases again at 0.3. When Arc/SD is -0.2 and 0.1, the median and mean DA/G are highest, with a relatively even data distribution. When Arc/SD is -0.3, the median and mean DA/G are lower, with a wider data distribution range. When Arc/SD is -0.2 and -0.1, the median and mean DA/G are higher, with some data points exceeding 0.75. When Arc/SD is 0.3, the median and mean DA/G decrease again. When Arc/SD is -0.2 and 0.1, the median and mean DA/G are higher, and the data distribution is more concentrated, indicating that these arcs provide better daylight autonomy.

From Figure 6.14 (c), it can be seen that there is no clear monotonic trend in useful daylight illuminance (UDI/Min) as Arc/SD varies from -0.3 to 0.3. When Arc/SD is -0.3, -0.1, and 0.3, the median and mean UDI/Min are higher, with a more concentrated data distribution. When Arc/SD is -0.3 and -0.1, the median and mean UDI/Min are higher, with a narrow data distribution range. When Arc/SD is 0.1 and 0.2, the median and mean UDI/Min are close to the target value of 0.75, with a wider data distribution range. When Arc/SD is 0.3, the median and mean UDI/Min rise again, with a narrow data distribution range. When Arc/SD is -0.3, -0.1, and 0.3, more data points meet the requirement of being greater than 0.50, with some data points close to or exceeding 0.75.

In summary, the shading arc significantly impacts annual cumulative illuminance, daylight autonomy, and useful daylight illuminance. Choosing an appropriate arc can optimize the use of natural light and improve the quality of the indoor lighting environment.

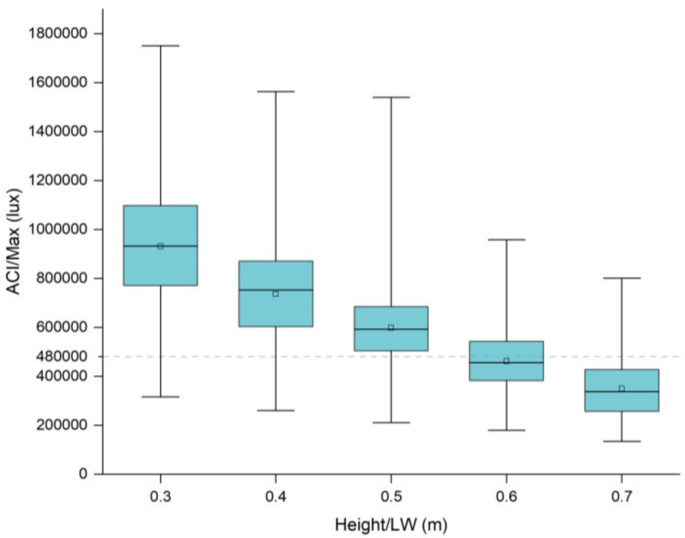

(a) Height/LW and ACI/Max

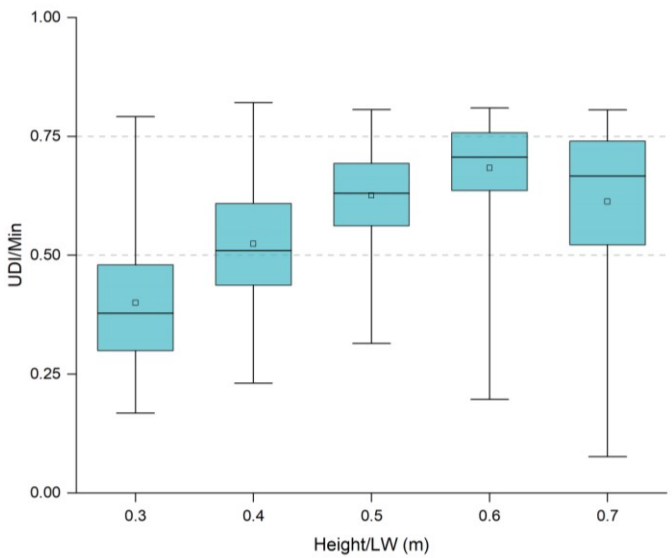

(b) Height/LW and UDI/Min

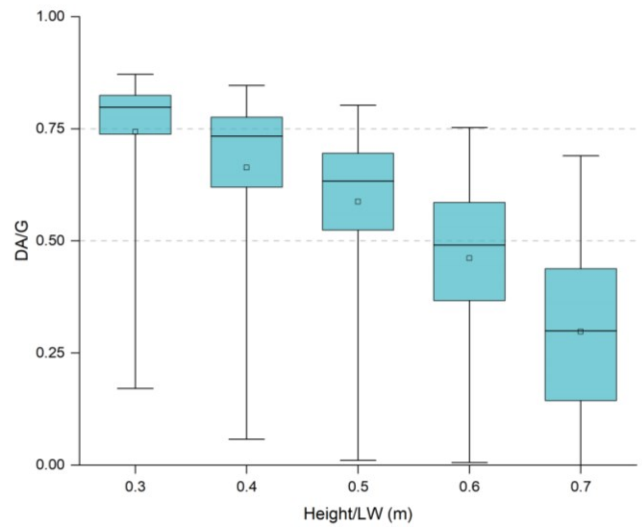

(c) Height/LW and DA/G

Figure 6.12 The impact of different Height/LW on three lighting objectives

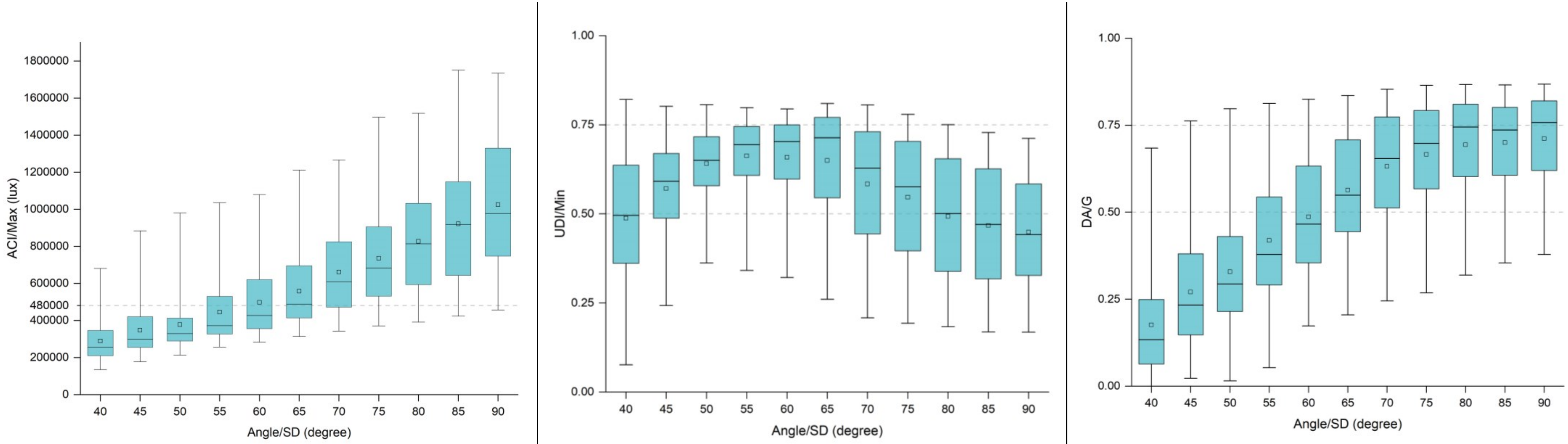

(a) Angle/SD and ACI/Max

(b) Angle/SD and UDI/Min

(c) Angle/SD and DA/G

Figure 6.13 The impact of different Angle/SD on three lighting objectives

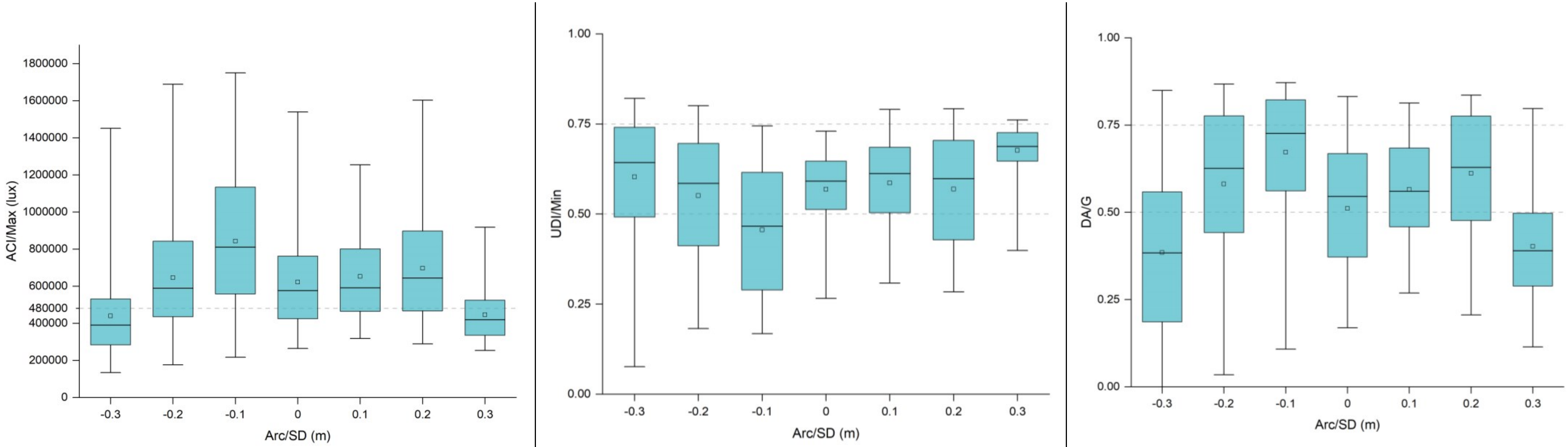

(a) Arc/SD and ACI/Max

(b) Arc/SD and UDI/Min

(c) Arc/SD and DA/G

Figure 6.14 The impact of different Arc/SD on three lighting objectives

6.9.4. Baseline-model simulation

In Figure 6.15, without roof shading, although the DA/G of the floor is fully satisfied, the ACI of all four walls of the baseline model 01 greatly exceeds 480,000lux; and the ACI values of the north and south walls are extremely different, which implies that the indoor illuminance is not uniform. Through the optimization in baseline model 02, the ACI/Max of baseline model 01 is reduced from 106748304lux to 780060lux, the UDI/min is increased from 0% to 47.48%, and the DA/G is still higher than 50% although it has been reduced. The $ACI_{480000lx}$ and $UDI_{50\text{-}200lx}$ of all four walls reach a similar value, meaning that the indoor light environment is more uniform than baseline model 01. However, the ACI/Max of baseline model 02 is still over 480,000 lux and the UDI/min is slightly below 50%, which means that there is still room for optimization of this skylight system.

6.9.5. Optimal solutions

Table 6.9.1, Figure 6.15 and Figure 6.16 display the top 10 attributes of the optimal solutions ranked based on the fitness function value. As evident from the table, among the top 10 solutions, the peak performance for target ACI/Max ranges from 424,211 lux in model No. 2881 to 451,920 lux in model No. 4388, with all ten results meeting the requirement of an annual insolation total below 480,000 lux. The UDI/MIN percentage ranges from 78.15% in model No. 1597 to 80.61% in model No. 2881. DA/G percentage spans from 50.93% in model No. 2881 to 57.16% in model No. 1597.

In terms of the input parameter range, Height/LW is limited to 0.6 meters and 0.7 meters, with 0.6 meters occurring 6 times and 0.7 meters occurring 4 times. In the Angle/LW parameter, there are 10 degrees, 20 degrees, and 30 degrees, with 10 degrees representing 60% of the total. In the Angle/OP parameter, the minimum value is 80 degrees, and the maximum value is 120 degrees. However, 80 degrees occurs 3 times, 90 degrees 2 times, 100 degrees 3 times, and 120 degrees 2 times. This indicates a uniform distribution. In the Length/SD parameter, ranging from the minimum value of 1.3 to the maximum value of 1.5, where 1.3 offset occurs 2 times, 1.4 occurs 4 times, and 1.5 occurs 4 times, showing a relatively close distribution. In the Angle/SD parameter, 65 occurs 6 times, and 70 occurs 4 times. In the Arc/SD parameter, ranging from the minimum value of -0.3 to the maximum value of -0.2, where -0.3 offset occurs 9 times, dominating the distribution.

Solution	ACI	UDI	DA
B-01	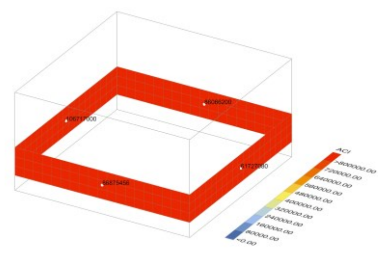	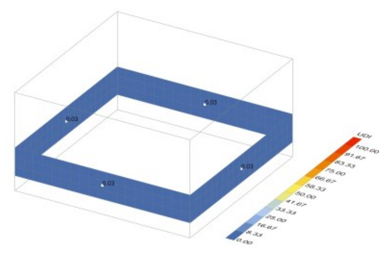	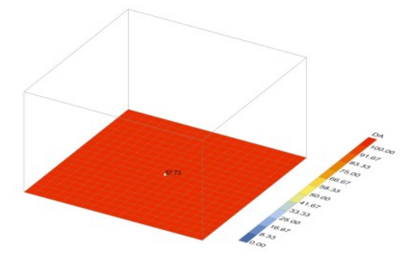
B-02	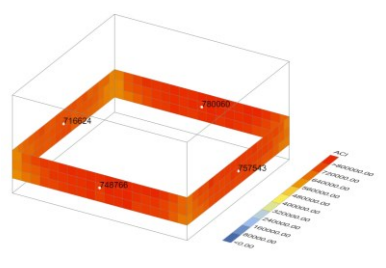	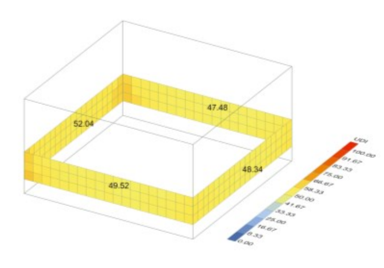	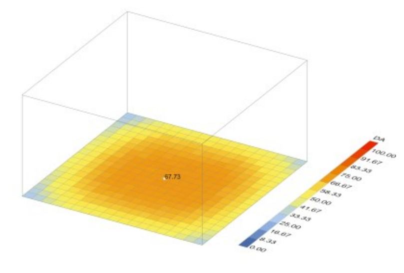
Op-01	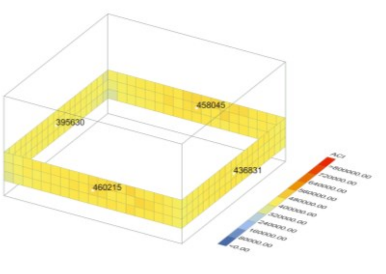	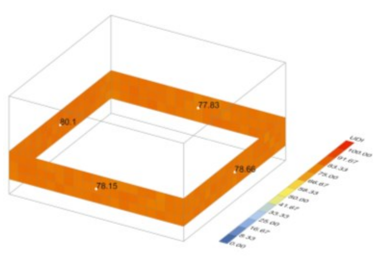	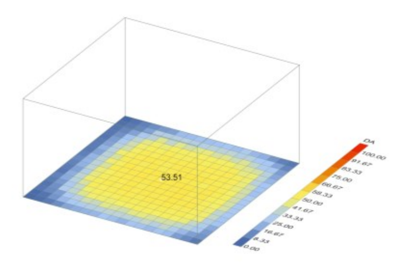
Op-02	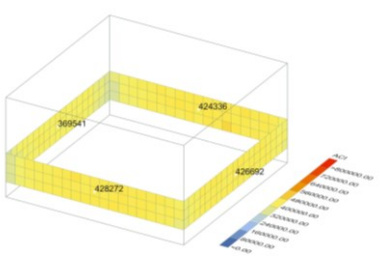	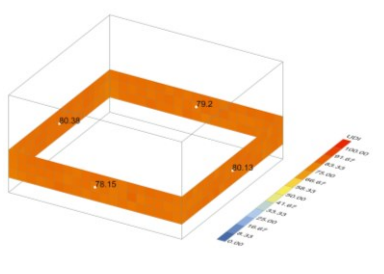	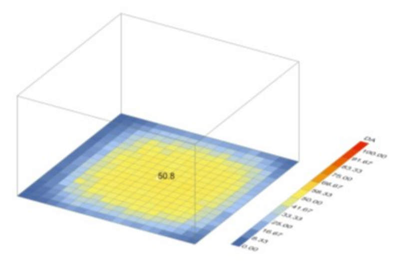

Op-03	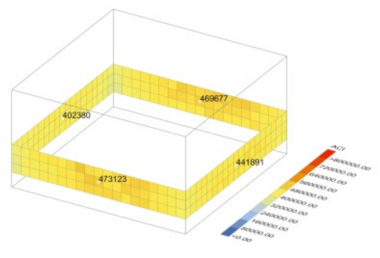	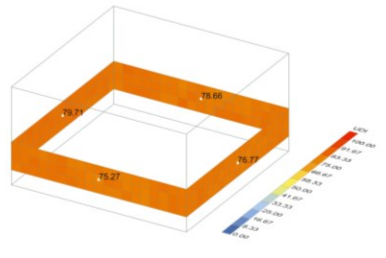	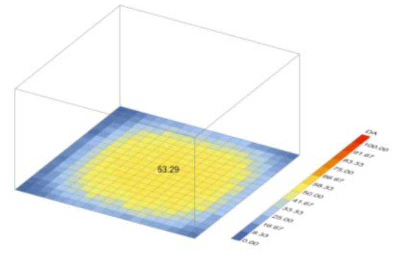
Op-04	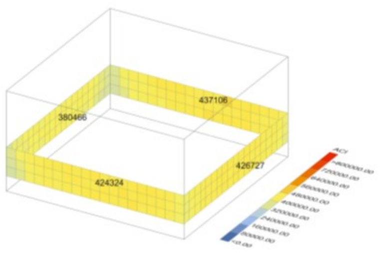	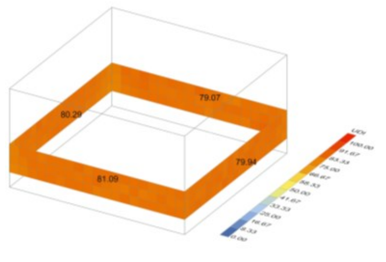	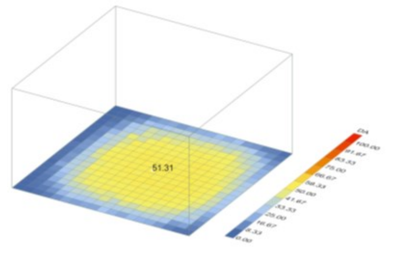
Op-05	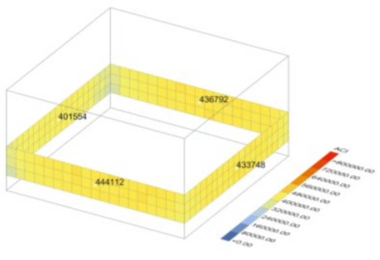	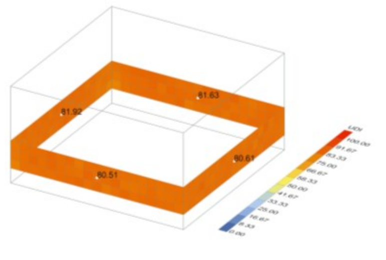	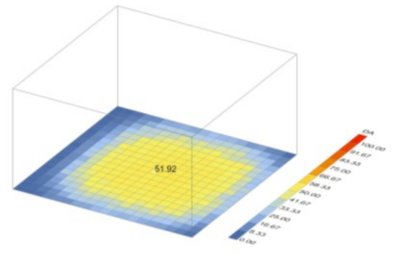
Op-06	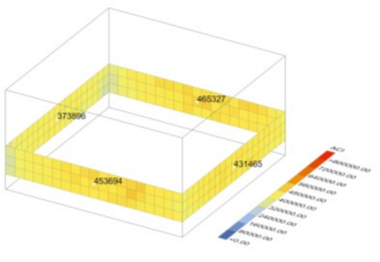	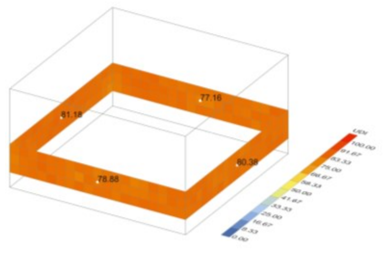	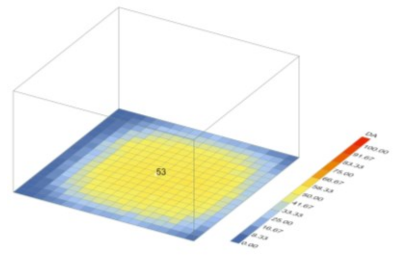
Op-07	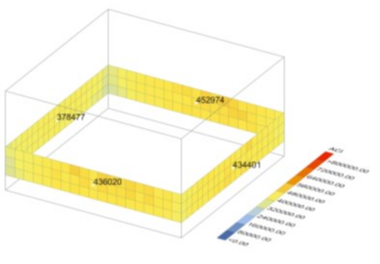	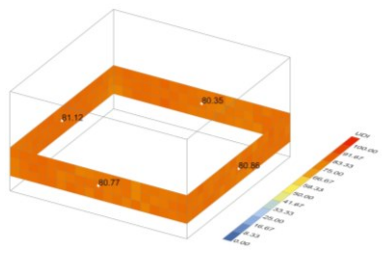	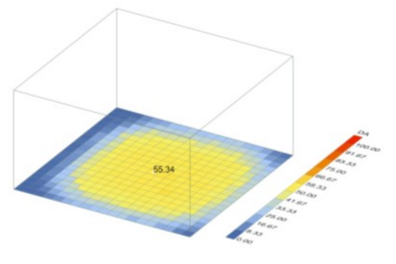

Op-08	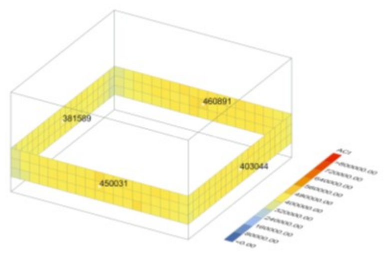	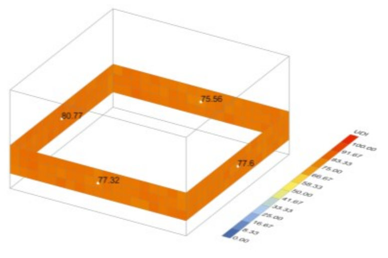	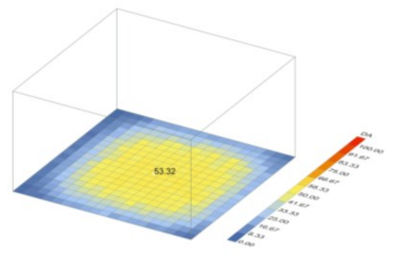
Op-09	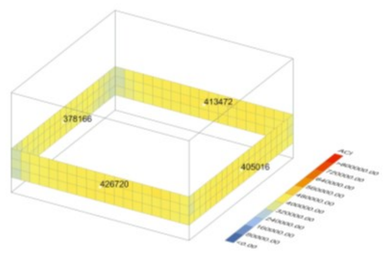	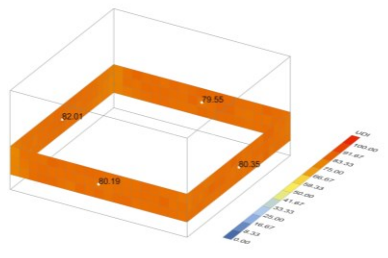	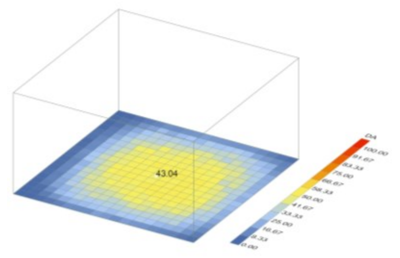
Op-10	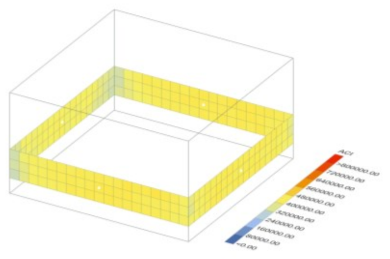	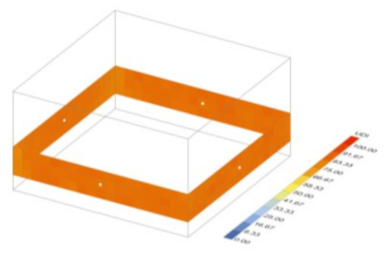	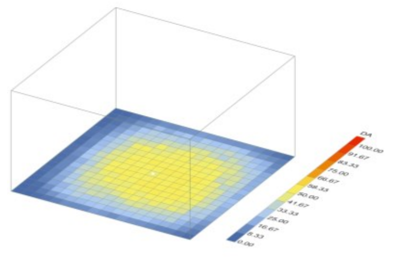

Figure 6.15 The simulating results of baseline models the 10 best solutions.

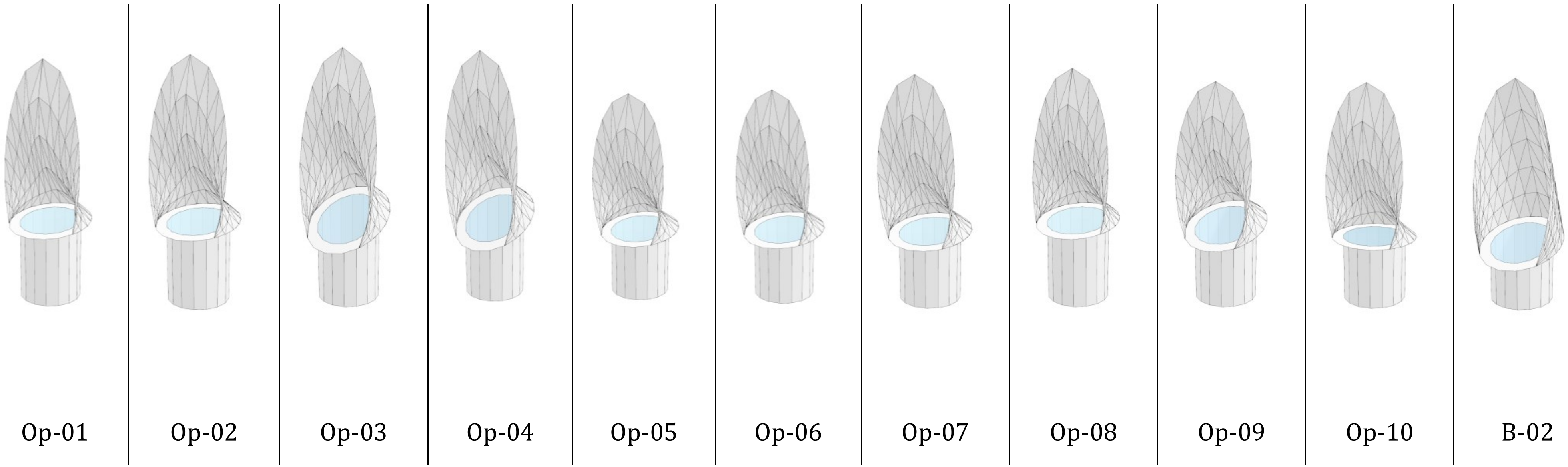

Figure 6.16 Shape of selected solutions based on fitness-function calculations.

Table 6.9.1 The selected solutions based on fitness-function calculations.

Solution rank	Model number	Parameters						Objectives			Fitness Function
		Height/LW (m)	Angle/LW (degree)	Angle/OP (degree)	Length/SD (m)	Angle/SD (degree)	Arc/SD (m)	ACI/Max Lux	UDI/Min %	DA/G %	
B-01	Baseline 01	-	-	-	-	-	-	106748304	0.03	97.73	
B-02	Baseline 02	0.438	20	93.8	1.425	70	0	780060	47.48	67.73	
Op-01	1597	0.7	10	120	1.5	70	-0.3	446699	78.15	57.16	140.94
Op-02	2108	0.7	10	100	1.5	70	-0.3	425116	79.84	53.39	140.22
Op-03	4388	0.6	30	80	1.4	70	-0.3	451920	78.85	55.56	139.72
Op-04	3428	0.6	30	80	1.5	65	-0.3	437106	79.07	51.31	139.24
Op-05	2907	0.6	10	90	1.4	65	-0.3	434938	80.16	52.65	139.19
Op-06	3592	0.6	10	100	1.4	65	-0.3	447481	79.2	54.41	139.15
Op-07	3430	0.6	10	90	1.5	65	-0.3	446937	78.69	54.79	138.93
Op-08	1890	0.7	10	120	1.4	70	-0.3	443416	78.24	54.89	138.66
Op-09	2881	0.6	20	80	1.3	65	-0.3	424211	80.61	50.93	138.49
Op-10	4135	0.7	20	100	1.3	65	-0.2	446203	78.79	53.8	137.98

6.9.6. Middle point study of optimal solutions

The midpoint of a wall typically represents the brightest section and often becomes the focal point of visual attention. This subsection concentrates on the midpoint of walls as the subject of study, exploring variations in Annual Cumulative Illuminance (ACI), Useful Daylight Illuminance (UDI), Annual Illuminance Factor (AIF), Daylight Autonomy (DA), Daylight Glare Probability (DGP), and Annual Daylight Illuminance across interior walls facing four different orientations.

ACI of walls

From Figure 6.17 (a), it is evident that the ACI at the midpoints of all four walls in the baseline-02 scenario exceeds 650,000 lux, well surpassing the standard value of 480,000 lux. In contrast, all midpoints in the ten optimized scenarios exhibit ACI values below 480,000 lux. The north wall continues to receive the least illuminance among the four walls, experiencing a reduction of approximately 300,000 lux compared to baseline-02. The ACI values on the other three walls also exhibit a significant decrease compared to the baseline-02.

UDI of walls

In Figure 6.17 (b), within the baseline-02 scenario, only the UDI values for the north-facing wall exceed 50%, notably higher than those of the other three walls. In the ten optimized scenarios, all models exhibit UDI values exceeding 75%, ranging from 78% to 82%. This represents an increase of nearly 30% compared to baseline-02, indicating a significant improvement. The UDI values for the four walls do not exhibit a consistent pattern; however, in most cases, the UDI for the north-facing wall tends to be slightly superior to those of the other three walls.

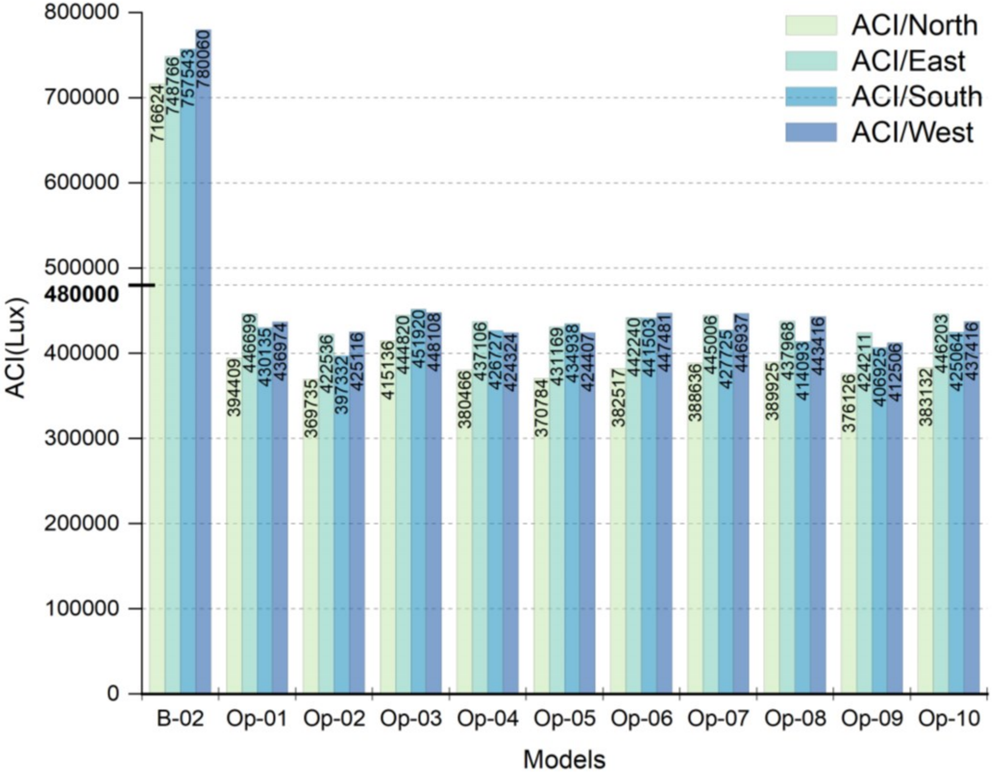

(a) ACI of middle points

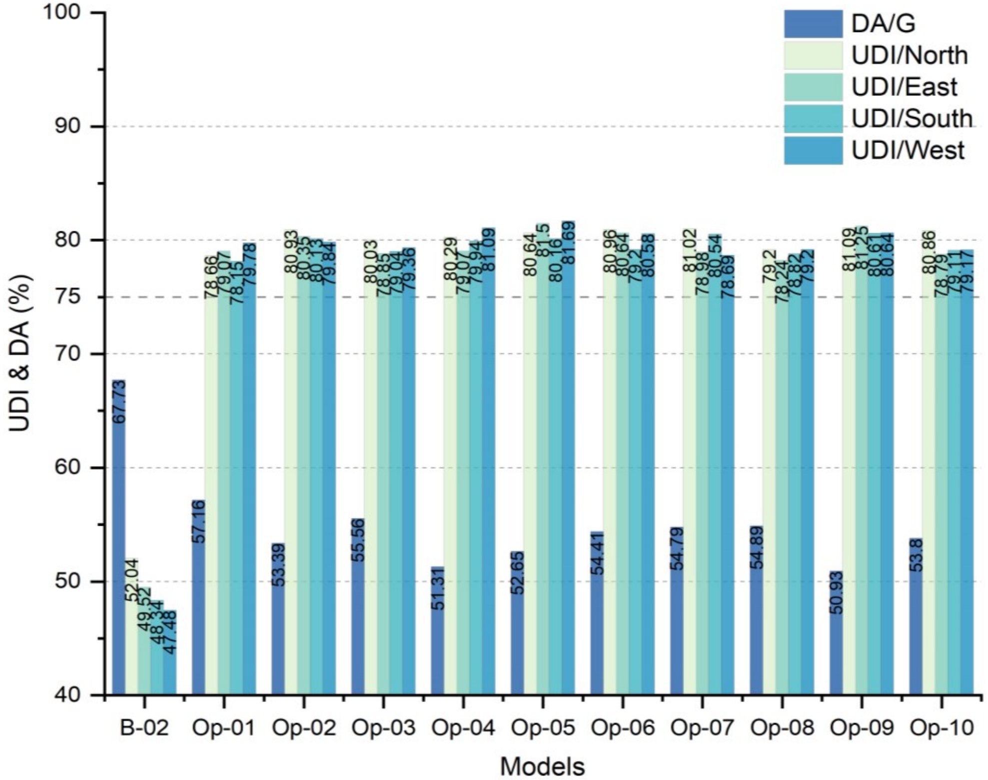

(b) UDI and DA of middle points

Figure 6.17 ACI, UDI and DA of middle points.

AIF of walls

AIF refers to the percentage values representing the annual daytime hours with illuminance within a specific range. It is evident from Figure 6.18 that all models exhibit a similar pattern of illuminance distribution across the four walls. In the baseline-02 scenario, the percentage of time with various illuminance levels is relatively uniform, with most being below 10%. Although the proportion of natural light within the range of 50-200 lux is slightly higher, there are also instances exceeding 200 lux, with an average of about 5% for each interval. In the ten optimized outcomes, compared to baseline-02, the percentage of time exceeding 200 lux significantly decreases, often dropping to about 0%. Conversely, the percentage of time with illuminance within the 50-150 lux range exceeds that of baseline-02, forming a noticeable peak. Among the four walls, the peak for the north-facing wall is notably higher than the other three walls, while the percentage of time with illuminance exceeding 200 lux is significantly lower than the other three walls.

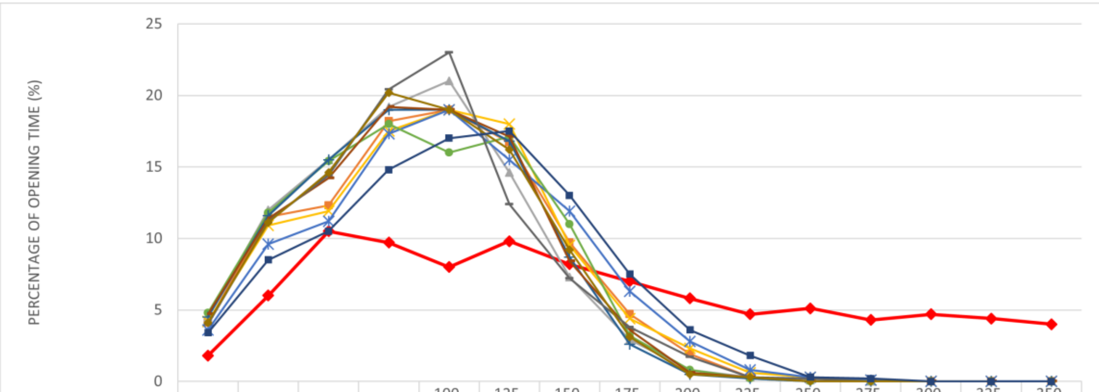

	0-25	25-50	50-75	75-100	100-125	125-150	150-175	175-200	200-225	225-250	250-275	275-300	300-325	325-350	350-375
B-02 (North)	1.8	6	10.5	9.7	8	9.8	8.2	7	5.8	4.7	5.1	4.3	4.7	4.4	4
Op-01 (North)	4.1	11.5	12.3	18.2	19	16.7	9.7	4.7	1.9	0.3	0.1	0	0	0	0
Op-02 (North)	4.5	12	15.5	19.2	21	14.6	7.3	2.9	0.8	0.3	0.1	0	0	0	0
Op-03 (North)	4.2	10.9	11.9	17.5	19	18	9.5	4.4	2.3	0.6	0.3	0.1	0	0	0
Op-04 (North)	3.6	9.6	11.2	17.3	19	15.5	11.9	6.3	2.8	0.8	0.3	0.1	0	0	0
Op-05 (North)	4.8	11.8	15.4	18	16	17.1	11	3.2	0.8	0.2	0	0	0	0	0
Op-06 (North)	4.5	11.6	15.5	19	19	16.8	8.7	2.6	0.5	0.2	0	0	0	0	0
Op-07 (North)	4.7	11.4	14.2	19.2	19	17.1	8.4	3.6	0.6	0.3	0	0	0	0	0
Op-08 (North)	4	11.2	14.4	20.4	23	12.4	7.2	3.8	1.7	0.3	0.2	0	0	0	0
Op-09 (North)	4.1	11.1	14.6	20.2	19	16.2	9.2	3.1	0.5	0.3	0	0	0	0	0
Op-10 (North)	3.4	8.5	10.5	14.8	17	17.5	13	7.5	3.6	1.8	0.3	0.2	0	0	0

(a) AIF of north wall

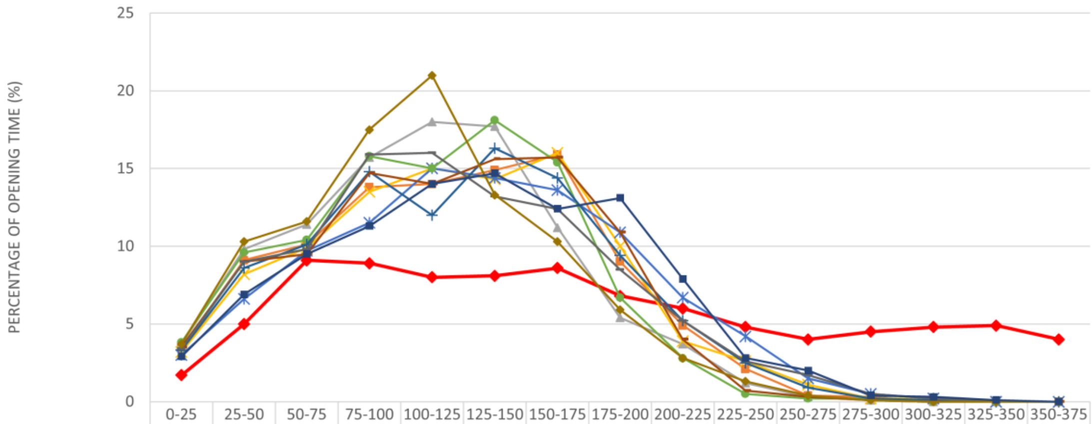

	0-25	25-50	50-75	75-100	100-125	125-150	150-175	175-200	200-225	225-250	250-275	275-300	300-325	325-350	350-375
B-02 (East)	1.7	5	9.1	8.9	8	8.1	8.6	6.8	6	4.8	4	4.5	4.8	4.9	4
Op-01 (East)	3.4	9.1	10.1	13.8	14	14.9	15.9	9	4.9	2.1	0.4	0.3	0	0	0
Op-02 (East)	3.7	9.8	11.4	15.7	18	17.7	11.2	5.4	3.7	1.2	0.3	0.1	0	0	0
Op-03 (East)	3.2	8.2	9.9	13.5	15	14.3	16	10	3.9	2.6	1.1	0.2	0.2	0	0
Op-04 (East)	3	6.6	9.7	11.5	15	14.4	13.6	10.9	6.7	4.2	1.5	0.5	0.2	0	0
Op-05 (East)	3.8	9.6	10.4	15.8	15	18.1	15.4	6.7	2.8	0.5	0.2	0.2	0	0	0
Op-06 (East)	3.3	8.6	10.1	14.8	12	16.3	14.4	9.4	5.2	2.5	0.9	0.2	0.1	0	0
Op-07 (East)	3.5	9	9.5	14.7	14	15.6	15.7	10.9	4	0.7	0.3	0.1	0	0	0
Op-08 (East)	3.4	9	9.8	15.9	16	13.2	12.4	8.5	5.2	2.6	1.7	0.5	0.2	0	0
Op-09 (East)	3.7	10.3	11.6	17.5	21	13.3	10.3	5.9	2.8	1.3	0.4	0.1	0	0	0
Op-10 (East)	2.9	6.9	9.5	11.3	14	14.7	12.4	13.1	7.9	2.8	2	0.4	0.3	0.1	0

RANGE OF ILLUMINANCE (LUX)

(b) AIF of east wall

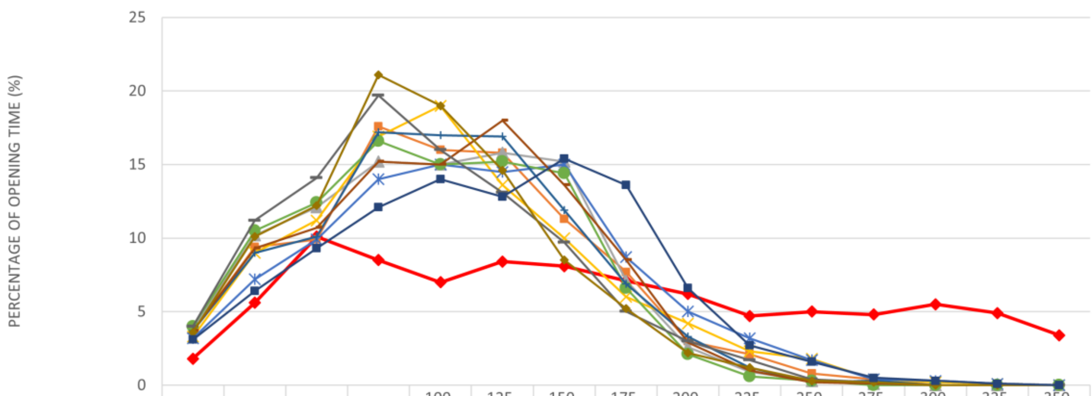

	0-25	25-50	50-75	75-100	100-125	125-150	150-175	175-200	200-225	225-250	250-275	275-300	300-325	325-350	350-375
B-02 (South)	1.8	5.6	10.1	8.5	7	8.4	8.1	7.1	6.2	4.7	5	4.8	5.5	4.9	3.4
Op-01 (South)	3.7	9.4	9.9	17.6	16	15.8	11.3	7.7	3	2.1	0.8	0.4	0	0	0
Op-02 (South)	3.9	10.2	12.1	15.2	15	15.8	15.2	7.1	2.6	0.9	0.3	0.1	0	0	0
Op-03 (South)	3.3	9	11.2	16.9	19	13.6	10	6	4.2	2.3	1.8	0.4	0.2	0.1	0
Op-04 (South)	3.2	7.2	9.9	14	15	14.5	15	8.7	5	3.2	1.7	0.4	0.3	0.1	0
Op-05 (South)	4	10.5	12.4	16.6	15	15.2	14.4	6.6	2.1	0.6	0.3	0	0	0	0
Op-06 (South)	3.7	9	10.1	17.2	17	16.9	11.9	6.9	3.3	1.2	0.2	0.3	0	0	0
Op-07 (South)	3.7	9.3	10.7	15.2	15	18	13.6	8.5	2.9	1	0.2	0.1	0	0	0
Op-08 (South)	4	11.2	14.1	19.7	16	13.1	9.7	5	3	1.7	0.4	0.2	0	0	0
Op-09 (South)	3.6	10.1	12.2	21.1	19	14.6	8.5	5.2	2.2	1.2	0.3	0.2	0	0	0
Op-10 (South)	3.1	6.4	9.3	12.1	14	12.8	15.4	13.6	6.6	2.7	1.6	0.5	0.3	0.1	0

RANGE OF ILLUMINANCE (LUX)

(c) AIF of south wall

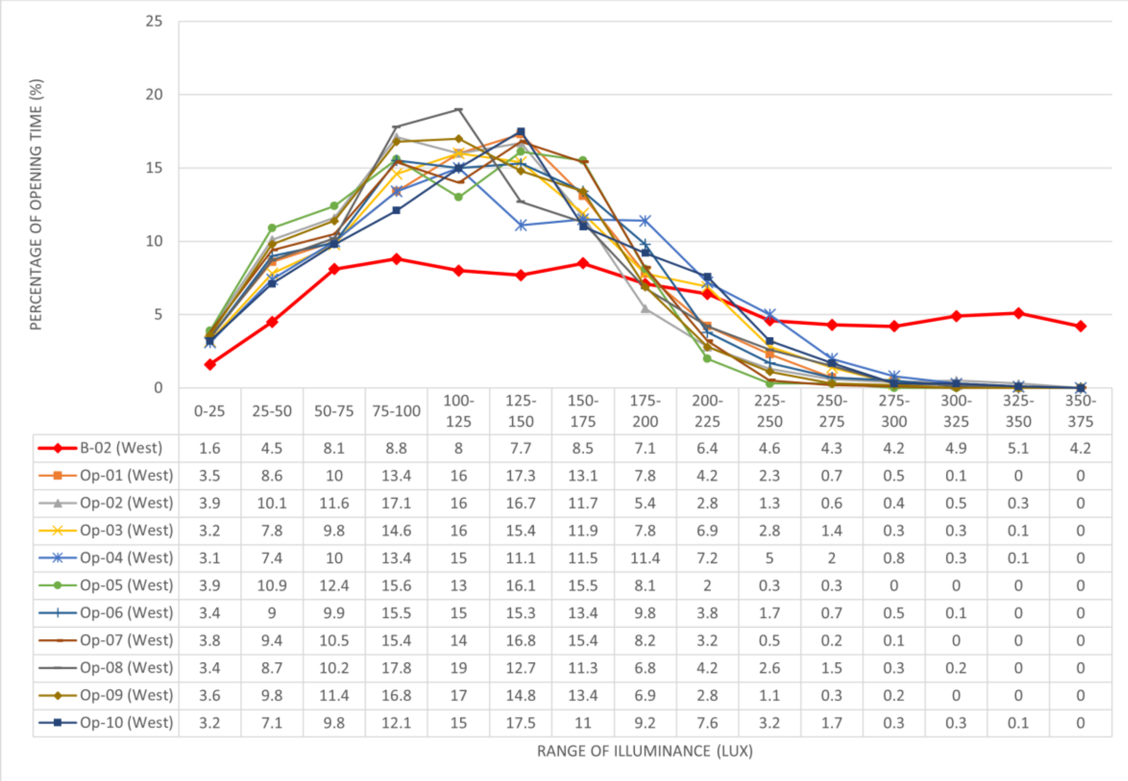

	0-25	25-50	50-75	75-100	100-125	125-150	150-175	175-200	200-225	225-250	250-275	275-300	300-325	325-350	350-375
B-02 (West)	1.6	4.5	8.1	8.8	8	7.7	8.5	7.1	6.4	4.6	4.3	4.2	4.9	5.1	4.2
Op-01 (West)	3.5	8.6	10	13.4	16	17.3	13.1	7.8	4.2	2.3	0.7	0.5	0.1	0	0
Op-02 (West)	3.9	10.1	11.6	17.1	16	16.7	11.7	5.4	2.8	1.3	0.6	0.4	0.5	0.3	0
Op-03 (West)	3.2	7.8	9.8	14.6	16	15.4	11.9	7.8	6.9	2.8	1.4	0.3	0.3	0.1	0
Op-04 (West)	3.1	7.4	10	13.4	15	11.1	11.5	11.4	7.2	5	2	0.8	0.3	0.1	0
Op-05 (West)	3.9	10.9	12.4	15.6	13	16.1	15.5	8.1	2	0.3	0.3	0	0	0	0
Op-06 (West)	3.4	9	9.9	15.5	15	15.3	13.4	9.8	3.8	1.7	0.7	0.5	0.1	0	0
Op-07 (West)	3.8	9.4	10.5	15.4	14	16.8	15.4	8.2	3.2	0.5	0.2	0.1	0	0	0
Op-08 (West)	3.4	8.7	10.2	17.8	19	12.7	11.3	6.8	4.2	2.6	1.5	0.3	0.2	0	0
Op-09 (West)	3.6	9.8	11.4	16.8	17	14.8	13.4	6.9	2.8	1.1	0.3	0.2	0	0	0
Op-10 (West)	3.2	7.1	9.8	12.1	15	17.5	11	9.2	7.6	3.2	1.7	0.3	0.3	0.1	0

(d) AIF of west wall

Figure 6.18 AIF of middle points fs walls.

DA of floor

In Figure 6.17, the DA performance across all models shows no significant differences. For the baseline-02 scenario, DA on the floor is measured at 67.73%. Among the other ten models, Op-01 achieves the highest DA at 57.16%, while Op-09 records the lowest at 50.93%. Contrary to the improvements observed in UDI, DA does not show enhancement and actually exhibits a slight decrease. This indicates that optimizing wall UDI and limiting overall wall illuminance also correspondingly restricts the floor's DA.

DGP study

From Figure 6.19, it is evident that, owing to the morphology of the skylight model, both the baseline-02 and the ten optimized results models have achieved optimal control over glare. The glare intensity remains within 0.35 throughout the year, indicating imperceptible glare, and thus, there is no room for further optimization.

Annual daylight illuminance

The Annual Daylight Illuminance serves as an indicator reflecting the specific distribution of annual sunlight exposure over time periods. From Figure 6.19, it is observed that in the daylight performance of the baseline-02 scenario, time periods with illuminance exceeding 200 lux are primarily concentrated from February to October annually. Notably, during the months of May to July, the duration of illuminance exceeding 200 lux is the longest, approximately 10 to 11 hours daily. Post-optimization, the time periods exceeding 200 lux are primarily concentrated from May to July annually. Within this period, there is an improvement in the daily duration of illuminance exceeding 200 lux, with approximately 5 hours each day. This signifies that after optimization, not only is the overall duration of unacceptable illuminance reduced throughout the year, but there is also a notable enhancement in the daily duration of unacceptable illuminance.

	North	East	South	West	DGP
B02	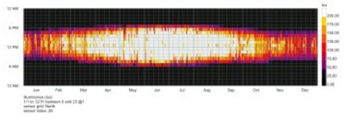	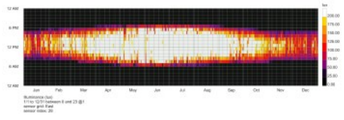	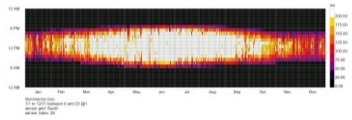	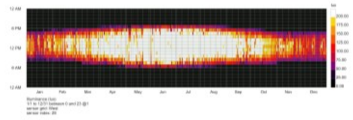	
Op01	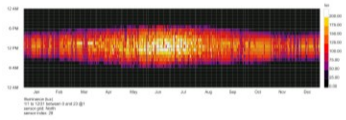	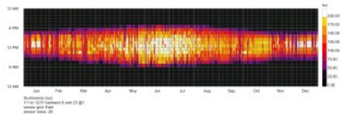	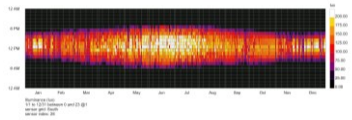	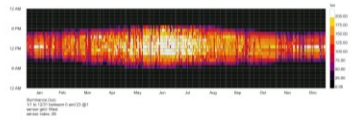	
Op02	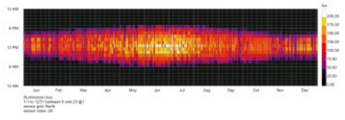	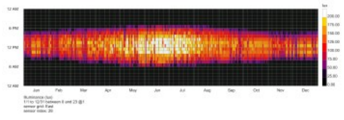	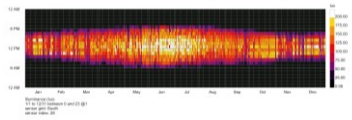	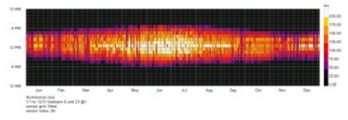	
Op03	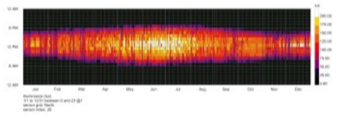	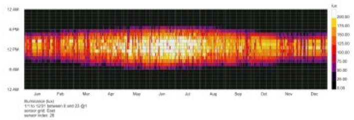	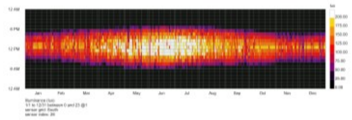	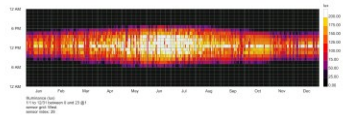	
Op04	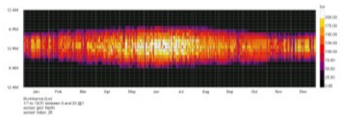	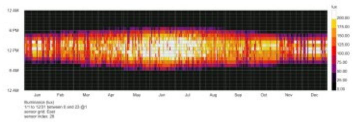	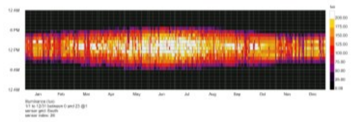	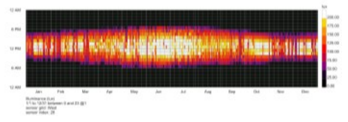	
Op05	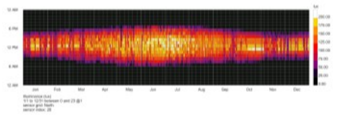	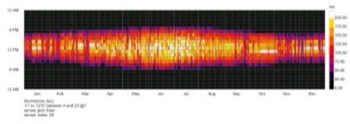	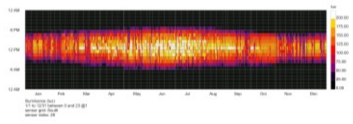	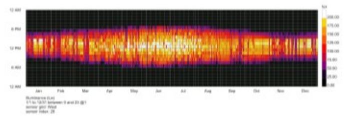	

Op06	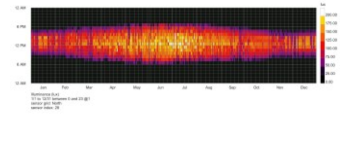	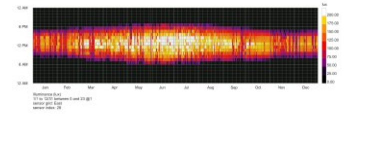	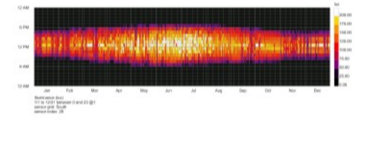	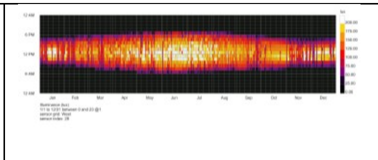	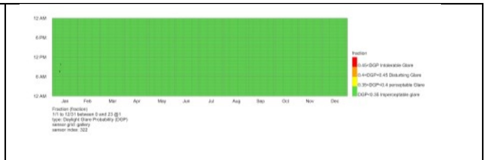
Op07	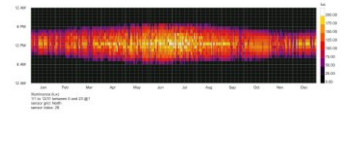	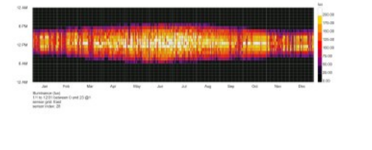	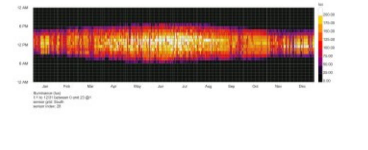	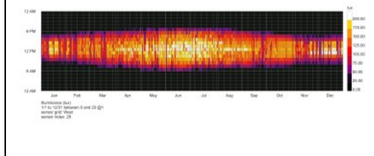	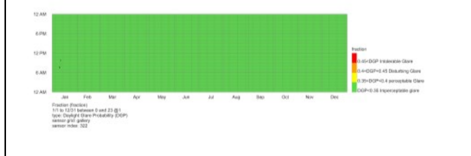
Op08	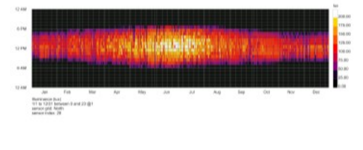	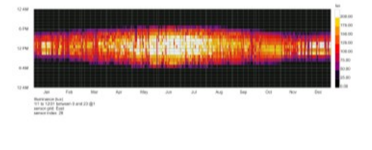	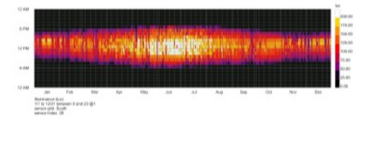	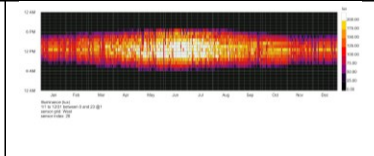	
Op09	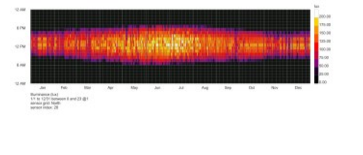	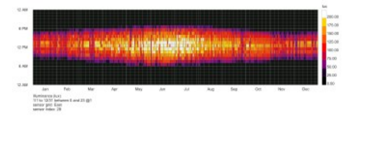	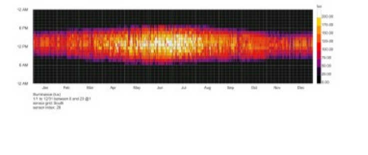	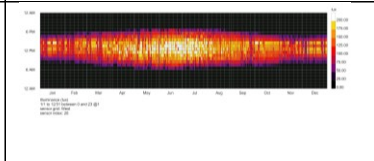	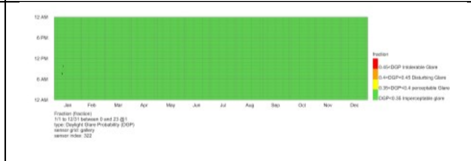
Op10	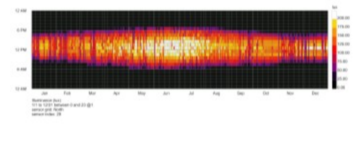	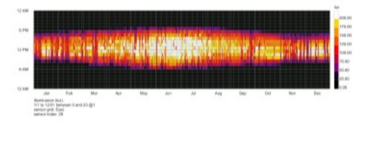	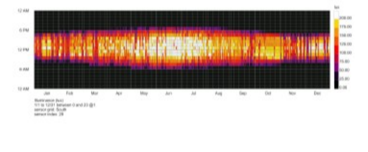	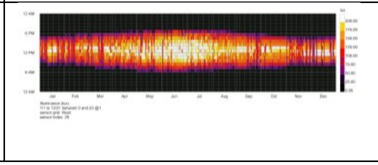	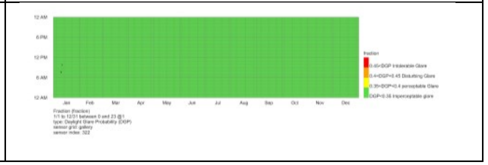

Figure 6.19 Hourly plot of annual daylight illuminance and DGP of baseline-02 and optimized results.

6.9.7. Cross-sectional study of optimal solutions

This section primarily explores the uniformity of illumination on the walls, with a particular focus on the numerical variations recorded by sensors located at a height of 1.55 meters on all walls within the room. Achieving more uniform illumination is beneficial for enhancing visual comfort for observers. Both Figure 6.20 and Figure 6.21 depict the specific values and trends of the continuous distribution of ACI and UDI across all four walls inside the room. The first five optimized results are selected for comparison.

ACI of walls

From Figure 6.20, it is evident that both the baseline-02 model and the optimized models exhibit a noticeable annual illuminance distribution trend, with the ACI significantly higher in the central part of the walls than in the corners. The ACI curves for each wall segment present distinct arch-shaped patterns. Notably, the ACI peak on the north-facing wall is the lowest among the four walls, while the east and west-facing walls have the highest ACI peaks. In baseline-02, the peak ACI on the north-facing wall reaches 716,624 lux, while the peak values on the other walls approach 800,000 lux. In the optimized results, in the majority of cases, wall ACI is below 480,000 lux. While achieving absolute uniformity may be challenging, the optimized results demonstrate a noticeable reduction in the disparity between the highest and lowest ACI values compared to baseline-02.

UDI of walls

In this section, the focus is primarily on comparing the continuity of UDI between baseline-02 and optimized results. From Figure 6.21, it is evident that baseline-02's UDI exhibits a clear trend, with lower UDI in the middle of the walls compared to the corners. Except for the north-facing wall where UDI slightly exceeds 50%, UDI on the remaining walls is below 50%. In optimized results, the UDI for all points is consistently above 75%, without displaying a distribution trend similar to baseline-02. The disparity in UDI between wall corners and wall surfaces is minimal. There is also no significant difference in UDI among the four walls, presenting an overall uniform linear pattern.

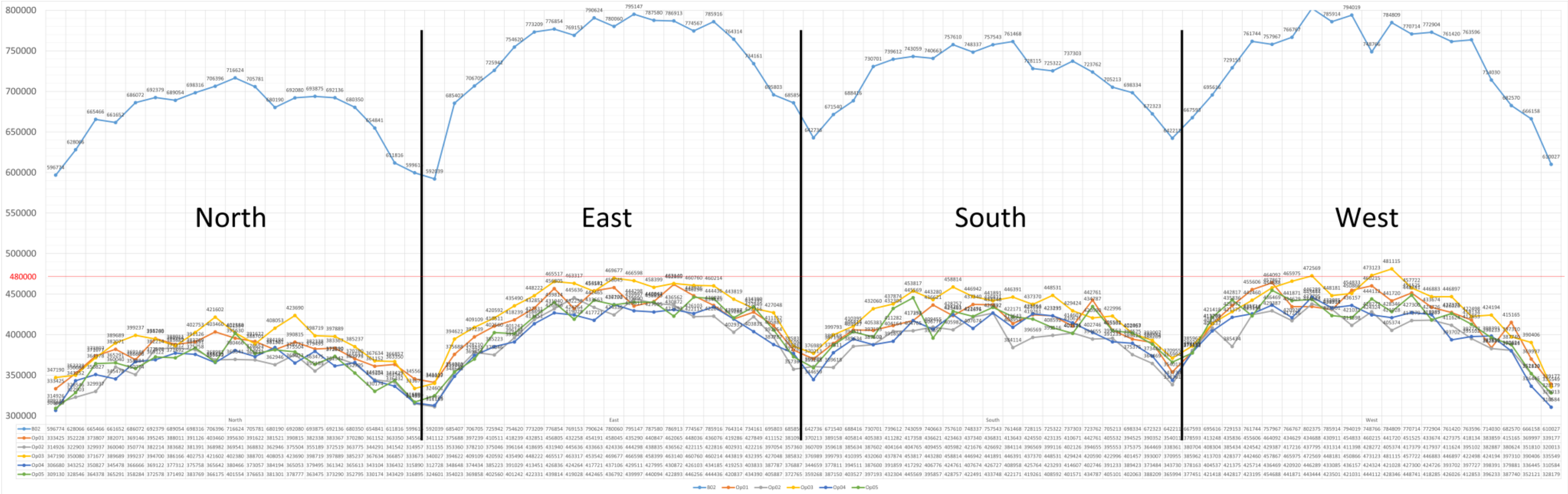

Figure 6.20 Cross-sectional study of all walls of ACI (lux)

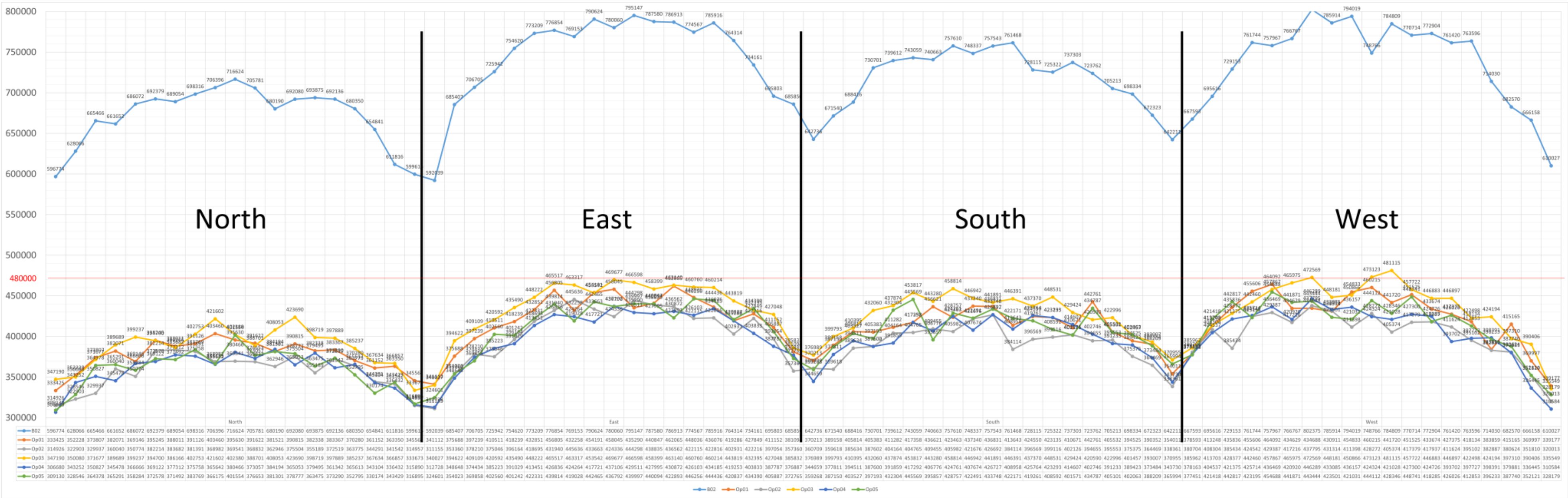

Figure 6.21 Cross-sectional study of all walls of UDI (%)

6.9.8. Comparison with physical test (Point in time)

Figure 6.22 and Figure 6.23 respectively showcase the hourly illuminance data for the mock-up model and the Op-01 model on November 21, 2023, from 9 AM to 4 PM. Despite differences in values, which could be attributed to the day's lighting conditions and the materials' light transmission and reflection properties, the overall trend of the curves is similar.

Observing the curve progression, both models exhibit a continuous arch-like shape, with the highest points at the central points near each wall (N3,W3,S3,E3) and the lowest points at the corners (N1,N5,W1,W5,S1,S5,E1,E5). The illuminance measured on the north-facing walls is lower than that on the other three walls.

A comparison of the values at each measurement point across different times reveals a commonality: the highest values are recorded at noon, and the lowest values at 4 PM. The values from 9 AM to noon are relatively close, while the values at 4 PM are significantly lower than at other times. As shown in Figure 6.24, both the mock-up model and the Op-01 model experience a gradual rise to a peak from 9 AM to noon, a slow decline from noon to 4 PM, followed by a sharp decrease.

Although there are differences in specific values, the shapes of the curves are broadly similar, indicating a similar trend in daylight changes throughout the day. The consistency in the trend of daylight changes provides a method for validating computer simulations. This method allows for the adjustment and calibration of simulation parameters to closely align with real-world conditions, thereby enhancing the accuracy and reliability of daylight analysis simulation results in architectural design.

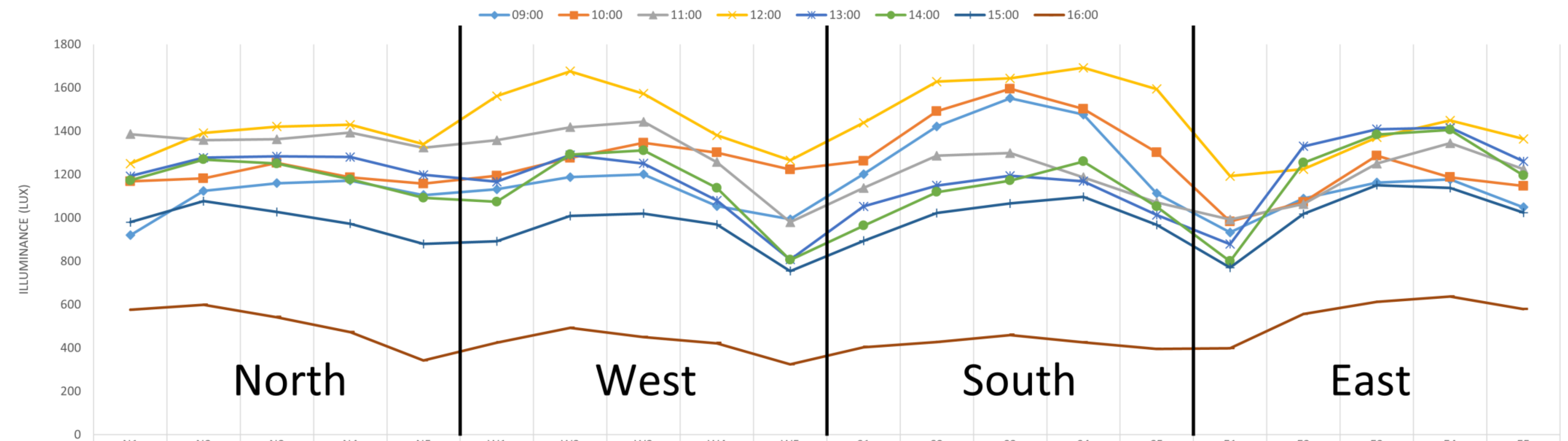

	N1	N2	N3	N4	N5	W1	W2	W3	W4	W5	S1	S2	S3	S4	S5	E1	E2	E3	E4	E5
09:00	920	1124	1160	1172	1105	1132	1188	1201	1054	994	1202	1422	1552	1476	1113	933	1089	1163	1177	1049
10:00	1168	1182	1253	1186	1158	1194	1276	1346	1301	1223	1262	1492	1595	1502	1302	983	1073	1287	1187	1147
11:00	1386	1359	1363	1393	1324	1358	1418	1443	1257	980	1138	1287	1299	1187	1072	992	1063	1250	1344	1224
12:00	1250	1391	1421	1429	1340	1561	1676	1573	1381	1265	1438	1628	1643	1692	1594	1193	1224	1371	1449	1364
13:00	1193	1278	1284	1281	1199	1167	1290	1251	1080	808	1053	1149	1194	1169	1013	879	1330	1409	1416	1261
14:00	1173	1269	1250	1177	1092	1074	1292	1311	1138	806	964	1119	1172	1260	1052	800	1254	1384	1406	1196
15:00	980	1077	1027	973	880	892	1009	1020	969	755	894	1022	1067	1097	968	770	1018	1151	1138	1024
16:00	576	599	542	473	342	425	493	450	422	324	404	427	460	426	395	398	556	613	637	579

POSITION OF SENSORS

Figure 6.22 The point in time test of mock-up model

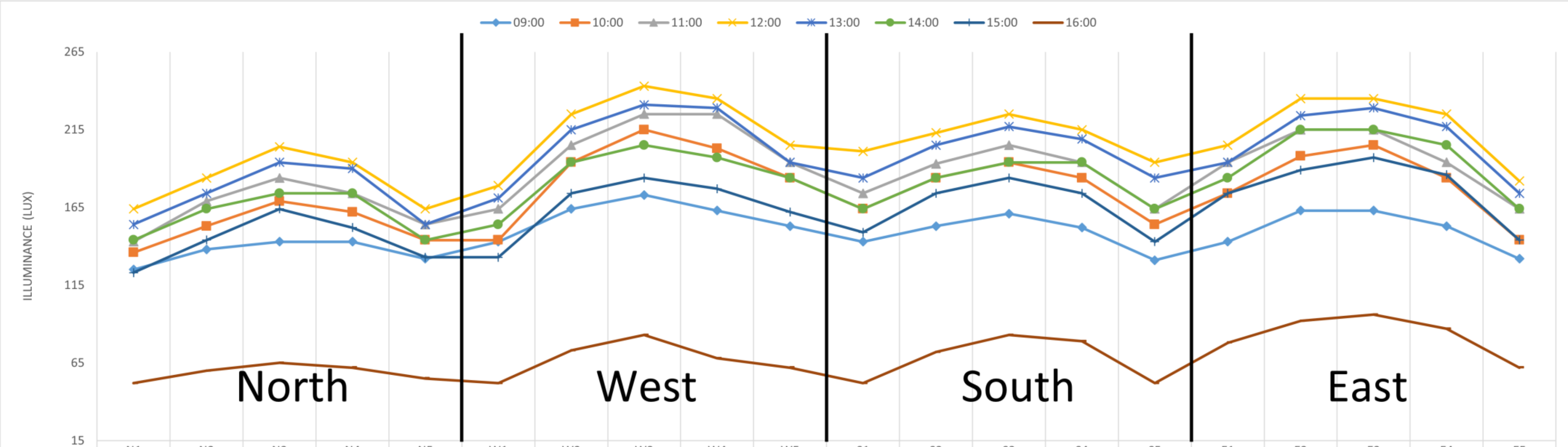

	N1	N2	N3	N4	N5	W1	W2	W3	W4	W5	S1	S2	S3	S4	S5	E1	E2	E3	E4	E5
09:00	125	138	143	143	132	143	164	173	163	153	143	153	161	152	131	143	163	163	153	132
10:00	136	153	169	162	144	144	194	215	203	184	164	184	194	184	154	174	198	205	184	144
11:00	143	169	184	174	154	164	205	225	225	194	174	193	205	194	164	194	215	215	194	164
12:00	164	184	204	194	164	179	225	243	235	205	201	213	225	215	194	205	235	235	225	182
13:00	154	174	194	190	154	171	215	231	229	194	184	205	217	209	184	194	224	229	217	174
14:00	144	164	174	174	144	154	194	205	197	184	164	184	194	194	164	184	215	215	205	164
15:00	123	144	164	152	133	133	174	184	177	162	149	174	184	174	143	174	189	197	186	144
16:00	52	60	65	62	55	52	73	83	68	62	52	72	83	79	52	78	92	96	87	62

POSITION OF SENSORS

Figure 6.23 The point in time test of simulating model Op-01

Figure 6.24 Comparison of mock-up model and Op-01 illuminance curve progression (N3)

6.10. **Discussion**

The point skylight system comprises uniformly arranged individual skylights, each with identical attributes, forming a matrix sequence similar to point light sources indoors. Annual daylighting simulations of interior spaces clearly demonstrate that, compared to traditional sawtooth-shaped skylight systems, the point skylight system effectively reduces direct sunlight exposure and minimizes glare to a great extent, creating a uniform natural lighting environment. The illumination intensity on the four interior walls is essentially maintained at a uniform level, with only a slight decrease observed at the corners. Following optimization, indoor lighting conditions have significantly improved, aligning with the standards specified by the IESNA.

Detailed examination of the optimization process, as depicted in Figure 6.10 and Figure 6.11, indicates that setting the Arc/SD to -0.2m or -0.3m enhances indoor natural lighting. This is evidenced by a notable reduction in ACI and an increase in UDI. Such improvement is likely attributed to the saddle-shaped shading panels which, owing to their hyperbolic shape, diminish the intensity of reflected light, unlike single-curved panels that exhibit higher reflectance. Additionally, these saddle-shaped panels may align more effectively with the solar angle's dynamic and periodic variations throughout the year. It is hypothesized that during periods of higher solar angles, such as summer noon, this configuration may efficiently block substantial portions of direct sunlight. However, these observations remain preliminary and require further experimentation and validation to ascertain the impact of shading panel shape on indoor daylight variation.

6.11. **Conclusion**

This study focuses on the natural lighting conditions within galleries, optimizing and balancing visual comfort and the protection of artifacts. Given the variety of exhibit materials that may be displayed on the floors and walls of art museums, targeted evaluations were set based on the different types of materials. With the aid of computers, lighting simulations were conducted according to predetermined parameters; moreover, genetic algorithms were applied to adjust these parameters to derive optimal solutions and ascertain the impact of each parameter on indoor natural lighting.

The results of this study are as follows:

-When the parameters of the point skylight system are set to: Height/LW at 0.7 and 0.6 meters, Angle/LW between 10 to 30 degrees, Angle/OP from 80 to 120 degrees, Length/SD ranging from 1.3 to 1.5 meters, Angle/SD between 65 to 70 degrees, and Arc/SD from -0.2 to -0.3 meters, the system achieves optimal lighting conditions. Under these settings, the annual sunlight exposure is maintained below 480,000 lux, and the Useful Daylight Illuminance (UDI) of 50-200 lux persists for over 75% of the year.

-Among the design parameters, Height/LW notably impacts the quality of interior lighting in the art museum. A skylight height within the range of 0.6 to 0.7 meters is effective in reducing annual ACI and enhancing UDI, albeit with a decrease in DA. Angle/SD also significantly affects the indoor lighting environment. For example, angles of 65 and 70 degrees between the shading panels and the horizontal plane increase indoor ACI, with a marginal improvement in UDI.

-The curvature of the shading metal panels, specifically Arc/SD, is also a finding of this study. While not as impactful as Height/LW and Angle/SD, Arc/SD plays a noticeable role. Minimized Arc/SD values, indicating a saddle-shaped configuration, improve ACI reduction and UDI enhancement indoors. The selected configurations for Arc/SD consistently fall at -0.2 or -0.3.

In conclusion, this study presents a design framework that offers designers, researchers, stakeholders, and architects a unique perspective on optimizing natural lighting effects. With the aid of computer simulation and genetic algorithms, it creates solutions that are cost-effective, time-efficient, and resource-efficient. Supported by the latest developments in computational simulation, this paper demonstrates that Multi-objective Optimization (MOO) through computational algorithms can guide architects in finding high-performance solutions at the early stages of design, across various parameter requirements. This research also serves as a starting point for implementing the proposed methods in practical design processes.

Future work should build upon this study to extend research into various daylight shading applications and architectural styles. The point skylight system, as an innovative shading system, harnesses natural light reflection for interior illumination in environments without windows. Further exploration into curved shading panels, such as hyperbolic surfaces, and their impact on indoor lighting compared to flat panels, is necessary. With a global emphasis on low-carbon energy efficiency, it is crucial to maximize natural light utilization while meeting specific lighting conditions for different types of buildings. Therefore, further investigation into passive shading systems, especially those incorporating curved shading elements, holds promise for advancing our understanding of daylight optimization in a wide range of architectural contexts.

Chapter 7. Discussion

Considering the development of computational architecture and the crucial role of introducing generative process thinking in the early stages of building design to fully utilize natural daylight and achieve energy efficiency, this dissertation presents a method that investigates the relationship between design parameters and performance goals through the use of generative and parametric approaches combined with multi-objective optimization via genetic algorithms. This study aims to explore potential design solutions generated during the optimization process and identify the best design alternatives for specific given environments. Additionally, it examines the relationship between design parameters and objectives, identifying the most influential parameters on a micro level to determine whether parametric and generative algorithm methods can assist designers or engineers in optimizing building performance during the early design stages by discovering connections between parameters and objectives and pinpointing the most impactful parameters.

This dissertation comprises nine chapters. Chapter 1 provides the background, research aims and objectives, originality and contributions, and the structure of the dissertation. Chapter 2 compiles and explains recent literature on the use of parametric and multi-objective optimization platforms in the building design process. Topics include daylight, geometric shapes, and shading-related issues, including the use of various skylights and their materials. Chapter 3 describes the broader computational process, including the use of parametric and generative optimization, followed by data collection and analysis mechanisms. Chapter 4 covers the preliminary study conducted before the formal research began, including variations in solar angles and sky illuminance, specific daylight requirements for museums and libraries, and studies on various skylight forms and materials.

7.1.1. Discussion of Chapter 5

The main body consists of three chapters, each providing detailed results from a specific experimental scenario. Chapter 5 describes the methodology of using genetic algorithms to optimize the geometric configuration of sawtooth skylights. In the realm of museum design, adept management of natural light stands as a cornerstone for achieving energy efficiency, fostering a comfortable indoor ambiance, and ensuring the preservation and display of exhibits. Among popular skylight systems, the sawtooth skylight draws significant attention and finds widespread application in museum architectural paradigms.

However, challenges emerge when a building's orientation deviates from true north, potentially resulting in localized variations of light intensity. This study extensively investigates the application of genetic algorithms as a forward-looking approach to optimizing the geometric configuration of sawtooth skylights, ensuring optimal natural light distribution in museums situated away from the polar regions. The genetic algorithm framework is leveraged as a feasible problem-solving method. The research utilizes the Octopus and Ladybug tools to define the shading system's design parameters, fitness function, and genetic algorithm settings, all based on comprehensive year-round sunlight simulations to facilitate the optimization process. Through an iterative approach, the study generates and assesses diverse shading system configurations, progressively honing in on the optimal design solution.

Ultimately, this research tailors an optimized shading system for buildings oriented at 45 degrees northeast, effectively ensuring an ideal balance of interior luminosity while meeting necessary exhibit protection standards. The simulation calculations in Octopus stopped running after generating 931 results. It was observed that most simulated results for spatial Useful Daylight Illuminance (sUDI) were distributed within the range of 0% to 60%, while Spatial Daylight Autonomy (sDA) values ranged from 0% to 100%, with a significant portion between 40% and 100%. Most Daylight Glare Probability (DGP) values were below 5%, and those above 5% were not considered optimized since their corresponding sUDI was 0. From this group of test results, a suitable optimization result was selected. The sunshade of the optimized sunroof presents a waveform. By comparing the baseline models with the optimized results, patterns of lighting variations were identified. It was found that the optimized result had higher sUDI and sDA values compared to the baseline models. Specifically, the optimized sUDI increased from 24% in the baseline model to 39.81%, and sDA increased from 52.20% to 61.73%.

Under the same skylight shading system, the orientation of the building significantly impacts daylighting performance. For instance, in one baseline scenario, more daylight accumulated on the south-facing wall, whereas, in another baseline, more daylight accumulated on the east-facing wall. Year-round illumination in one baseline was significantly higher than in the other, indicating that building orientation has a considerable impact on daylight performance. The overall acceptable sUDI shifted from the north side in one baseline to the northwest side in the other, with sUDI decreasing from 32.4% to 24% and sDA increasing from 49.3% to 59.2%. Comparing another baseline with the optimized result under the same orientation, it was noted that although higher ACI values were concentrated on the east-facing wall in both models, the optimized scenario had significantly less year-round insolation. The UDI in the optimized results was significantly higher due to the decrease in overall indoor ACI, increasing acceptable sUDI from 24% to 39.81% and DA from 52.20% to 61.73%. These comparisons demonstrate that optimizing the skylight system can significantly enhance daylight performance. The research highlights that genetic algorithms can quickly determine the optimal type of lighting to achieve desired light harvesting goals, resulting in significant improvements in interior lighting performance. The findings are expected to inform the design decision-making process based on performance criteria in the early stages of design.

7.1.2. Discussion of Chapter 6

Chapter 6 describes the methodology and findings related to optimizing natural lighting in museum galleries using advanced computational tools and genetic algorithms. The primary goal of this research is to enhance visual comfort, preserve artifacts, and achieve energy efficiency in museum lighting design.

In the realm of museum design, the meticulous planning of natural lighting plays a vital role in enhancing energy efficiency, improving the indoor atmosphere, and preserving and showcasing artifacts. One significant challenge is ensuring visitors' visual comfort while minimizing excessive natural light to prevent damage to exhibits. This study uses the High Museum Expansion by Renzo Piano as a case study, employing the medium sensitivity exhibit standards from the Illuminating Engineering Society of North America (IESNA) as the evaluation criteria.

During the preliminary design phase, computer modeling was utilized, and daylighting simulations were carried out using the Ladybug tool. The Octopus genetic algorithm plugin was applied to investigate, optimize, and evaluate the performance of point skylight systems in museum interiors. The findings indicate that optimized point skylight systems not only block direct sunlight, reducing indoor glare, but also ensure that the Annual Cumulative Illuminance (ACI) on interior surfaces stays below 480,000 lux, while the annual effective Useful Daylight Illuminance (UDI) is increased to 75%. In terms of design parameters, a skylight height of 0.6 to 0.7 meters, combined with a shading panel to horizontal angle of 65 to 70 degrees, is found to be effective in enhancing indoor lighting conditions.

The study focuses on the natural lighting conditions within galleries, aiming to optimize and balance visual comfort and artifact protection. Given the variety of exhibit materials that may be displayed on the floors and walls of art museums, targeted evaluations were set based on different types of materials. With the aid of computers, lighting simulations were conducted according to predetermined parameters; genetic algorithms were applied to adjust these parameters to derive optimal solutions and ascertain the impact of each parameter on indoor natural lighting.

The point skylight system comprises uniformly arranged individual skylights, each with identical attributes, forming a matrix sequence similar to point light sources indoors. Annual daylighting simulations of interior spaces clearly demonstrate that, compared to traditional sawtooth-shaped skylight systems, the point skylight system effectively reduces direct sunlight exposure and minimizes glare to a great extent, creating a uniform natural lighting environment. The illumination intensity on the four interior walls is essentially maintained at a uniform level, with only a slight decrease observed at the corners. Following optimization, indoor lighting conditions have significantly improved, aligning with the standards specified by the IESNA.

A key aspect of this research is the construction of a physical model based on the optimized design from the computer simulations. After selecting the best result using the fitness function, a physical model was built to conduct actual daylight testing. The results from the physical model were then compared and calibrated against the computer simulation results, providing a robust validation of the findings.

Detailed examination of the optimization process indicates that setting the Arc/SD to -0.2m or -0.3m enhances indoor natural lighting. This is evidenced by a notable reduction in ACI and an increase in UDI. Such improvement is likely attributed to the saddle-shaped shading panels which, owing to their hyperbolic shape, diminish the intensity of reflected light, unlike single-curved panels that exhibit higher reflectance. Additionally, these saddle-shaped panels may align more effectively with the solar angle's dynamic and periodic variations throughout the year. It is hypothesized that during periods of higher solar angles, such as summer noon, this configuration may efficiently block substantial portions of direct sunlight. However, these observations remain preliminary and require further experimentation and validation to ascertain the impact of shading panel shape on indoor daylight variation.

The study's findings suggest that optimizing the skylight system can significantly enhance daylight performance. By iterating using a genetic algorithm, computer simulations can rapidly determine the optimal type of lighting to achieve desired light harvesting goals, resulting in significant improvements in interior lighting performance. This innovative methodology introduces new strategies for refining architectural designs within specific lighting constraints, enriching the spectrum of strategies employed for comprehensive light control.

Furthermore, this study emphasizes the importance of integrating advanced computational tools in architectural design, highlighting their role in achieving sustainable and efficient buildings. The use of genetic algorithms, in conjunction with tools like Octopus and Ladybug, exemplifies the potential of these technologies to transform traditional architectural practices. By facilitating a more precise and controlled approach to daylight management, these tools help create environments that are both energy-efficient and conducive to the preservation of cultural artifacts.

The research demonstrates that employing genetic algorithms can significantly improve natural light management in museum spaces, offering valuable insights for architects and engineers aiming to optimize building performance in varying orientations. The study also highlights the necessity for further experiments to determine how to improve and optimize the skylight system and quantify the potential increase in lighting performance. The findings are expected to inform the design decision-making process based on design performance in the early stages of design.

7.1.3. Discussion of the methodology

The methods proposed in this thesis underscore the significant role of computational architecture in identifying and optimizing design solutions based on a given dataset of parameters. These methods have demonstrated how leveraging advanced computational tools can streamline the design process, making it more efficient and effective. However, several limitations have been identified. Firstly, a fundamental understanding of informatics is necessary to comprehend the logic of the computational process, which can be a barrier for some practitioners. Secondly, the reliance on the EPW file, a historical database, could be improved by incorporating actual measurements from the field to enhance the accuracy of material properties and weather conditions. This approach would ensure that the data used in simulations are as close to real-world conditions as possible.

Additionally, the hypothetical virtual model in this research neglects thickness due to hardware limitations. This simplification can impact the accuracy of the simulation results. Future research should include the thickness and detailed definitions of model surfaces in virtual models. Moreover, enhancing simulations using real-time weather data and increasing the number of design iterations could lead to more optimized solutions. These improvements would make the simulation results more reliable and applicable to real-world scenarios.

The methods discussed in this thesis highlight the benefits of computational architecture by laying a foundation for these strategies, allowing future research to build upon them and drive further advancements. This research is expected to benefit architects, designers, regulators, manufacturers, and other professionals in the built environment. The proposed methodology can be applied to various materials and climate models, providing insights into design goal optimization during the early stages of design using less time-consuming and cost-effective tools compared to on-site measurements with actual materials. Additionally, this approach offers potential in reducing the negative environmental impacts of buildings, aligning with sustainability goals.

By employing genetic algorithms and advanced simulation tools like Octopus and Ladybug, the research demonstrates how these technologies can transform traditional architectural practices. This thesis contributes to establishing a framework for such strategies, enabling future research to enhance and expand upon it. The findings suggest that computational methods can significantly improve natural light management in museum spaces, offering valuable insights for architects and engineers aiming to optimize building performance in varying orientations. Furthermore, the construction of a physical model based on the optimized design from computer simulations adds a layer of validation, ensuring that theoretical models align with practical applications.

The study emphasizes the importance of integrating advanced computational tools in architectural design, highlighting their role in achieving sustainable and efficient buildings. The use of genetic algorithms in conjunction with tools like Octopus and Ladybug exemplifies the potential of these technologies to innovate and improve traditional architectural methods. By facilitating a more precise and controlled approach to daylight management, these tools help create environments that are both energy-efficient and conducive to the preservation of cultural artifacts.

In conclusion, this thesis lays the groundwork for future advancements in architectural design, particularly in optimizing natural lighting for museums. The methodologies and findings presented here are expected to inform the design decision-making process, providing a robust framework for achieving optimal design solutions. This study's contributions are anticipated to benefit a wide range of stakeholders, including architects, designers, regulators, manufacturers, and other practitioners in the built environment, ultimately advancing the field of computational architecture.

Chapter 8. Conclusion

Researchers and practitioners have undertaken extensive work in utilizing parametric and multi-objective optimization methods for environmentally sustainable design. However, comprehensive optimization approaches from inception to the ranking of design solutions are still limitedly reported. To address the time-consuming and costly issue of comprehensive light testing in the early stages of architectural design, this thesis proposes a computational design platform using parametric and generative algorithm optimization methods at the initial design phase. The platform aims to investigate the relationship between design parameters and design objectives, as well as the potential for optimizing design objectives concerning environmental performance metrics. This thesis challenges design thinking by attempting to answer how the proposed computational methods contribute to optimizing design objectives and identifying the role of parameters in driving design goals. It emphasizes the hypothesis that computational and generative methods can achieve optimization and identify the influence of parameters on design objectives. The proposed method is particularly significant when handling multiple design objectives and dynamic parameters, such as climate data or material properties, requiring additional data input. By defining the design logic for the intended design objects, the computational design mechanism is applied to building skylight systems and daylighting studies.

8.1.1. Conclusion of Chapter 5

Chapter 5 describes the methods of investigating and optimizing the use of expanded metal as a shading device in architectural design. The research results indicate that the optimized expanded metal shading system can effectively reduce direct sunlight and indoor glare while ensuring that the annual cumulative illuminance (ACI) of interior surfaces remains below 480,000 lux. Additionally, the annual useful daylight illuminance (UDI) was improved to 75%. The study found that a skylight height of 0.6 to 0.7 meters and a shading panel angle of 65 to 70 degrees significantly enhance indoor lighting conditions.

A detailed examination of the optimization process revealed that setting the Arc/SD to -0.2m or -0.3m enhances natural indoor lighting. This improvement is attributed to the saddle-shaped shading panels, which, due to their hyperbolic shape, reduce the intensity of reflected light compared to single-curved panels. Moreover, these saddle-shaped panels align more effectively with the dynamic and periodic changes in the sun's angle throughout the year. During periods of high solar angles, such as midday in summer, this configuration effectively blocks a significant portion of direct sunlight.

This study underscores the potential of advanced computational tools and genetic algorithms in transforming traditional architectural practices, particularly in museum design. The innovative approach proposed introduces new strategies for optimizing architectural design within specific lighting constraints, expanding the application of comprehensive light control strategies. The findings are expected to provide valuable insights into the design decision-making process at early stages, offering practical solutions for architects, designers, and other stakeholders in the built environment.

The research demonstrates that employing genetic algorithms can significantly improve the management of natural light in museum spaces, offering practical solutions for optimizing building performance. The results also highlight the necessity for further experiments to determine how to improve and optimize skylight systems and quantify potential enhancements in lighting performance. The contributions of this study are anticipated to benefit a wide range of stakeholders, including architects, designers, regulators, manufacturers, and other practitioners in the field of the built environment, ultimately advancing the field of computational architecture.

8.1.2. Conclusion of Chapter 6

Chapter 6 describes the methods employed in optimizing natural lighting for museum galleries using advanced computational tools and genetic algorithms. The primary goal of this research is to enhance visual comfort, protect artifacts, and achieve energy efficiency in museum lighting design. Through the application of computer modeling and the use of tools such as Ladybug for daylight simulations and the Octopus genetic algorithm plugin, the study investigated, optimized, and evaluated the performance of point skylight systems within museum interiors.

The findings demonstrate that optimized point skylight systems not only block direct sunlight and reduce indoor glare but also ensure that the Annual Cumulative Illuminance

(ACI) on interior surfaces remains below 480,000 lux. Additionally, the annual effective Useful Daylight Illuminance (UDI) increased to 75%. In terms of design parameters, it was found that a skylight height of 0.6 to 0.7 meters and a shading panel angle of 65 to 70 degrees are effective in enhancing indoor lighting conditions.

Detailed examination of the optimization process revealed that setting the Arc/SD to -0.2m or -0.3m enhances indoor natural lighting. This improvement is likely due to the saddle-shaped shading panels, which reduce the intensity of reflected light more effectively than single-curved panels. These panels align better with the dynamic and periodic variations of solar angles throughout the year, particularly during high solar angle periods like summer noon, efficiently blocking significant portions of direct sunlight.

The study emphasizes the potential of advanced computational tools and genetic algorithms in transforming traditional architectural practices, particularly in museum design. The innovative methodology presented introduces new strategies for refining architectural designs within specific lighting constraints, enhancing the array of strategies for comprehensive light control. The results are expected to inform the design decision-making process early on, providing valuable insights for architects, designers, and other stakeholders in the built environment.

Furthermore, the research confirms that employing genetic algorithms can significantly improve natural light management in museum spaces, offering practical solutions for optimizing building performance. The study highlights the necessity of further experiments to refine skylight systems and quantify potential improvements in lighting performance. These contributions are expected to benefit a wide range of stakeholders, including architects, designers, regulators, manufacturers, and other practitioners in the built environment, ultimately advancing the field of computational architecture.

8.1.3. Conclusion for thesis

Overall, the series of experiments conducted in this study introduce novelty and contributions in two significant domains. Firstly, there is a broad contribution that encompasses the overarching idea behind this research. Secondly, there are specific novelties and contributions presented in more detail based on the case studies examined.

According to the results and findings of this research, the field of architecture can be both subjectively and quantitatively validated and confirmed at a micro-level within specific parameter value ranges. In architectural design, when this approach is applied at the early stages of design, countless design alternatives and outcomes emerge. Consequently, the design decision-making process can become more rational. "Good" will no longer be subjective but can be evaluated and generalized. As confirmed in the findings of each case study, the research results approach design theory by introducing an alternative method of evaluating the design process early on, thus saving time in addressing uncertainties. This mindset may tend to bring performance considerations forward to the early stages of design rather than during the evaluation phase.

The study contributes to the field of computational architectural design by demonstrating how morphological exploration can lead to the optimization of design objectives and by providing a method to investigate the relationship between design parameters and design goals at different scales of the design process. In the early stages of architectural design, understanding the relationship and trends between parameters and design objectives allows for the quantitative validation of design goals, achieving more optimized solutions.

References

[1] S. Sharples, D. Lash, Daylight in Atrium Buildings: A Critical Review, Archit. Sci. Rev. 50 (2007) 301–312. https://doi.org/10.3763/asre.2007.5037.
[2] M. DeKay, Daylighting and urban form: An urban fabric of light, J. Archit. Plan. Res. (2010) 35–56.
[3] U.G.B. Council, US green building council, US Green Building Council Washington, DC, USA, 1998.
[4] U.G.B. Council, LEED v4 for building design and construction, USGBC Inc 332 (2014).
[5] D. Phillips, Daylighting, Routledge, 2012.
[6] L. Edwards, P. Torcellini, Literature review of the effects of natural light on building occupants, (2002).
[7] D. Purves, S.M. Williams, eds., Neuroscience, 2. ed, Sinauer Associates, Sunderland, Mass, 2001.
[8] N. Lechner, Heating, cooling, lighting: Sustainable design methods for architects, John wiley & sons, 2014.
[9] Lighting, IEA (n.d.). https://www.iea.org/energy-system/buildings/lighting (accessed June 27, 2024).
[10] R. Páramo, Environmental repercussions of artificial lighting, Segur. Medio Ambiente 28 (2008) 112.
[11] Daylighting | WBDG - Whole Building Design Guide, (n.d.). https://wbdg.org/resources/daylighting (accessed June 27, 2024).
[12] D.C. CABE, The impact of office design on business performance, (2005).
[13] J. Natanian, O. Aleksandrowicz, T. Auer, A parametric approach to optimizing urban form, energy balance and environmental quality: The case of Mediterranean districts, Appl. Energy 254 (2019) 113637. https://doi.org/10.1016/j.apenergy.2019.113637.
[14] K. Konis, A. Gamas, K. Kensek, Passive performance and building form: An optimization framework for early-stage design support, Sol. Energy 125 (2016) 161–179. https://doi.org/10.1016/j.solener.2015.12.020.
[15] A. Eltaweel, Y. Su, Q. Lv, H. Lv, Advanced parametric louver systems with bi-axis and two-layer designs for an extensive daylighting coverage in a deep-plan office room, Sol. Energy 206 (2020) 596–613. https://doi.org/10.1016/j.solener.2020.06.035.
[16] H. Kim, M.J. Clayton, Parametric behavior maps: A method for evaluating the energy performance of climate-adaptive building envelopes, Energy Build. 219 (2020) 110020. https://doi.org/10.1016/j.enbuild.2020.110020.
[17] A. Agha, A. Shibani, D.H. Hassan, A. Salmon, Building research establishment environmental assessment methodology on the UK residential projects, Int. J. Constr. Eng. Manag. 9 (2020) 183–189.
[18] Ar. Kirti Varandani, Ar.Vibhuti Joshi, Ar. Sangeeth S Pillai, OPTIMIZATION OF DAYLIGHT IN MUSUEMS AND ART GALLERIES, EPRA Int. J. Res. Dev. IJRD (2021) 259–265. https://doi.org/10.36713/epra7327.
[19] I. Acosta, J. Navarro, J.J. Sendra, Daylighting design with lightscoop skylights: Towards an optimization of shape under overcast sky conditions, Energy Build. 60 (2013) 232–238. https://doi.org/10.1016/j.enbuild.2013.01.006.
[20] D. Behar, G. Capeluto, M. Levin, Light restoration proposal for the Ein Harod Museum of Art, Archit. Sci. Rev. 58 (2015) 300–313. https://doi.org/10.1080/00038628.2013.809687.
[21] E.O. O, Achieving Effective Internal Visibility through Daylighting at National War Museum Umuahia, Abia, Nigeria, Int. J. Res. Appl. Sci. Eng. Technol. 7 (2019) 949–957. https://doi.org/10.22214/ijraset.2019.9132.
[22] H. Sharif-Askari, B. Abu-Hijleh, Review of museums' indoor environment conditions studies and guidelines and their impact on the museums' artifacts and energy

consumption, Build. Environ. 143 (2018) 186–195. https://doi.org/10.1016/j.buildenv.2018.07.012.
[23] C.W. Kesner, Analysis of the Museum Lighting Environment, J. Inter. Des. 23 (1997) 28–41. https://doi.org/10.1111/j.1939-1668.1997.tb00247.x.
[24] InformeDesign, Green Build. Elem. (n.d.). https://greenbuildingelements.com/informedesign/ (accessed July 3, 2024).
[25] D. CIBSE, W. Design, Lighting Guide LG10, Chart. Inst. Build. Serv. Eng. (1999).
[26] K.M. Al-Obaidi, A.M.A. Rahman, Toplighting systems for improving indoor environment: A review, in: Renew. Energy Sustain. Technol. Build. Environ. Appl. Options Greener Future, Springer International Publishing, 2016: pp. 117–136. https://doi.org/10.1007/978-3-319-31840-0_7.
[27] N. Ruck, Ø. Aschehoug, S. Aydinli, Daylight buildings. A source book on daylighting systems and components, (2000).
[28] L. Heschong, Resources, Skylighting Guidelines, Southern California Edison, Calif. USA (1998).
[29] Global irradiance, (n.d.). https://serc.carleton.edu/details/images/45952.html (accessed July 3, 2024).
[30] E.S. Lee, Demonstration of a light-redirecting skylight system at the Palm Springs Chamber of Commerce, (1996).
[31] R.C. Cabús, F.O. Pereira, Luminous efficacy of daylighting in intertropical region: an analysis for toplighting systems, Renew. Energy 8 (1996) 210–213.
[32] Ž. Kristl, A. Krainer, Light wells in residential building as a complementary daylight source, Sol. Energy 65 (1999) 197–206.
[33] J. McHugh, P. Manglani, R. Dee, L. Heschong, F. Oaks, Modular skylight wells: design guidelines for skylights with suspended ceilings, Des. Guidel. Calif. Energy Comm. (2004).
[34] L.O. Beltran, Toplighting for the Tropics, Passive Low Energy Archit.-Environ. Sustain. Chall. Aware. Dev. Soc. (2005) 1–4.
[35] S. Darula, R. Kittler, M. Kocifaj, Luminous effectiveness of tubular light-guides in tropics, Appl. Energy 87 (2010) 3460–3466.
[36] A. Chel, G.N. Tiwari, H.N. Singh, A modified model for estimation of daylight factor for skylight integrated with dome roof structure of mud-house in New Delhi (India), Appl. Energy 87 (2010) 3037–3050.
[37] C.S. Kim, S.J. Chung, Daylighting simulation as an architectural design process in museums installed with toplights, Build. Environ. 46 (2011) 210–222. https://doi.org/10.1016/j.buildenv.2010.07.015.
[38] J. Yunus, S.S. Ahmad, A. Zain-Ahmed, Analysing the impact of roof obstructions on daylight levels in atrium buildings: physical scale model measurements under real sky conditions, in: Proc. Int. Conf. Environ. Sci. Technol. ICEST 2011, 2011.
[39] I. Acosta, J. Navarro, J.J. Sendra, P. Esquivias, Daylighting design with lightscoop skylights: Towards an optimization of proportion and spacing under overcast sky conditions, Energy Build. 49 (2012) 394–401. https://doi.org/10.1016/j.enbuild.2012.02.038.
[40] K. Yildirim, M. Lutfi Hidayetoglu, A. Sen, Effects on sustainability of various skylight systems in buildings with an atrium, Smart Sustain. Built Environ. 1 (2012) 139–152. https://doi.org/10.1108/20466091211260587.
[41] L. Ghobad, W. Place, J. Hu, The impact of systems integration on the daylighting performance of skylights in offices, in: Conf. Proceeding SimBuild, 2012.
[42] A. Laouadi, A.D. Galasiu, H.H. Saber, C. Arsenault, Tubular daylighting devices. Part I: Development of an optical model (1415-RP), Hvacr Res. 19 (2013) 536–556.

[43] P. Schumacher, Design Research within the Parametric Paradigm, (n.d.). https://www.patrikschumacher.com/Texts/Design Research at Zaha Hadid Architects.htm.
[44] I. Caetano, L. Santos, A. Leitão, Computational design in architecture: Defining parametric, generative, and algorithmic design, Front. Archit. Res. 9 (2020) 287–300. https://doi.org/10.1016/j.foar.2019.12.008.
[45] R. Oxman, Thinking difference: Theories and models of parametric design thinking, Des. Stud. 52 (2017) 4–39. https://doi.org/10.1016/j.destud.2017.06.001.
[46] A. Stals, S. Jancart, C. Elsen, Parametric modeling tools in small architectural offices: Towards an adapted design process model, Des. Stud. 72 (2021) 100978. https://doi.org/10.1016/j.destud.2020.100978.
[47] T. Wortmann, B. Tunçer, Differentiating parametric design: Digital workflows in contemporary architecture and construction, Des. Stud. 52 (2017) 173–197. https://doi.org/10.1016/j.destud.2017.05.004.
[48] W. Jabi, Parametric design for architecture, Laurence King Publishing, London, 2013.
[49] R. Woodbury, S. Williamson, P. Beesley, PRARMETRIC MODELLING AS A DESIGN REPRESENTATION IN ARCHITECTURE: A PROCESS ACCOUNT, Proc. Can. Eng. Educ. Assoc. CEEA (2011). https://doi.org/10.24908/pceea.v0i0.3827.
[50] R. Aish, R. Woodbury, Multi-level Interaction in Parametric Design, in: A. Butz, B. Fisher, A. Krüger, P. Olivier (Eds.), Smart Graph., Springer Berlin Heidelberg, Berlin, Heidelberg, 2005: pp. 151–162. https://doi.org/10.1007/11536482_13.
[51] A. Zani, M. Andaloro, L. Deblasio, P. Ruttico, A.G. Mainini, Computational Design and Parametric Optimization Approach with Genetic Algorithms of an Innovative Concrete Shading Device System, Procedia Eng. 180 (2017) 1473–1483. https://doi.org/10.1016/j.proeng.2017.04.310.
[52] P.K. Rendy, Study on Optimization Method of Architectural Design Process based on Environmental Performance Indicators and Implementation of Generative Algorithm, (2022).
[53] P.J. Bentley, D.W. Corne, An introduction to Creative Evolutionary Systems, in: Creat. Evol. Syst., Elsevier, 2002: pp. 1–75. https://doi.org/10.1016/B978-155860673-9/50035-5.
[54] D.J. Gerber, S.-H.E. Lin, B.P. Pan, A.S. Solmaz, Design optioneering: multi-disciplinary design optimization through parameterization, domain integration and automation of a genetic algorithm, in: Proc. 2012 Symp. Simul. Archit. Urban Des., 2012.
[55] W. Pan, M. Turrin, C. Louter, S. Sariyildiz, Y. Sun, Integrating multi-functional space and long-span structure in the early design stage of indoor sports arenas by using parametric modelling and multi-objective optimization, J. Build. Eng. 22 (2019) 464–485. https://doi.org/10.1016/j.jobe.2019.01.006.
[56] M. Li, S. Yang, X. Liu, Shift-Based Density Estimation for Pareto-Based Algorithms in Many-Objective Optimization, IEEE Trans. Evol. Comput. 18 (2014) 348–365. https://doi.org/10.1109/TEVC.2013.2262178.
[57] R.P. Khidmat, H. Fukuda, Kustiani, B. Paramita, M. Qingsong, A. Hariyadi, Investigation into the daylight performance of expanded-metal shading through parametric design and multi-objective optimisation in Japan, J. Build. Eng. 51 (2022) 104241. https://doi.org/10.1016/j.jobe.2022.104241.
[58] Z. Shirzadnia, A. Goharian, M. Mahdavinejad, Designerly approach to skylight configuration based on daylight performance; toward a novel optimization process, Energy Build. 286 (2023) 112970. https://doi.org/10.1016/j.enbuild.2023.112970.

[59] Y.K. Yi, A. Tariq, J. Park, D. Barakat, Multi-objective optimization (MOO) of a skylight roof system for structure integrity, daylight, and material cost, J. Build. Eng. 34 (2021). https://doi.org/10.1016/j.jobe.2020.102056.
[60] A. Hariyadi, H. Fukuda, Q. Ma, The effectiveness of the parametric design 'Sudare' blind as external shading for energy efficiency and visibility quality in Jakarta, Archit. Eng. Des. Manag. 13 (2017) 384–403. https://doi.org/10.1080/17452007.2017.1296811.
[61] A. Eltaweel, S. Yuehong, Using integrated parametric control to achieve better daylighting uniformity in an office room: A multi-Step comparison study, Energy Build. 152 (2017) 137–148. https://doi.org/10.1016/j.enbuild.2017.07.033.
[62] Y. Fang, S. Cho, Design optimization of building geometry and fenestration for daylighting and energy performance, Sol. Energy 191 (2019) 7–18. https://doi.org/10.1016/j.solener.2019.08.039.
[63] D.J. Gerber, E. Pantazis, A. Wang, A multi-agent approach for performance based architecture: Design exploring geometry, user, and environmental agencies in façades, Autom. Constr. 76 (2017) 45–58. https://doi.org/10.1016/j.autcon.2017.01.001.
[64] Y. Grobman, G. Austern, Y. Hatiel, I. Capeluto, Evaluating the Influence of Varied External Shading Elements on Internal Daylight Illuminances, Buildings 10 (2020) 22. https://doi.org/10.3390/buildings10020022.
[65] P. Bakmohammadi, E. Noorzai, Optimization of the design of the primary school classrooms in terms of energy and daylight performance considering occupants' thermal and visual comfort, Energy Rep. 6 (2020) 1590–1607. https://doi.org/10.1016/j.egyr.2020.06.008.
[66] H. Kim, M.J. Clayton, A multi-objective optimization approach for climate-adaptive building envelope design using parametric behavior maps, Build. Environ. 185 (2020) 107292. https://doi.org/10.1016/j.buildenv.2020.107292.
[67] E. Taveres-Cachat, G. Lobaccaro, F. Goia, G. Chaudhary, A methodology to improve the performance of PV integrated shading devices using multi-objective optimization, Appl. Energy 247 (2019) 731–744. https://doi.org/10.1016/j.apenergy.2019.04.033.
[68] E. Taveres-Cachat, F. Goia, Co-simulation and validation of the performance of a highly flexible parametric model of an external shading system, Build. Environ. 182 (2020) 107111. https://doi.org/10.1016/j.buildenv.2020.107111.
[69] E. Taveres-Cachat, K. Bøe, G. Lobaccaro, F. Goia, S. Grynning, Balancing competing parameters in search of optimal configurations for a fix louvre blade system with integrated PV, Energy Procedia 122 (2017) 607–612. https://doi.org/10.1016/j.egypro.2017.07.357.
[70] E. Elbeltagi, H. Wefki, S. Abdrabou, M. Dawood, A. Ramzy, Visualized strategy for predicting buildings energy consumption during early design stage using parametric analysis, J. Build. Eng. 13 (2017) 127–136. https://doi.org/10.1016/j.jobe.2017.07.012.
[71] M. Marzouk, M. ElSharkawy, A. Eissa, Optimizing thermal and visual efficiency using parametric configuration of skylights in heritage buildings, J. Build. Eng. 31 (2020). https://doi.org/10.1016/j.jobe.2020.101385.
[72] P. Pilechiha, M. Mahdavinejad, F. Pour Rahimian, P. Carnemolla, S. Seyedzadeh, Multi-objective optimisation framework for designing office windows: quality of view, daylight and energy efficiency, Appl. Energy 261 (2020) 114356. https://doi.org/10.1016/j.apenergy.2019.114356.

[73] J. Zhang, N. Liu, S. Wang, A parametric approach for performance optimization of residential building design in Beijing, Build. Simul. 13 (2020) 223–235. https://doi.org/10.1007/s12273-019-0571-z.
[74] R. Talami, J.A. Jakubiec, Early-design sensitivity of radiant cooled office buildings in the tropics for building performance, Energy Build. 223 (2020) 110177. https://doi.org/10.1016/j.enbuild.2020.110177.
[75] A. Tabadkani, M. Valinejad Shoubi, F. Soflaei, S. Banihashemi, Integrated parametric design of adaptive facades for user's visual comfort, Autom. Constr. 106 (2019) 102857. https://doi.org/10.1016/J.AUTCON.2019.102857.
[76] F. Demarco, F. Bertacchini, C. Scuro, E. Bilotta, P. Pantano, The development and application of an optimization tool in industrial design, Int. J. Interact. Des. Manuf. IJIDeM 14 (2020) 955–970. https://doi.org/10.1007/s12008-020-00679-4.
[77] S.R. Samant, A parametric investigation of the influence of atrium facades on the daylight performance of atrium buildings, University of Nottingham, 2011.
[78] Lighting Design Glossary, (n.d.). https://www.schorsch.com/en/kbase/glossary/ (accessed June 27, 2024).
[79] C.F. Reinhart, Tutorial on the use of daysim simulations for sustainable design, Ott. Inst. Res. Constr. Natl. Res. Counc. Can. (2006).
[80] J.M. Stellman, Encyclopaedia of occupational health and safety, International Labour Organization, 1998.
[81] M.-C. Dubois, Impact of shading devices on daylight quality in offices, Simul. Radiance (2001).
[82] International Recommendations for the Calculation of Natural Daylight, J. Illum. Eng. Inst. Jpn. 52 (1968) 300–306. https://doi.org/10.2150/jieij1917.52.6_300.
[83] E.I. Network, Sun, Wind & Light–Architectural Design Strategies, UPDATE (2007).
[84] A. Marsh, CIE Sky Generator, (n.d.). https://andrewmarsh.com/software/cie-sky-web/.
[85] Brooklyn Museum Director Anne Pasternak: Interview, (n.d.). https://lh3.googleusercontent.com/Wu9tEdcLeXdigBubnBYIU1AowX7Iiewk910_1bYuRl8zQAUuvw0qcT5SvJg-Z-LxU3IL0AVb2C6P6NLFMT1g?filename=jeremy-deller-iggy-pop-brooklyn-museum.jpg (accessed June 27, 2024).
[86] L. Cone, Material Matters: The Conservation of Modern Sculpture, Stud. Conserv. 48 (2003) 139–140. https://doi.org/10.1179/sic.2003.48.2.139.
[87] F.D. Martin, Some Irritating Observations about Museums in the U.S.A. and Italy, Leonardo 13 (1980) 42. https://doi.org/10.2307/1577921.
[88] M. Hall, On display: A Design Grammar for Museum Exhibitions, Mus. Int. 40 (1988) 119–119. https://doi.org/10.1111/j.1468-0033.1989.tb00741.x.
[89] O. Omar, B. García-Fernández, A.Á. Fernández-Balbuena, D. Vázquez-Moliní, Optimization of daylight utilization in energy saving application on the library in faculty of architecture, design and built environment, Beirut Arab University, Alex. Eng. J. 57 (2018) 3921–3930. https://doi.org/10.1016/j.aej.2018.10.006.
[90] Y. Jeanneret, A. Depoux, J. Luckerhoff, V. Vitalbo, D. Jacobi, Written signage and reading practices of the public in a major fine arts museum, Mus. Manag. Curatorship 25 (2010) 53–67. https://doi.org/10.1080/09647770903529400.
[91] R. Clark, M. Barger, The Artist Initiative at San Francisco Museum of Modern Art, Stud. Conserv. 61 (2016) 24–28. https://doi.org/10.1080/00393630.2016.1193692.
[92] X. Huang, S. Wei, S. Zhu, Study on daylighting optimization in the exhibition halls of museums for Chinese calligraphy and painting works, Energies 13 (2020). https://doi.org/10.3390/en13010240.

[93] D.L. Loe, E. Rowlands, N.F. Watson, Preferred lighting conditions for the display of oil and watercolour paintings, Light. Res. Technol. 14 (1982) 173–192. https://doi.org/10.1177/096032718201400401.
[94] M.S. Rea, Illuminating Engineering Society of North America, eds., The IESNA lighting handbook: reference & application, 9. ed, Iluminating Engineering Society of North Amercia, New York, NY, 2000.
[95] C. Cuttle, Light for art's sake: lighting for artworks and museum displays, 1st ed., Routledge, Milton Park New York, 2007.
[96] S. Liu, Y.T. Kwok, K.K.-L. Lau, W. Ouyang, E. Ng, Effectiveness of passive design strategies in responding to future climate change for residential buildings in hot and humid Hong Kong, Energy Build. 228 (2020) 110469. https://doi.org/10.1016/j.enbuild.2020.110469.
[97] M. Buffoli, S. Capolongo, M. Cattaneo, C. Signorelli, [Project, natural lighting and comfort indoor], Ann. Ig. Med. Prev. E Comunita 19 (2007) 429–441.
[98] K. Konis, E.S. Lee, Measured daylighting potential of a static optical louver system under real sun and sky conditions, Build. Environ. 92 (2015) 347–359. https://doi.org/10.1016/j.buildenv.2015.04.024.
[99] A. Zayed, M. Elkhateib, M. Mahdy, I. Elwy, Exploring dynamic slat system for enhancing daylighting distribution at deep office spaces in hot arid regions, Energy Procedia 153 (2018) 290–294. https://doi.org/10.1016/j.egypro.2018.10.003.
[100] S.M. Al-Masrani, K.M. Al-Obaidi, Dynamic shading systems: A review of design parameters, platforms and evaluation strategies, Autom. Constr. 102 (2019) 195–216. https://doi.org/10.1016/j.autcon.2019.01.014.
[101] A. Figueiredo, J. Kämpf, R. Vicente, Passive house optimization for Portugal: Overheating evaluation and energy performance, Energy Build. 118 (2016) 181–196. https://doi.org/10.1016/j.enbuild.2016.02.034.
[102] S. Carlucci, F. Causone, F. De Rosa, L. Pagliano, A review of indices for assessing visual comfort with a view to their use in optimization processes to support building integrated design, Renew. Sustain. Energy Rev. 47 (2015) 1016–1033. https://doi.org/10.1016/j.rser.2015.03.062.
[103] D. Haas-Arndt, F. Ranft, N. Hüttenhölscher, Tageslichttechnik in Gebäuden, 1. Aufl, Müller, Heidelberg, Neckar, 2007.
[104] National Renewable Energy Laboratory, PASSIVE SOLAR DESIGN, (n.d.). https://www.nrel.gov/docs/fy01osti/29236.pdf.
[105] The American Society of Heating, Refrigerating and Air-Conditioning Engineers, RESEARCH ON GUIDELINES FOR WINDOW DESIGN STRATEGIES IN HIGH PERFORMANCE OFFICE BUILDINGS, (n.d.). https://www.ashrae.org/file%20library/conferences/specialty%20conferences/2020%20building%20performance/papers/d-bsc20-c054.pdf.
[106] E. Stach, Renzo Piano Building Workshop, Renzo Piano Building Workshop : space - detail - light, n.d.
[107] W.S. Brown, Daylight vs. Sunlight in Sawtooth-Roof Construction, (n.d.).
[108] E. CHPS, Collaborative for High Performance Schools, Natl. Mov. Improve Stud. Perform. Entire Educ. Exp. Build. Best Possible Sch. Www Chps Net (2003).
[109] L. Heschong, Daylight Metrics: PIER Daylighting Plus Research Program, Final Proj. Rep. Public Interest Res. PIER Program (2012).
[110] T. Kazanasmaz, L.O. Grobe, C. Bauer, M. Krehel, S. Wittkopf, Three approaches to optimize optical properties and size of a South-facing window for spatial Daylight Autonomy, Build. Environ. 102 (2016) 243–256. https://doi.org/10.1016/j.buildenv.2016.03.018.

[111] I. Acosta, M.Á. Campano, S. Domínguez, J. Fernández-Agüera, Minimum daylight autonomy: a new concept to link daylight dynamic metrics with daylight factors, Leukos (2019).
[112] J. Wienold, J. Christoffersen, Evaluation methods and development of a new glare prediction model for daylight environments with the use of CCD cameras, Energy Build. 38 (2006) 743–757. https://doi.org/10.1016/j.enbuild.2006.03.017.
[113] M. Hakimazari, M. Baghoolizadeh, S.M. Sajadi, P. Kheiri, M.Y. Moghaddam, M. Rostamzadeh-Renani, R. Rostamzadeh-Renani, M.B. Hamooleh, Multi-objective optimization of daylight illuminance indicators and energy usage intensity for office space in Tehran by genetic algorithm, Energy Rep. 11 (2024) 3283–3306. https://doi.org/10.1016/j.egyr.2024.03.011.
[114] F. Kharvari, An empirical validation of daylighting tools: Assessing radiance parameters and simulation settings in Ladybug and Honeybee against field measurements, Sol. Energy 207 (2020) 1021–1036. https://doi.org/10.1016/j.solener.2020.07.054.
[115] C. Hopfe, Uncertainty and sensitivity analysis in building performance simulation for decision support and design optimization, 2009.
[116] N. Delgarm, B. Sajadi, K. Azarbad, S. Delgarm, Sensitivity analysis of building energy performance: A simulation-based approach using OFAT and variance-based sensitivity analysis methods, J. Build. Eng. 15 (2018) 181–193. https://doi.org/10.1016/j.jobe.2017.11.020.
[117] M. Nayyeri, S.A. Hosseini, Sensitivity analysis to determine the importance of input variables in groundwater stress, Phys. Chem. Earth Parts ABC 135 (2024) 103628. https://doi.org/10.1016/j.pce.2024.103628.
[118] S. Tarantola, F. Ferretti, S. Lo Piano, M. Kozlova, A. Lachi, R. Rosati, A. Puy, P. Roy, G. Vannucci, M. Kuc-Czarnecka, A. Saltelli, An annotated timeline of sensitivity analysis, Environ. Model. Softw. 174 (2024) 105977. https://doi.org/10.1016/j.envsoft.2024.105977.
[119] A. Pellegrino, S. Cammarano, V. Savio, Daylighting for Green Schools: A Resource for Indoor Quality and Energy Efficiency in Educational Environments, Energy Procedia 78 (2015) 3162–3167. https://doi.org/10.1016/j.egypro.2015.11.774.
[120] Rethinking lighting in museums and galleries - Arup, (n.d.). https://www.arup.com/perspectives/publications/promotional-materials/section/rethinking-lighting-in-museums-and-galleries (accessed December 19, 2023).
[121] I.L. Wong, A review of daylighting design and implementation in buildings, Renew. Sustain. Energy Rev. 74 (2017) 959–968. https://doi.org/10.1016/j.rser.2017.03.061.
[122] Lu Na, Exhibits protection in light environment design of Art gallery, in: 2009 IEEE 10th Int. Conf. Comput.-Aided Ind. Des. Concept. Des., IEEE, Wenzhou, China, 2009: pp. 1739–1742. https://doi.org/10.1109/CAIDCD.2009.5375341.
[123] T. De Graaf, M. Dessouky, H.F.O. Müller, Sustainable lighting of museum buildings, Renew. Energy 67 (2014) 30–34. https://doi.org/10.1016/j.renene.2013.11.035.
[124] C. Cuttle, A Proposal to Reduce the Exposure to Light of Museum Objects Without Reducing Illuminance or the Levelofvisual Satisfaction of Museum Visitors, J. Am. Inst. Conserv. 39 (2000) 229–244. https://doi.org/10.1179/019713600806082720.
[125] W. El-Abd, B. Kamel, M. Afify, M. Dorra, Assessment of skylight design configurations on daylighting performance in shopping malls: A case study, Sol. Energy 170 (2018) 358–368. https://doi.org/10.1016/j.solener.2018.05.052.

[126] J. Cabeza-Lainez, J.-M. Almodovar-Melendo, I. Dominguez, Daylight and Architectural Simulation of the Egebjerg School (Denmark): Sustainable Features of a New Type of Skylight, Sustainability 11 (2019) 5878. https://doi.org/10.3390/su11215878.
[127] A. Laouadi, M.R. Atif, A. Galasiu, Methodology towards developing skylight design tools for thermal and energy performance of atriums in cold climates, Build. Environ. 38 (2003) 117–127. https://doi.org/10.1016/S0360-1323(02)00009-4.
[128] F.R. Piano, High Museum of Art Expansion, (n.d.).
[129] A. Nabil, J. Mardaljevic, Useful daylight illuminances: A replacement for daylight factors, Energy Build. 38 (2006) 905–913. https://doi.org/10.1016/j.enbuild.2006.03.013.
[130] A. Nabil, J. Mardaljevic, Useful daylight illuminance: a new paradigm for assessing daylight in buildings, Light. Res. Technol. 37 (2005) 41–57.
[131] C.F. Reinhart, O. Walkenhorst, Validation of dynamic RADIANCE-based daylight simulations for a test office with external blinds, Energy Build. 33 (2001) 683–697. https://doi.org/10.1016/S0378-7788(01)00058-5.
[132] Ö. Erlendsson, Daylight optimization: A parametric study of atrium design, R. Inst. Technol. Stockh. Httpwww Diva-Portal Orgsmashgetdiva2 723644 (2014).
[133] T.K. Þórðardóttir, DAYLIGHTING IN BUILDINGS IN ICELAND, Aalborg: sn, 2016.
[134] The RADIANCE Lighting Simulation and Rendering System, (n.d.). https://floyd.lbl.gov/radiance/refer/long.html#Table.
[135] R.A. Mangkuto, D.K. Dewi, A.A. Herwandani, M.D. Koerniawan, Faridah, Design optimisation of internal shading device in multiple scenarios: Case study in Bandung, Indonesia, J. Build. Eng. 24 (2019) 100745. https://doi.org/10.1016/j.jobe.2019.100745.
[136] M.C. Peel, B.L. Finlayson, T.A. McMahon, Updated world map of the Köppen-Geiger climate classification, Hydrol. Earth Syst. Sci. 11 (2007) 1633–1644. https://doi.org/10.5194/hess-11-1633-2007.
[137] X.-S. Yang, Genetic Algorithms, in: Nat.-Inspired Optim. Algorithms, Elsevier, 2021: pp. 91–100. https://doi.org/10.1016/B978-0-12-821986-7.00013-5.
[138] W. Roetzel, X. Luo, D. Chen, Optimal design of heat exchanger networks, in: Des. Oper. Heat Exch. Their Netw., Elsevier, 2020: pp. 231–317. https://doi.org/10.1016/B978-0-12-817894-2.00006-6.
[139] S. Sansri, S.W. Kielarova, Multi-Objective Shape Optimization in Generative Design: Art Deco Double Clip Brooch Jewelry Design, in: K.J. Kim, H. Kim, N. Baek (Eds.), IT Converg. Secur. 2017, Springer Singapore, Singapore, 2018: pp. 248–255. https://doi.org/10.1007/978-981-10-6451-7_30.
[140] K. Negendahl, T.R. Nielsen, Building energy optimization in the early design stages: A simplified method, Energy Build. 105 (2015) 88–99. https://doi.org/10.1016/j.enbuild.2015.06.087.
[141] Z. Luo, Y. Lu, Y. Cang, L. Yang, Study on dual-objective optimization method of life cycle energy consumption and economy of office building based on HypE genetic algorithm, Energy Build. 256 (2022) 111749. https://doi.org/10.1016/j.enbuild.2021.111749.
[142] A. Eltaweel, Y. Su, M.A. Mandour, O.O. Elrawy, A novel automated louver with parametrically-angled reflective slats; design evaluation for better practicality and daylighting uniformity, J. Build. Eng. 42 (2021) 102438. https://doi.org/10.1016/j.jobe.2021.102438.

[143] R.A. Rizi, A. Eltaweel, A user detective adaptive facade towards improving visual and thermal comfort, J. Build. Eng. 33 (2021) 101554. https://doi.org/10.1016/j.jobe.2020.101554.
[144] A. Toutou, M. Fikry, W. Mohamed, The parametric based optimization framework daylighting and energy performance in residential buildings in hot arid zone, Alex. Eng. J. 57 (2018) 3595–3608. https://doi.org/10.1016/j.aej.2018.04.006.
[145] A. Zhang, R. Bokel, A. van den Dobbelsteen, Y. Sun, Q. Huang, Q. Zhang, Optimization of thermal and daylight performance of school buildings based on a multi-objective genetic algorithm in the cold climate of China, Energy Build. 139 (2017) 371–384. https://doi.org/10.1016/j.enbuild.2017.01.048.
[146] D. Zhuang, X. Zhang, Y. Lu, C. Wang, X. Jin, X. Zhou, X. Shi, A performance data integrated BIM framework for building life-cycle energy efficiency and environmental optimization design, Autom. Constr. 127 (2021) 103712. https://doi.org/10.1016/j.autcon.2021.103712.
[147] J. Bader, E. Zitzler, HypE: An Algorithm for Fast Hypervolume-Based Many-Objective Optimization, Evol. Comput. 19 (2011) 45–76. https://doi.org/10.1162/EVCO_a_00009.
[148] S. Samadi, E. Noorzai, L.O. Beltrán, S. Abbasi, A computational approach for achieving optimum daylight inside buildings through automated kinetic shading systems, Front. Archit. Res. 9 (2020) 335–349. https://doi.org/10.1016/j.foar.2019.10.004.
[149] H. Samuelson, S. Claussnitzer, A. Goyal, Y. Chen, A. Romo-Castillo, Parametric energy simulation in early design: High-rise residential buildings in urban contexts, Build. Environ. 101 (2016) 19–31. https://doi.org/10.1016/j.buildenv.2016.02.018.
[150] K. Asadi, H. Ramshankar, H. Pullagurla, A. Bhandare, S. Shanbhag, P. Mehta, S. Kundu, K. Han, E. Lobaton, T. Wu, Vision-based integrated mobile robotic system for real-time applications in construction, Autom. Constr. 96 (2018) 470–482. https://doi.org/10.1016/j.autcon.2018.10.009.